# Book of Abstracts

APiP 2025 TOKYO

July 21 – 25, 2025, Tokyo, JAPAN

International Center, Tokyo Metropolitan University

## 22nd International Conference on Atomic Processes in Plasmas
## 1st NIFS Conference on Atomic and Molecular Processes in Plasmas

in cooperation with IAEA 大学共同利用機関法人 自然科学研究機構 核融合科学研究所 National Institute for Fusion Science

# CONTENTS

About ··· 2
Committee ··· 3
Sponsors ··· 4
Program ··· 5
Abstracts
  Invited talks ··· 10
  Memorial talks ··· 31
  Oral talks ··· 34
  Posters A ··· 58
  Posters B ··· 86
Author index ··· 114

# ABOUT

Welcome to the Joint Conference of the 22nd International Conference on Atomic Processes in Plasmas (APiP 2025) and the NIFS Conference on Atomic and Molecular Processes in Plasmas. This conference will be held from July 21 to July 25, 2025, on the campus of Tokyo Metropolitan University in Hachioji, Tokyo, Japan. Since 1977, the APiP conference has focused on atomic processes that are involved in the study of various plasmas over a wide range of densities and temperatures (eV to a few keVs). The topics cover Astrophysical plasmas; Fundamental Data and Modeling; High Energy Density Plasmas; Low Temperature and Industrial Plasmas; Magnetic-Fusion Plasmas; Measurements of Atomic Processes; Powerful Light Sources (XFEL, etc.); Small-scale Plasmas (table-top lasers, EBITs, etc.); Warm Dense Matter.

This time the NIFS conference is jointly held with the APiP conference and various atomic and molecular processes in fusion plasmas are focused to discuss in particular. We hope to bring researchers in fusion plasmas to this conference to join the discussion and find new sights on plasma physics.

APiP 2025 is organized in cooperation with the International Atomic Energy Agency (IAEA).

# COMMITTEE

## INTERNATIONAL PROGRAM COMMITTEE

Annette CALISTI (France)
Christian HILL (Austria)
Curt JOHNSON (USA)
Hae Ja LEE (USA)
Oleksandr MARCHUK (Germany)
Gerard MASSACRIER (France)
Izumi MURAKAMI (Japan)
Taisuke NAGAYAMA (USA)
Nobuyuki NAKAMURA (Japan)
Mi-Young SONG (Korea)

## LOCAL ORGANIZING COMMITTEE

Nobuyuki NAKAMURA (UEC, Chair)
Izumi MURAKAMI (NIFS, Co-Chair)
Shin KAJITA (UTokyo)
Daiji KATO (NIFS)
Naoki KIMURA (NIFS)
Shinichi NAMBA (Hiroshima U.)
Hayato OHASHI (U. Toyama)
Hiroyuki A. SAKAUE (NIFS)
Chihiro SUZUKI (NIFS)
Hajime TANUMA (TMU)
Hiroya YAMAGUCHI (ISAS)

# SPONSORS

公益財団法人
鹿島学術振興財団
THE KAJIMA FOUNDATION

Society for Promotion of Space Science
公益財団法人 宇宙科学振興会

# PROGRAM

## Day0: July 21 (Mon)

| | | |
|---|---|---|
| 16:00 –18:00 | | Registration and Reception (International Center, Tokyo Metropolitan University) |

## Day1: July 22 (Tue)

| | | |
|---|---|---|
| 8:30 | | Registration |
| 9:20 | | Opening<br>Nobuyuki Nakamura (LOC Chair, U. Electro-Comm.)<br>Hiroshi Yamada (Director of General, NIFS)<br>Takaya Ohashi (President, Tokyo Metro. Univ.) |
| 9:50 | I-01 | Motoshi Goto (NIFS)<br>Spectroscopic studies in LHD focusing on atomic processes |
| 10:20 | I-02 | Andreas Langenberg (IPP)<br>Tungsten Spectroscopy at W7-X: Diagnostics, Models, and Applications |
| 10:50 | Coffee | |
| 11:10 | M-01 | Martin O'Mullane (U. Strathclyde)<br>Approaching complexity for atomic data and models |
| 11:40 | I-03 | Tomoko Kawate (QST)<br>Electron collision processes for BH and $BH^+$ molecules |
| 12:10 | O-01 | Ritu Dey (IITT)<br>Simulating the Low Charge State Emissions from Tungsten for Fusion Applications |
| 12:30 | O-02 | Ibtissem Hannachi (U. Batna 1)<br>Hydrogen Stark broadening revisited for magnetic fusion plasma diagnostics |
| 12:50 | Lunch | |
| 14:10 | I-04 | Conor Perks (MIT)<br>High-resolution laboratory measurements of tungsten M-shell x-ray spectra for burning plasma diagnostics in SPARC and ITER |
| 14:40 | I-05 | Masahiro Kobayashi (NIFS)<br>Thermal Instability in Magnetically Confined Toroidal Plasmas Induced by Radiative Emission of Highly Charged Ions |
| 15:10 | O-03 | Yuki Hayashi (NIFS) |

| | | |
|---|---|---|
| | | Dynamic response of atomic processes in recombining helium plasmas to high-density pulse in Magnum-PSI |
| 15:30 | Coffee | |
| 15:50 | I-06 | Ulises Losada (Auburn U.)<br>Advances in Tungsten Ultraviolet Spectroscopy via Improved Atomic Physics Calculations for Erosion Diagnostics in Fusion Plasmas |
| 16:20 | O-04 | Tsunehiro Morita (Kyoto U.)<br>A numerical study on the feasibility of the recombination front measurements by analyzing the Zeeman effect on the chord integrated deuterium Paschen $\alpha$ line spectrum in JT-60SA |
| 16:40 | O-05 | Keisuke Fujii (ORNL)<br>Analytic Scaling of Neutral Transport in High-Temperature Plasma Edges through Repetitive Charge Exchange Collisions |
| 17:00<br>-19:00 | Poster Session B | |

## Day2: July 23 (Wed)

| | | |
|---|---|---|
| 9:30 | I-07 | Yuri Ralchenko (NIST)<br>Till 120! Triumph and Twilight of Atomic Spectroscopy at NIST |
| 10:00 | O-06 | Jianmin Yuan (Jilin U.)<br>Influences on the continuum atomic processes in hot and dense plasmas due to IPD and changes of continuum electron wavefunctions |
| 10:20 | O-07 | Shivam Gupta (NCKU)<br>Theoretical Investigation of Electron Impact Excitation and Radiative Processes in Highly Charged Tin Ions Using a Collisional-Radiative Model |
| 10:40 | Coffee | |
| 11:00 | M-02 | John Sheil (ARCNL)<br>Howard Scott: The scientist, the colleague, the mentor |
| 11:30 | I-08 | Shinsuke Fujioka (ILE)<br>X-ray Spectroscopy of High Energy Density Plasma for Inertial Fusion Energy Development |
| 12:00 | O-08 | Patrick Renaudin (CEA/DAM)<br>Cooling and recombination dynamics of an Al plasma in AlTi or AlAu mixtures heated by an ultraintense laser pulse |
| 12:20 | O-09 | Xing Wang (Xi'an Jiaotong U.)<br>Enhanced x-ray absorption and heating in medium-Z-doped CHO foams under laser-driven hohlraum radiation |
| 12:40 | Lunch | |

| | | |
|---|---|---|
| 14:00 | I-09 | Evgeny Stambulchik (WIS)<br>Fast evaluation of complex line shapes in plasma |
| 14:30 | I-10 | Marc-Andre Schaeuble (SNL)<br>Using deep learning to develop a fast, versatile NLTE spectral model for application to HED systems |
| 15:00 | O-10 | Hai P Le (LLNL)<br>Impact of super-Gaussian electron distributions on plasma K-shell emission |
| 15:20 | Coffee | |
| 15:40 | I-11 | Bob Nagler (SLAC)<br>Direct measurement of ion temperature and electron-ion equilibration in warm dense matter |
| 16:10 | I-12 | Oliver Humphries (EuXFEL)<br>Ionization dynamics and electronic structure of x-ray heated plasmas |
| 16:40 | O-11 | Moto Togawa (EuXFEL)<br>Nonlinear response of highly charged ions to ultraintense XFEL radiation |
| 17:00 | O-12 | Hae Ja Lee (SLAC)<br>Understanding of hot dense plasmas isochorically heated by XFEL using X-ray emission spectroscopy |
| 17:20 | Break | |
| 17:35 | I-13 | Canelia Miron (Nagoya U.)<br>Cold atmospheric pressure plasma-treated liquids and formulations for cancer treatment |
| 18:05 | I-14 | Marc Sackers (FZ Jülich)<br>On the line shape of sputtered atoms in low-temperature magnetized plasmas |
| 18:35 | O-13 | Mi-Yong Song (KIFE)<br>Development of Ar and $N_2$ Plasma Spectroscopy Reference Data for Plasma Characterization using Collision-Radiation Models and Machine Learning |
| 18:55 | End | |

## Day3: July 24 (Thu)

| | | |
|---|---|---|
| 9:30 | I-15 | Thomas Gawne (CASUS)<br>M-shell Rebinding in Hot, Solid-density Mg and Al |
| 10:00 | O-14 | Pedro Velarde (IFN, UPM)<br>Probing dense plasmas with high harmonics |
| 10:20 | O-15 | Lucas Ansia Fernadez (GoLP, IST)<br>Shake-off in XFEL Heated Solid-Density Plasma |

| | | |
|---|---|---|
| 10:40 | Coffee | |
| 11:10 | I-16 | Maria Teresa Belmonte Sainz-Ezquerra (U. Valladolid)<br>Experimental Plasma Spectroscopy: meeting data needs for astrophysics |
| 11:40 | I-17 | Hiroya Yamaguchi (ISAS/JAXA)<br>High-Resolution X-Ray Spectroscopy of Astrophysical Plasmas with XRISM |
| 12:10 | O-16 | Yuki Amano (ISAS/JAXA)<br>A Laboratory plasma experiment for X-ray astronomy using a compact electron beam ion trap (EBIT) |
| 12:30 | O-17 | Masahiro Tsujimoto (ISAS/JAXA)<br>X-ray Microcalorimeter Spectroscopy and Radiative Transfer Modeling of Astrophysical Plasmas around Neutron Stars and Black Holes |
| 12:50 | Lunch (IPC meeting) | |
| 14:10 | I-18 | Ryohko Ishikawa (NAOJ)<br>Exploring the Sun with Ultraviolet SpectroPolarimetry: The CLASP Sounding Rocket Series |
| 14:40 | O-18 | Roi Avraham Rahin (NASA)<br>The structure of the AGN narrow-line region as probed by emission line ratios |
| 15:00 -17:00 | Poster Session A | |
| 18:30 -20:30 | Banquet (Royal Garden Palace Hachioji Nihonkaku) | |

## Day4: July 25 (Fri)

| | | |
|---|---|---|
| 9:30 | I-19 | Patricial Cho (LLNL)<br>Testing High Density XSTAR Models with Fe Photoionized Plasma Experiments on the Z Machine |
| 10:00 | I-20 | Jerome Deprince (U. Mons)<br>Large scale computation of atomic data in heavy elements for kilonova modeling |
| 10:30 | O-19 | Chunyu Zhang (U. Strathclyde )<br>Dielectronic Recombination of Fe $3d^k$ Ions |
| 10:50 | O-20 | Hiroaki Nakamura (NIFS)<br>Molecular Dynamics Study of Amino Acid Precursor Formation under Space-like Conditions |
| 11:10 | Coffee | |

| | | |
|---|---|---|
| 11:40 | O-21 | Kirsten Dowd (UCD)<br>Visible-Near Infrared Photo-absorption in Zirconium Plasmas for Kilonova Studies |
| 12:00 | O-22 | Mourad Telmini (UTM)<br>Mapping Rydberg states of $H_2$ with the Halfium R-matrix method |
| 12:20 | O-23 | Ayushi Agrawal (IIT Roorkee)<br>Detailed Collisional-Radiative Analysis of Iodine Plasma for Plasma Diagnostics |
| 12:40 | Closing | |

# INVITED TALKS

**I-01**

# Spectroscopic studies in LHD focusing on atomic processes

**Motoshi Goto**

National Institute for Fusion Science, Toki 509–5292, Japan

The Large Helical Device (LHD) at the National Institute for Fusion Science is equipped with various types of spectrometers to cover a wide range of wavelengths from the visible to the X-ray region, and many studies based on spectral measurements are being performed. Among these, recent researches focused on atomic processes are presented.

Helium gas was injected into the LHD plasma and the intensities of several visible emission lines of neutral helium atoms were measured simultaneously. The helium atom emissions are known to occur in the outermost region of the plasma. Using a collisional radiative model, the electron temperature and electron density were derived from the line intensity ratios and it was found that these parameters vary strongly with plasma conditions. It was also found that the radial position of the helium atom emission was almost fixed at the location where the magnetic field line connection length to the divertor plates suddenly increases to over 100 m [1]. This result indicates that the magnetic field structure is important for determining the neutral particle transport in the plasma boundary region.

It is known that atomic emission lines due to electron collision excitation are generally polarized. If the electron velocity distribution function in the plasma is anisotropic, the atomic emission lines can be polarized. Inspired by CLASP (Chromospheric Lyman-Alpha Spectro-Polarimeter) by the National Astronomical Observatory of Japan [2], a polarization measurement in the LHD was attempted and a few percent polarization was detected, with a tendency for the polarization to relax with increasing collisionality. A collisional radiation model was constructed and the anisotropy of the electron temperature was evaluated from the detected degree of polarization [3]. It was successfully demonstrated the atomic emission line polarization can be used as a method for measuring plasma anisotropy.

Hydrogen pellets were injected into the LHD plasma and a spectral measurement was conducted for the ablation cloud surrounding the pellet. The discrete lines show large Stark broadening, and the electron temperature and density of the ablation cloud were obtained by fitting the experimental data with a spectral model assuming the complete local thermodynamic equilibrium. The penetration characteristics of the pellet changed depending on the state of the target plasma, and in particular, it was confirmed that the penetration length became shorter as the temperature of the target plasma increased. In addition, it was found that the maximum electron density of the ablation cloud little changed irrespective of the penetration length [4]. These results are helpful for developing pellet ablation simulation models.

References

[1] M. Goto and K. Sawada, J. Quant. Spectrosc. Radiat. Transf. **137**, 23 (2014)

[2] R. Kano et al., APjL **839**, L10 (2017).

[3] M. Goto et al., Plasma Fusion Res. **16**, 2402029 (2021).

[4] M. Goto et al., Atoms **12**, 1 (2024).

**I-02**

# Tungsten Spectroscopy at W7-X: Diagnostics, Models, and Applications

**A. Langenberg[1]**, T. Gonda[2], O. Marchuk[3], N. Pablant[4], Th. Wegner[1], O. Ford[1], B. Buttenschön[1], N. Tamura[1], and the W7-X Team

[1] Max-Planck-Institute for Plasma Physics, 17491 Greifswald, Germany
[2] Auburn University, 36849 Auburn, United States of America
[3] Forschungszentrum Jülich, 52425 Jülich, Germany
[4] Princeton Plasma Physics Laboratory, 08542 Princeton, United States of America

This work reports on recent developments on the spectroscopic analysis of Tungsten emission lines over a wide spectral range from ultra-violet to high-resolution x-ray data of various spectrometers [1,2] at the magnetically confined fusion Stellarator experiment Wendelstein 7-X [3].
A new method for an absolute calibration of X-ray spectrometers using well defined impurity injections [4,5], line identifications of highly resolved $W^{41+}$-$W^{46+}$ spectra (Fig.1), as well as validations of W rate coefficients through diagnostics cross calibrations will be discussed in detail.

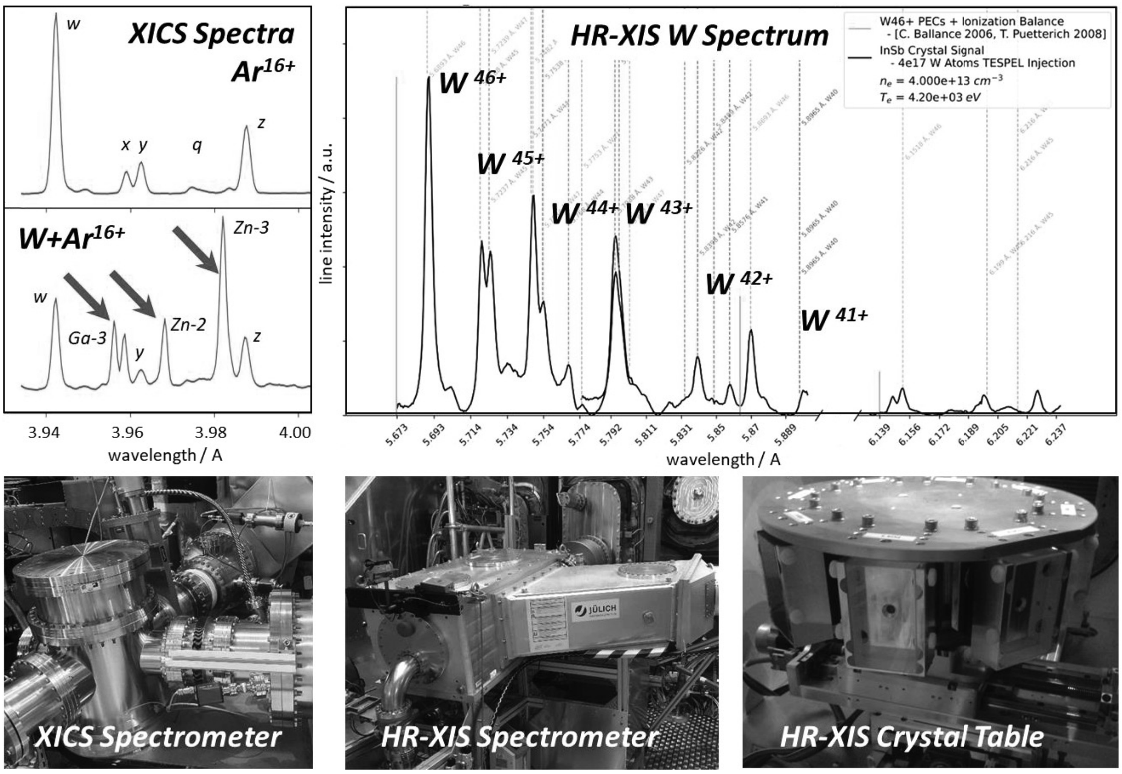


Fig.1: High resolution tungsten spectra observed at W7-X with imaging spectrometers XICS and HR-XIS [1] after tungsten injections via laser blow off and solid pellet injections into high electron temperature plasmas.

[1] A. Langenberg, N.A. Pablant, Th. Wegner *et al*. Review of Scientific Instruments **89**, 10G101 (2018)
[2] B. Buttenschön, R. Burhenn, M. Kubkowska et al. 43rd EPS Conference on Plasma Physics (2016)
[3] O. Grulke, C. Albert, J.A. Alcuson Belloso *et al.* Nuclear Fusion **64**, 112002 (2024)
[4] R. Bussiahn, N. Tamura, K.J. Mc Carthy *et al.* Plasma Phys. Control. Fusion **66**, 115020 (2024)
[5] Th. Wegner, F. Kunkel *et al.* Fusion Engineering and Design **193**, 113691 (2023)

**I-03**

# Electron collision processes for BH and $BH^+$ molecules

**Tomoko Kawate**[1,2,3], Izumi Murakami[2,3], Motoshi Goto[2,3]

[1]National Institutes for Quantum Science and Technology, 801-1 Mukoyama, Naka, Ibaraki 311-0193, JAPAN
[2]National Institute for Fusion Science, 322-6 Oroshi, Toki, Gifu 509-5292, JAPAN
[3]The Graduate Institute for Advanced Studies, SOKENDAI, 322-6 Oroshi, Toki, Gifu 509-5292, JAPAN

In magnetically confined fusion devices, BH spectral emission is a good diagnostic of boron deposition onto plasma-facing materials. BH (or boron deuteride, BD) molecular bands have been confirmed in discharges after fresh boronization. Kawate et al.[1] performed impurity powder dropping experiments[2] with boron powders in the Large Helical Device toward real-time wall conditioning. Their spatially-resolved spectroscopic measurements of BH molecular bands suggest deposition and desorption of boron on the divertor plates.

Especially aiming at fusion plasmas, electron collisional cross sections for hydride molecules related to plasma-wall interactions are crucial and have been discussed intensively. Despite the importance in fusion plasma applications and the long discussions of the spectroscopic characteristics, systematic investigations of cross sections and rate coefficients of $e^-$–$BH^{(+)}$ collision had not been in the literature.

In this study, we numerically investigate electronic excitation and ionization cross sections for the $e^-$–BH and $e^-$–$BH^+$ collision processes and the rate coefficients. In addition, we derive S/XB and compare it to the preceding study, aiming for an application to plasma diagnostics and modeling near plasma-facing materials in fusion devices. The calculations were performed by the R-matrix and Binary Encounter Bethe methods by using the UKRmol+ software suite[4]. To examine the uncertainty due to the calculation conditions, we compared the results by different basis sets and internuclear distances of the target model. We found that the uncertainties are typically within 10%. Rate coefficients were derived and fitted to an Arrhenius function. The derived S/XB values for $e^-$–BH collisions agreed with the value presented by Lieder et al.[5].

References

[1] T. Kawate, N. Ashikawa, M. Goto et al., Nucl. Fusion **62**, 126052 (2022)

[2] A. Nagy, A. Bortolon, D. M. Mauzey et al., Rev. Sci. Instrum. **89**, 10K121 (2018)

[3] T. Kawate, I. Murakami, M. Goto, Plasma Sources Sci. Technol. **32**, 085006 (2023)

[4] Z. Mašín, J. Benda, J. Gorfinkiel et al., Comput. Phys. Commun. **249**, 107092 (2020)

[5] G. Lieder et al. (the ASDEX-Upgrade Team), Eur. Phys. Soc. Conf. Plasma Phys., **2**, 722 (1994)

**I-04**

# High-resolution laboratory measurements of tungsten M-shell x-ray spectra for burning plasma diagnostics in SPARC and ITER

**C. Perks[1]**, J.E. Rice[1], N. Hell[2], A.J. Fairchild[2], G.V. Brown[2],
D. Vezinet[3], S.B. Hansen[4], M.F. Gu[5], M.L. Reinke[3]

*[1]Plasma Science and Fusion Center, Massachusetts Institute of Technology, Cambridge, MA 02139, USA*
*[2]Lawrence Livermore National Laboratory, Livermore, CA 94550, USA*
*[3]Commonwealth Fusion Systems, Cambridge, MA 02139, USA*
*[4]Sandia National Laboratory, Albuquerque, NM 87123, USA*
*[5]Prism Computational Sciences, Madison, WI 53711, USA*

High-resolution x-ray crystal spectroscopy (XRCS) is routinely used on tokamaks to measure the ion temperature and toroidal rotation profiles by monitoring the Doppler broadening and Doppler line shifts, respectively, of intrinsic or seeded impurity line emission. The SPARC tokamak, currently under construction, will similarly employ this diagnostic method. The designed XRCS system is optimized to view the Ne-like Xe 3D line (3d-2p, 2.72 Å, 4.5 keV) for low-temperature operations (Te(0)~4-10 keV) and the He-like Kr w resonance line (2p-1s, 0.945 Å, 13.1 keV) for high-temperature operations (Te(0)>10 keV) [1]. A low-resolution survey spectrometer is also being designed to monitor L-shell W emission from 8-10 keV (1.6-1.2 Å). However, similar XRCS systems have shown that high-Z impurity emission (Mo, W) can contaminate the spectrum leading to errors in the inferred plasma parameters [2,3]. As SPARC will feature an all-tungsten wall design, it is crucial to fully characterize the tungsten emission spectrum within the spectral ranges relevant to SPARC's XRCS system.

OpenADAS and FLYCHK indicate W lines nearly degenerate with the Ne-like Xe 3D line, but these sources do not always provide accurate wavelengths or complete line lists. To address this, we have performed high-resolution W measurements at the electron beam ion trap (EBIT-I) facility at Lawrence Livermore National Laboratory (LLNL) using the EBIT Calorimeter Spectrometer (ECS). These measurements were done by systematically varying the electron beam energy to isolate and associate emission lines with the emitting charge state. Using the EBIT-I data to identify the brightest lines in this spectral range, we preformed high-fidelity simulations using the SCRAM, FAC and ColRadPy codes to deduce the transitions as well as generate emissivity data. Wavelengths were measured using the SPECTRALLY spectral fitting code and reported here. We then apply these data for throughput modeling using the ToFu and XICSRT ray-tracing codes to scope the impact of the relative W-to-Xe concentration on inferred ion temperature. We will use these lines, along with the survey spectrometer, for W density measurements and transport studies, such as profile peaking.

Work at LLNL is performed under the auspices of the U.S. Department of Energy under contract No. DE-AC52-07NA27344. SNL is managed and operated by NTESS under DOE NNSA contract DE-NA0003525.

1. C. Perks *et al., Rev. Sci. Instrum.* **95,** 083555 (2024)
2. J.E. Rice *et al., J. Phys. B: At. Mol. Opt. Phys.* **54,** 095701 (2021)
3. A. Da Ros *et al., Rev. Sci. Instrum.* **95,** 043505 (2024)

**I-05**

# Thermal Instability in Magnetically Confined Toroidal Plasmas Induced by Radiative Emission of Highly Charged Ions

**Masahiro Kobayashi**, Masato. I.N. Kobayashi*, Ryohtaroh T. Ishikawa, Ken-ichi. Nagaoka, and the LHD Experiment group

National Institute for Fusion Science, Toki, 509-5292, Japan.
* Physikalisches Institut, Universität zu Köln, Zülpicher Straße 77, 50937 Köln, Germany

Excessive heat load on divertor plates in magnetically confined fusion reactors poses significant risks, potentially leading to substantial damage and jeopardizing stable reactor operation. One promising approach for mitigating this heat load is the cooling of peripheral plasmas through radiative emission from deliberately introduced highly charged ions, known as impurities. Impurities with low atomic number (Z) are preferred to avoid unintended cooling of the hot core plasma, as high-Z impurities can result in excessive radiation at the high temeprature range of order of several keV.

The cooling function ($L$), defined as the sum of all impurity line radiations, exhibits a notable dependence on electron temperature ($T_e$). Initially, $L$ increases with $T_e$ as electrons in plasma attain sufficient energy to excite orbital electrons in impurity ions, resulting in radiation through subsequent de-excitation. However, as the impurity charge states progress to closed-shell configurations (e.g., He-like shell), excitation energies rise and radiation significantly diminishes, causing $L$ to decrease by orders of magnitude. Consequently, low-Z impurities show peak radiation efficiency at electron temperatures around 10–30 eV, followed by a decline as $T_e$ approaches 100 eV.

This temperature-dependent behavior of $L$ is a critical factor in the thermal instability of plasmas. When the condition $\frac{\partial}{\partial T}\left(\frac{L}{T_e}\right) < 0$ is met, plasma cooling accelerates in a runaway manner until reaching a new thermal equilibrium [1]. Our study investigates the thermal instability in magnetically confined toroidal plasmas, focusing on the role of peripheral magnetic field structures where radiative cooling predominantly occurs.

In the Large Helical Device (LHD) experiment at NIFS, Japan, the thermal instability growth rate $\gamma_{th}$ was analyzed during radiative cooling operation with carbon impurities as a major impurity originating from graphite divertor plates. As plasma density increased, edge $T_e$ gradually decreased with fixed heating power, enhancing total plasma radiation according to the function $n_e n_{imp} L(T_e)$, where $n_e$ and $n_{imp}$ are densities of electrons and impurities, respectively. During cooling, $\gamma_{th}$ became positive in the peripheral region, with the unstable zone moving radially inward until plasma collapse due to uncontrollable radiation occurred.

Interestingly, introducing magnetic perturbation fields stabilized radiative cooling by altering edge magnetic topology. The resulting "magnetic island," analogous to phase-space structures in nonlinear Hamiltonian systems, consist of X-points (hyperbolic singular point) and O-points (elliptic cell) surrounded by separatrices. By inspecting energy transport at the island, the $\gamma_{th}$ becomes large at the O-point and the X-point, where the stabilizing effect by energy transport is reduced significantly because of the singularities. Thermal instability analysis within the island revealed that while radiation intensified, $\gamma_{th}$ at the O-point became negative, reaching thermal stability. Thermal condensation at the O-point led to reduced $T_e$ (down to several eV) and increased density (up to $10^{20}$ $m^{-3}$), avoiding the unstable condition $\frac{\partial}{\partial T}\left(\frac{L}{T_e}\right) < 0$.

Details of this analysis will be presented and the thermal equilibrium achieved during radiative cooling operations will be discussed at the conference.

[1] S.A. Balbus, The Astrophysical Journal **303**, L79 (1986) L79.

**I-06**

# Advances in Tungsten Ultraviolet Spectroscopy via Improved Atomic Physics Calculations for Erosion Diagnostics in Fusion Plasmas

**U. Losada[1]**, D. A. Ennis[1], S. D. Loch[1], C. A. Johnson[2], C. Ballance[3], T. Abrams[4], A. G. McLean[5], D. L. Rudakov[6], W. R. Wampler[7]

[1]Auburn University, Auburn, AL, USA; [2]Oak Ridge National Laboratory, Oak Ridge, TN, USA; [3]Queens University Belfast, Belfast, United Kingdom; [4]General Atomics, San Diego, CA; USA; [5]Lawrence Livermore National Laboratories, Livermore, CA, USA;[6]University of California San Diego, San Diego, CA, USA; [7]Sandia National Laboratories, Sandia, NM, USA

Measurements of tungsten (W) gross-erosion and re-deposition rates have been derived from high-resolution ultraviolet (UV) spectroscopy in the lower divertor of the DIII-D tokamak. These results leverage new spectrometric capabilities in the DIII-D device along with improved atomic data for neutral [1] and near neutral charge states of W [2,3] and lead to substantial advances in understanding processes governing W erosion under conditions relevant for future fusion devices. The atomic data consists of R-matrix calculations for the electron-impact excitation [2,3] and exchange classical impact parameter data for ionization [1]. W erosion and transport in future fusion devices could cause unacceptable levels of high-*Z* impurities in the core, reducing plasma performance by radiation losses. For ionizing conditions ($T_e > 10$ eV), W erosion fluxes can be quantified by atomic line spectroscopy combined with ionization per photon coefficients (S/XBs) obtained from collisional-radiative (CR) atomic physics models [4]. The intensity of the W I emission line at 400.88 nm, commonly used for erosion measurements, can depend on metastable state populations [5]. Conversely, measuring several neutral tungsten emission lines (W I) in the UV wavelength range allows for precise W gross-erosion measurements. In addition, most emission from higher W charge states occurs below 400 nm, enabling W re-deposition measurements.

W-coated graphite samples were exposed over a range of plasma conditions ($n_e \sim 1$ - $2 \times 10^{19}$ m$^{-3}$, $T_e$ ~15 - 35 eV) using the Divertor Material Evaluation System (DiMES) manipulator. W erosion rates during experiments were of the order of $\sim 1 \times 10^{19}$ atoms m$^{-2}$ s$^{-1}$, like previous DIII-D experiments [6]. Emission observed at 255.13 nm is the most intense W I line and is not dependent on metastable levels, while a W I line at 265.65 nm is populated from the same metastable states as the 400.88 nm line. Spectroscopic data from W I emission lines combined with post-mortem Rutherford backscattering measurements of material erosion from W samples yield empirical S/XBs values systematically larger than CR predictions, consistent with underestimated ionization rates [1].

Furthermore, the simultaneous observation of W I and W II emission provides lower bound of W re-deposition estimations, while higher tungsten charge states (W III, …) are needed for more accurate measurements. Post-exposure re-deposition fractions of ~75 – 80% have been measured from W samples of 1.5 cm in diameter. Additionally, pairs of W I emission lines can be used as line ratio diagnostics for $T_e$ in the plasma edge, giving $T_e$ values slightly below Langmuir probe measurements.

References

[1] Smyth et al 2018, PRA, 97, 052705
[2] Dunleavy et al. 2022, JPB, 55, 175002
[3] McCann et al. 2024, JPB, 57, 235202
[4] K. Behringer *et al.*, 1989, PPCF 31 2059
[5] C.A. Johnson *et al.*, 2023, NF 63 096017
[6] T. Abrams *et al.* 2017, NF 57 056034

Work supported by US DOE: DE-SC0015877 and DE-FC02-04ER54698.

**I-07**

# Till 120! Triumph and Twilight of Atomic Spectroscopy at NIST

**Yuri Ralchenko**

Associate, National Institute of Standards and Technology, Gaithersburg, MD 20899, USA

The 120-year-long history of atomic spectroscopy at NIST has come to completion with the recent termination of its Atomic Spectroscopy Group (ASG). Over many decades, NIST spectroscopists produced unique critically evaluated data for atomic parameters, performed exceptionally precise measurements of spectra from neutral to 70-times ionized atoms, developed powerful methods for diagnostics of diverse terrestrial and astrophysical plasmas. This talk will present an overview of ASG achievements over years with emphasis on the most recent work and offer an outlook for its path ahead.

# X-ray Spectroscopy of High Energy Density Plasma for Inertial Fusion Energy Development

**Shinsuke FUJIOKA**[1], Ryunosuke TAKIZAWA[1], Yuga KARAKI[2,1], Hiroki MATSUBARA[2,1], Rinya AKEMATSU[2,1], Ryo OOMURA[2,1], Muhammad Fauzan SYAHBANA[2,1], Kai KIMURA[2,1], Jinyuan DUN[2,1], Alessio MORACE[1], Yasunobu ARIKAWA[1], Akifumi IWAMOTO[1], Tomoyuki JOHZAKI[3,1], Yasuhiko SENTOKU[1], Ryosuke KODAMA[1]

[1] Institute of Laser Engineering, The University of Osaka,
[2] Graduate School of Sciences, The University of Osaka,
[3] Graduate School of Advanced Science and Engineering, Hiroshima University.

X-ray spectroscopy plays a vital role in the development of inertial fusion energy (IFE), particularly in the fast ignition (FI) scheme, where the separation of fuel compression and ignition phases requires precise control and understanding of high energy density (HED) plasmas. Accurate diagnosis of temperature, density, and ionization states in laser-compressed matter is essential for validating implosion symmetry, determining energy coupling efficiency, and optimizing fuel assembly.

This work presents x-ray-based diagnostics techniques developed at the University of Osaka to probe dense plasmas generated by high-power laser systems such as GEKKO XII and LFEX. We employ mid-Z tracer elements and high-sensitivity X-ray spectrometers to capture keV-range emission spectra from heated targets [1, 2, 3]. The observed spectra are analyzed using the atomic kinetics codes FLYCHK and PrismSPECT, allowing quantitative plasma parameter extraction under extreme conditions.

Particular focus is placed on diagnosing preheat, shock timing, and hot spot formation—all critical for fast ignition. We also discuss the application of X-ray diagnostics to solid-core targets with improved resistance to hydrodynamic instabilities and magnetized implosions, where sub-kilotesla-level fields are applied to suppress thermal conduction and enhance confinement.

These diagnostic capabilities support the experimental validation of IFE target designs and serve as feedback to improve hydrodynamic and radiation transport simulations. X-ray spectroscopy is thus a cornerstone of integrated research efforts toward realizing laser fusion energy.

## References

[1] S. Sakata *et al.*, Nature Communications **9**, 3937 (2018).

[2] K. Matsuo *et al.*, Physical Review Letters **124**, 035001 (2020), 1907.10447.

[3] R. Takizawa *et al.*, Physical Review Research **00**, 3000 (2025).

# Fast evaluation of complex line shapes in plasma

**Evgeny Stambulchik**, Ramy Doron, and Yitzhak Maron

Weizmann Institute of Science, Rehovot 7610001, Israel

Line-shape analysis is an invaluable tool for diagnostics of laboratory and space plasmas [1]. Line-shape calculations typically rely on complex numerical codes, consuming substantial computational resources. This is particularly true for computer simulation methods [2].

In practice, one often needs to repeat the calculations multiple times over a range of plasma parameters while, e.g., obtaining the best fit of an experimental spectrum. Moreover, due to a combination of instrumental limitations (finite spatial and temporal resolutions) and intrinsic plasma effects (such as fluctuations driven by turbulent motion), the experimental spectra inevitably represent a weighted average over a distribution of plasma parameters, leading to non-trivial alterations in the observed line shapes [3]. Accounting for such distributions of plasma parameters in a line-shape model further increases the number of calculations required.

Evidently, a fast interpolating procedure is desired to obtain a line profile based only on a limited number of pre-calculated line shapes. It can be done rather straightforwardly in specific applications (for example, see Ref. [4]), but not in the general case. Here, a technique for line-shape interpolation (or morphing) will be discussed, and examples of its application will be presented, including inlining accurate line shapes in a collisional-radiative model.

References

[1] H. R. Griem. *Principles of Plasma Spectroscopy*. Cambridge University Press, Cambridge, England, 1997.

[2] E. Stambulchik and Y. Maron. Plasma line broadening and computer simulations: A mini-review. *High Energy Density Phys.*, 6(1):9–14, 2010.

[3] E. Stambulchik and Y. Maron. Effects of density distribution on the Stark width and shift of spectral lines in plasma. *J. Quant. Spectrosc. Radiat. Transfer*, 315:108889, March 2024.

[4] K. W. Hill, L. Gao, B. F. Kraus, M. Bitter, P. C. Efthimion, N. Pablant, M. B. Schneider, D. B. Thorn, H. Chen, R. L. Kauffman, D. A. Liedahl, M. J. MacDonald, A. G. MacPhee, H. A. Scott, S. Stoupin, R. Doron, E. Stambulchik, Y. Maron, and B. Lahmann. Study of Stark broadening of krypton helium-$\beta$ lines and estimation of electron density and temperature in NIF compressed capsules. *Plasma Phys. Controlled Fusion*, 64(10):105025, September 2022.

# I-10

## Using deep learning to develop a fast, versatile NLTE spectral model for application to HED systems

**Marc-Andre Schaeuble**, Will Lewis, Stephanie Hansen, and Taisuke Nagayama

Sandia National Laboratories, P.O. Box 5800, Albuquerque, NM 87185, USA

Non-local thermodynamic equilibrium (NLTE) effects significantly influence radiation transport and atomic level populations of high energy density (HED) plasmas. Under optically thin conditions, NLTE effects lead to a deviation of atomic populations from their equilibrium values, which can significantly change plasma emissivities and opacities. Simulations and experimental analyses of HED systems must therefore accurately and efficiently account for these effects. Calculating the needed NLTE data requires substantial computational resources, leading simulations to utilize simplified, low-resolution NLTE spectra and experimental analyses to assume simple plasma structures. Deep learning (DL) has been used to develop efficient and accurate NLTE spectral models, but each is limited to a specific problem [1-3]. Using the published models as inspiration, we outline in this talk, our approach to developing a versatile DL NLTE spectral model that can predict optically thin spectra from 0.01 – 10 keV in electron temperature and $10^{19}$ – $10^{22}$ $cm^{-3}$ in ion density, a 4x/7x increase in each parameter over the largest published model [1]. Multiple DL models, each of which captures a charge state, are needed to achieve the desired accuracy over the entire parameter space. The resulting DL model predicts an optically thin, high-resolution (20x higher than other work) NLTE spectrum in ~160 ms with 99.5% accuracy, making it ~$10^5$ times faster than its source model, the NLTE code SCRAM. Our approach works equally well for Ar and Kr spectra, demonstrating the robustness of our approach (see Fig. 1). We also discuss our progress for including arbitrary radiation fields in our existing model. If successful, the model with arbitrary radiation fields could address many existing NLTE challenges encountered in HED physics simulations and analyses.

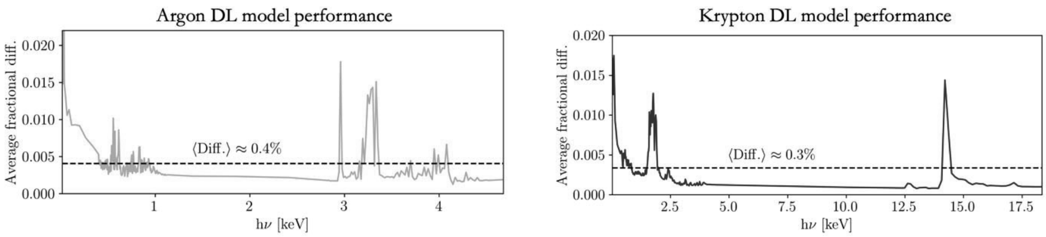


Figure 1: **Left** – Photon energy (hν) resolved average difference between DL model and independent validation set for Ar. **Right** – same as left, but for Kr. Model architecture is consistent for both elements, and performance surpasses expectations for each case.

References

[1] Kluth, G. et al., Phys. Of Plasmas, 27, 052707 (2020)
[2] Mariscal, D. A. et al., Phys. Of Plasmas, 29, 093901 (2022)
[3] Vander Wal, M. D. et al., IEEE Trans. on Plasma Science, 51, 1 (2023)

Sandia is managed and operated by NTESS under DOE NNSA contract DE-NA0003525.

# Direct measurement of ion temperature and electron-ion equilibration in warm dense matter

**Bob Nagler**

SLAC National Accelerator Laboratory, 2575 Sand Hill Road, Menlo Park, CA 94025, USA

To understand or model the behavior of a dense plasma or Warm Dense Matter, accurate knowledge of the temperature is crucial. Nevertheless, such measurements remain elusive. While some methods exist to determine the electron temperature, directly measuring the ion temperature in rapidly evolving (and potentially out-of-thermal-equilibrium) samples has eluded scientists. In this presentation, we will introduce a method to directly and model-independently measure the ion temperature of a gold sample with temperatures up to a few eV. Using a high-resolution ( 50 meV) x-ray scattering platform developed at the LCLS x-ray free-electron laser, we can measure the width of a quasi-elastic Rayleigh peak. In the back-scattering geometry, the width of this peak directly reveals the velocity distribution of the ions and their corresponding temperature, due to the Doppler shift of the scattered photons. We use this diagnostic to track the ion temperature evolution in thin gold samples after irradiation by a short-pulse laser. In this way, we unambiguously determine the electron-ion relaxation dynamics in Warm Dense Gold. Furthermore, in combination with x-ray diffraction, we can determine the Debye temperature when the heated gold remains crystalline, resolving a decades-old controversy regarding changes in bond strength in laser-excited gold.

I-12

# Ionization dynamics and electronic structure of x-ray heated plasmas

**Oliver Humphries**[1], Calum Prestwood[1,2], Thomas Preston[1], Hae Ja Lee[3], Bob Nagler[3], Sam Vinko[4], Mikhail Mishchenko[1], Ulf Zastrau[1], Michal Šmíd[5]

[1]European XFEL, D-22869 Schenefeld, Germany
[2]School of Mathematics and Physics, Queen's University Belfast, Belfast BT71NN, UK
[3]SLAC National Accelerator Laboratory, Menlo Park, CA 94025, USA
[4]Department of Physics, University of Oxford, Oxford OX1 3PU, UK
[5]Helmholtz-Zentrum Dresden-Rossendorf, D-01328 Dresden, Germany

I will present on recent experiments at the European XFEL, using the intense x-ray pulse to isochorically heat 3d metals to 100's of eV [1]. Details of the volumetric heating process of the nanofocused XFEL will be discussed, and the ways in which these prototypical systems can inform laser-driven experiments to benchmark models in well-defined conditions. The resulting x-ray emission and inelastic x-ray scattering – as well as resonant variants – of these plasmas will be detailed, along with the information we can extract on the electronic structure and rates.

Through a combination of experimental diagnostics, I will present a picture of how we are able to use the XFEL to diagnose L- and M-shell collisional rates in hot dense systems, and the time evolving ionization balance. A comparison will be made to resonant spectroscopy data using a high-intensity laser driver in conjunction with the XFEL on Cu foil targets, elucidating the difficult-to-model range of spatiotemporal scales needed for even ultra-short optical laser interaction, and how x-ray-only experiments have informed its analysis.

References

[1] M. Šmíd *et al.* arXiv preprint arXiv:2406.06233 (2024)
[2] O. S. Humphries *et al.* Physical Review Letters 125.19 (2020): 195001
[3] T. Gawne *et al.* Physical Review E 108.3 (2023): 035210.

**I-13**

# Cold atmospheric pressure plasma-treated liquids and formulations for cancer treatment

**Camelia Miron**[1], Luminita Marin[2], Taishi Yamakawa[1], Ryo Wakatsukasa[1], Koki Ono[1], Kotaro Sato[3], Shinya Toyokuni[1,4], Masaru Hori[1], Hiromasa Tanaka[1]

[1]Center for Low-temperature Plasma Sciences, Nagoya University, Furo-cho, Chikusa-ku, Nagoya 464-8601, Japan.

[2]Institute of Macromolecular Chemistry “Petru Poni”, Aleea Grigore Ghica Voda 41A, Iasi 700487, Romania

[3] Department of Oral and Maxillofacial Surgery, Nagoya University Graduate School of Medicine 65 Tsurumai-cho, Showa-ku, Nagoya, 466-8550, Japan.

[4]Department of Pathology and Biological Responses, Nagoya University, Graduate School of Medicine, 65 Tsurumai-cho, Showa-ku, Nagoya 466-8550, Japan.

Cold atmospheric pressure plasma is a partially ionized gas that has unveiled its considerable potential for cancer treatment as a new type of oncological therapy [1, 2]. The discharges are usually generated above the liquid surface, in a mixture of argon, nitrogen, and oxygen gases that facilitate the plasma generation and dictate the type of predominant reactive species that influence the effect of these irradiated liquids on normal and cancer cells [2]. It was observed that not only the gas mixture used in the discharge responsible for the selective cytotoxic effect on cancer cells, but also the chemical structure of the liquid precursor. Chitooligosaccharides, tricarballylic acid, ethyl acetate, glyceric acid, and their mixture generated in plasma in certain concentrations showed a selective cytotoxic effect on cancer cells [2]. The selectivity was not induced by only one chemical compound but by a mixture of several chemicals generated in low amounts, which act synergistically.

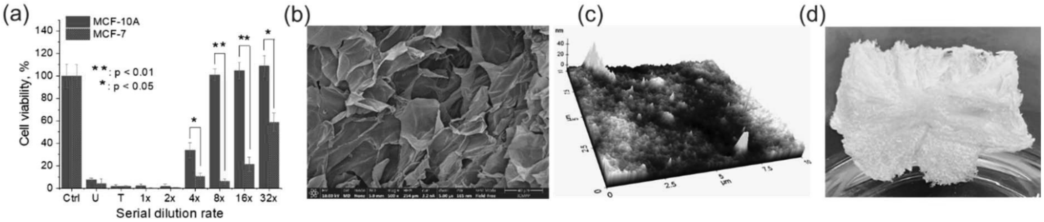


Figure 1. (a) Cell viability tests of MCF-10A (non-tumorigenic epithelial cell) and MCF-7 (breast cancer cell) lines after incubation in untreated chitosan 0.5% (U) and plasma-activated chitosan (T) solution. (b) and (c) SEM and AFM of plasma-activated chitosan-based hydrogel, respectively. (d) Photo of xerogel obtained from plasma-activated chitosan reticulated with natural mono-aldehyde.

Therefore, the plasma-activated liquids provide a foundation for clinical applications of combinatorial chemistry to enhance selectivity during therapy, offering patients a more effective and less harmful option. This also paves the way for engineering liquids by plasma for drug delivery systems, such as plasma-activated-based hydrogels, to preserve and improve bioavailability, and serve as a platform to deliver the plasma-activated liquid content to cells.

**[1]** H. Tanaka, M.. Mizuno, K. Ishikawa, C. Miron, Y. Okazaki, S. Toyokuni, K. Nakamura, H. Kajiyama, M. Hori, Free Radical Research **57** (2023) 14-20.

**[2]** C. Miron, B. Andreica, M. Iftime, A. Fifere, T. Yamakawa, S. Toyokuni, M. Mizuno, L. Mititelu-Tartau, Y. Motooka, A. Bejan, T. Kondo, I. Sava, V. Harabagiu, J. Kumagai, A. Tanaka, H. Tanaka, L. Marin, M. Hori, International Journal of Biological Macromolecules, **281,** 136513 (2024) 1-16.

# I-14

## On the line shape of sputtered atoms in low-temperature magnetized plasmas

**Marc Sackers**, Oleksandr Marchuk, Sebastijan Brezinsek*, Arkadi Kreter

Forschungszentrum Jülich GmbH, Institute of Fusion Energy & Nuclear Waste Management - Plasma Physics
(*) HHU Düsseldorf, Faculty of Mathematics and Natural Sciences

The erosion of plasma-facing components in magnetically confined fusion limits the operating scenarios of the reactors. In particular, high-Z elements, such as the first wall and divertor material of tungsten in ITER, create excessive radiative cooling of the plasma. Therefore, it is essential to measure and simulate the tungsten influx. The latter depends to a great extent on our knowledge of the plasma-wall interaction (PWI).

In this case, some uncertainty lies in the near-threshold regime of physical sputtering by the seeding gas impurities and diagnostic gases, e.g. that is the sputtering yield of tungsten and the distribution function of tungsten atoms which define the boundary condition for kinetic plasma models. Linear plasma devices, such as PSI-2, cover this regime and enable erosion studies under well-definable conditions. The approach for evaluating the PWI in this contribution is to analyze the line shape of optical transitions by sputtered atoms.

More precisely, the physics of interest, which is the velocity and angular distribution function (VDF, ADF), is contained within the Doppler broadening of the tungsten spectral lines. The accurate interpretation of these line-of-sight integrated signals requires accounting for the geometry of the source and plasma. The other relevant line shape perturbing mechanisms (light reflection, hyperfine structure splitting or the Zeeman effect) are presented as well. Particularly interesting is that the external magnetic field at PSI-2 of 90 mT creates conditions, where the perturbing Hamiltonian with hyperfine and Zeeman terms must be evaluated.

Resolving the details of the hyperfine-Zeeman mixing ($\sim$ 2 GHz) is impossible using the emission spectra of tungsten measured at PSI-2 due to the similar size of the instrumental broadening ($\sim$ 3 GHz) and (unknown) Doppler broadening ($\sim$ 4 GHz). Benchmarking experiments using laser absorption from xenon effectively circumvents these issues: the instrumental broadening is negligible and the Doppler broadening is well-known (Maxwellian, 0.8 GHz).

This contribution presents new experimental data on the near-threshold erosion of tungsten by argon ions obtained at the linear plasma device PSI-2. The data illustrates the difference in line shape due the surface structure – e.g. the crystall orientation exposed to plasma, strongly reformed surfaces. The modeling reveals reasonable agreement with the angular distribution estimated using molecular dynamics simulations. As a result, line shape emission spectroscopy is suitable for operando measurements monitoring the surface structure of plasma-facing components during plasma operation.

**I-15**

# M-shell Rebinding in Hot, Solid-density Mg and Al


**Thomas Gawne**

Center for Advanced Systems Understanding (CASUS), D-02826 Görlitz, Germany
Helmholtz-Zentrum Dresden-Rossendorf (HZDR), D-01328 Dresden, Germany


Ionization potential depression (IPD) plays an important role in the modelling of high energy density (HED) systems. Constructed using the chemical model, IPD models aim to accurately treat the complex many-body effect of continuum lowering (CL) in a computationally efficient way. However, a number of experiments [1-4] have now demonstrated that commonly-used IPD models do not treat CL sufficient accurately in HED conditions. This has spurred further investigations into the nature of CL, and resulted in the development of new IPD models.

Benchmarking IPD models is challenging due to the difficulties in directly measuring CL in experiments, meaning there is limited data to compare against. Therefore, the direct measurements of CL in numerous materials by Ciricosta *et al.* [3] has proved invaluable. There, the IPD values for the different charge states of solid-density Mg and Al were extracted by observing the onset of Kα emission when changing the photon energy of the incident XFEL. However, a key conclusion from these IPD values is that the Mg and Al M-shells never rebind to the ions, even at high charge states. This conclusion was in part drawn from the lack of direct observation of Kβ emission from these materials, but it could not be discounted that they were simply too weak to observe.

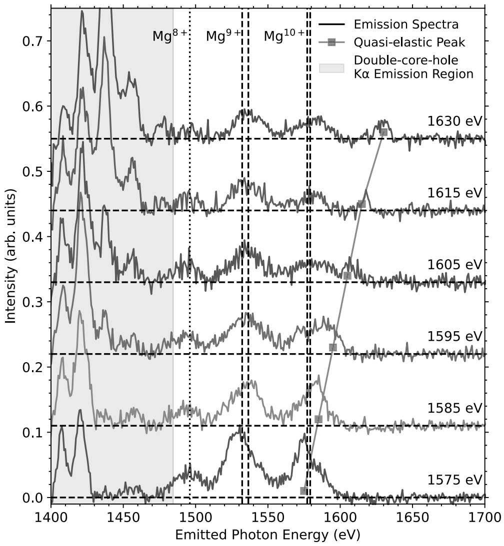


**Fig. 1**: Emission spectra [4] for different incident photon energies (labelled right) from solid-density Mg, showing Kβ emission from the Mg$^{8+}$ to Mg$^{10+}$ ions. Vertical lines indicate equivalent emission energies from isolated Mg ions from [6] (dashed) and [7] (dotted).

In this presentation, we discuss more recent experimental and theoretical investigations into the M-shell rebinding behaviour of highly-charged Mg. The key result is that Kβ emission has recently been directly observed in solid-density highly-ionized Mg [4] (see Fig. 1), indicating the M-shell can in fact rebind to the Mg ions. These findings are further supported by recent measurements of the Mg Heα lineshape [5], and finite-temperature density functional theory calculations [4]. Overall, these investigations strongly support that the IPD in the experiments lies somewhere between the Stewart-Pyatt and modified Ecker-Kröll models, and lower than inferred by [3]. Due to the similarities in the predicted ionization and localization behaviours of Mg and Al, we expect similar conclusions should be true for Al. Finally, we discuss the relevance of these results for the development of new IPD models.


References
[1] O. Ciricosta, S. M. Vinko, H.-K. Chung, *et al.*, Phys. Rev. Lett **109**, 065002 (2012)
[2] D. J. Hoarty, P. Allan, S. F. James, *et al.*, Phys. Rev. Lett **110**, 265003 (2013)
[3] O. Ciricosta, S. M. Vinko, B. Barbel, *et al.*, Nat. Comm. **7**, 11713 (2016)
[4] T. Gawne, T. Campbell, A. Forte, *et al.*, Phys. Rev. E **108**, 035210 (2023)
[5] G. Pérez-Callejo, T. Gawne, T. R. Preston, *et al.*, Phys. Rev. E **109**, 045204 (2024)
[6] NIST Atomic Spectra Database (ver. 5.12) [Online]. Available: https://physics.nist.gov/asd
[7] AAEXCITE [Online]. Available: https://www-amdis.iaea.org/AAEXCITE/

**I-16**

# Experimental Plasma Spectroscopy: meeting data needs for astrophysics

**Maria Teresa Belmonte***, Pratyush Ranjan Sen Sarma, Santiago Mar

University of Valladolid, Department of Theoretical and Atomic Physics and Optics,
Paseo de Belén 7, 47011 Valladolid (Spain)
(*) mariateresa.belmonte@uva.es

The vast majority of the information we have about astronomical objects comes from analysing the radiation they emit. In this context, plasma spectroscopy becomes an extraordinarily powerful tool, allowing us to decipher the physical and chemical properties of stars, nebulae and galaxies from their spectra. The widths and shifts of the spectral lines tell us about the electron densities and temperatures of the plasmas in which the radiation was produced, and the speeds at which they were moving. However, this decoding depends critically on the availability of accurate atomic parameters such as wavelengths, transition probabilities, Stark parameters, and hyperfine and isotope structure constants for many different neutral and ionised species.

These data are not only fundamental to astrophysics, but also play a key role in applications ranging from the lighting industry to plasma diagnostics in fusion research and benchmarking of theoretical and semi-empirical atomic calculations. Despite very impressive technological improvements in telescopes and spectrographs, studies of chemical composition are still held back by the lack of quantity and quality of the atomic data available. Thousands of transitions across the periodic table remain poorly characterised, highlighting the urgent need for sustained experimental efforts.

At the Atomic Spectroscopy Laboratory of the University of Valladolid (Spain) we have more than 40 years of experience in the measurement of accurate atomic parameters. Our current focus is on the measurement of rare earth parameters [1], which are urgently needed by astronomers for the study of kilonovae emitted by neutron star mergers [2]. We also put a lot of effort into determining the uncertainties of our newly measured data, which is essential to provide data users with a guide and a way to obtain the uncertainties of their own measurements and calculations. We have produced new open-source code for the determination of transition probability uncertainties from fitted spectra for plasmas that satisfy the assumption of partial local thermodynamic equilibrium [3].

The primary goal of this talk is to bridge the gap between experimental plasma spectroscopy laboratories and the users of atomic data. I will present the capabilities of our laboratory and discuss the challenges we face in measuring atomic data. I will also provide examples from our previous work on noble gases and our current research on rare earth elements. By promoting a better understanding of how these data are produced, we hope to strengthen the collaboration between the producers and users of atomic data, and help to fill this critical gap in the data.

**Acknowledgements:** M. T. Belmonte thanks the Ministerio de Ciencia, Innovación y Universidades of the Spanish Government for her Beatriz Galindo Fellowship and acknowledges funding from MICIU/AEI /10.130 39/501100011033 and by FEDER (UE) under project PID2021- 127786NA-100 P. R. Sen Sarma thanks the University of Valladolid for his Ph.D. grant.

References

[1] P. R. Sen Sarma, M. T. Belmonte, S. Mar, Eur. Phys. J. D 78:76 (2024)
[2] D. Kasen, B. Metzger, J. Barnes *et al.*, Nature, **551**, 80-84 (2017)
[3] M. T. Belmonte, S. Mar, S. Djurović *et al.*, Spectrochim. Acta B. **229**, 107190 (2025)

I-17

# High-Resolution X-Ray Spectroscopy of Astrophysical Plasmas with XRISM

**Hiroya Yamaguchi**, on behalf of XRISM Collaboration

*Institute of Space and Astronautical Science (ISAS), JAXA, Kanagawa, Japan*

The X-Ray Imaging and Spectroscopic Mission (XRISM)[1], developed by JAXA and NASA with ESA's participation, has been operating in orbit since September 2023. The X-ray microcalorimeter "Resolve" on board XRISM achieved an energy resolution of ~4.5 eV (FWHM) in the 2-10 keV band, providing us new insights into astrophysical plasmas in different spatial scales, including galaxy clusters[2], active galactic nuclei[3], supernova remnants[4], and X-ray binaries[5]. For instance, the Resolve successfully measured the bulk velocity of the hot intracluster medium in the Centaurus Cluster with an accuracy of 10-50 km $s^{-1}$ using the well-resolved K-shell emission lines of He-like and H-like Fe, revealing the evidence of past cluster mergers[2]. From the X-ray binary Cyg X-3, the Resolve detected both emission and absorption features of Fe ions in various charge states (Fig.1), allowing us to constrain the velocity and density profiles of the plasma surrounding the binary system and even the mass of the compact object[5]. In this talk, I will review some initial results from XRISM and describe successes and challenges in modelling of high-resolution spectra based on our current knowledge of atomic processes.

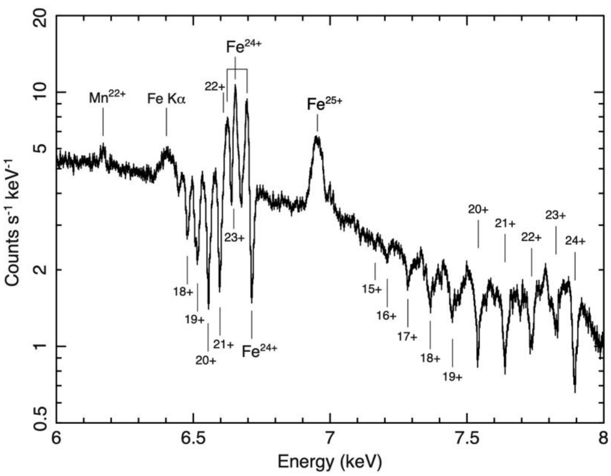


Figure 1: The Resolve spectrum of the X-ray binary Cygnus X-3 in the 6-8 keV band

References

[1] M. Tashiro et al., PASJ, in press. (2025) DOI: 10.1093/pasj/psaf023
[2] XRISM Collaboration, Nature, **638**, 365 (2025)
[3] XRISM Collaboration, ApJL, **973**, L25 (2024)
[4] XRISM Collaboration, PASJ, **76**, 1186 (2024)
[5] XRISM Collaboration, ApJL, **977**, L34 (2024)

# Exploring the Sun with Ultraviolet SpectroPolarimetry: The CLASP Sounding Rocket Series

**R. Ishikawa[1]**, R. Kano[1], A. Winebarger[2], D. McKenzie[2], J. Trujillo Bueno[3], Frédéric Auchère[4], N. Narukage[1], D. Song[5,1], T. J. Okamoto[1], L. Rachmeler[6], CLASP team

1: National Astronomical Observatory of Japan, Tokyo 181-8588, Japan
2: NASA Marshall Space Flight Center, Huntsville, AL 35812, USA
3 : Instituto de Astrofísica de Canarias, E-38205 La Laguna, Tenerife, Spain
4 : Institut d'Astrophysique Spatiale, F-91405 Orsay Cedex, France
5: Korea Astronomy and Space Science Institute, Daejeon 305-348, Republic of Korea
6: National Oceanic and Atmospheric Administration, National Centers for Environmental Information, Boulder, CO 80305, USA

The magnetic field in the solar atmosphere plays a crucial role in the transfer of energy from the relatively cool (6,000 K) visible surface of the photosphere to the overlying hot (>$10^6$ K) corona. The $\beta$=1 layer, where the ratio of gas pressure to magnetic pressure equals unity, is located in the chromosphere, a critical region situated between the photosphere and the corona. Above this layer (i.e., in the upper chromosphere), the magnetic field dominates the structuring and dynamics of the plasma. Therefore, measuring the magnetic field in this region is essential for understanding solar activity in both the chromosphere and the corona. To achieve this, we must measure and model the polarization of ultraviolet (UV) spectral lines that originate in the upper chromosphere, as they encode valuable information about the magnetic fields [1].

To demonstrate the capability of UV spectro-polarimetry, a series of sounding rocket experiments CLASP were conducted in 2015 (CLASP), 2019 (CLASP2), and 2021 (CLASP2.1). In the first flight, the mission successfully performed spectropolarimetric observations of the hydrogen Lyman-$\alpha$ line (121.57 nm) and the Si III resonance line (120.6 nm), achieving very high polarization sensitivity [2]. For the first time, CLASP detected linear polarization produced by the scattering of anisotropic radiation in VUV lines and observed polarization signals indicative of the Hanle effect in the upper solar chromosphere. In the second and third flights, following an upgrade of the CLASP instrument, we carried out spectropolarimetric observations across the Mg II h & k lines, which are also strong UV spectral lines of great interest for probing the magnetic fields in the upper chromosphere. These missions yielded unprecedented measurements of polarization signals caused by the joint action of scattering processes and the Hanle, Zeeman and Magneto-Optical effects. Furthermore, through coordinated observations with the Solar Optical Telescope (SOT) aboard the Hinode satellite, we produced magnetic field maps extending from the photosphere to the upper chromosphere in an active region [3]. In this talk, we summarize the scientific findings from the series of CLASP experiments.

References

[1] Trujillo Bueno, Landi Degl'Innocenti, Belluzzi, Space Sci. Rev. **210**, 183 (2017)
[2] Kano, Trujillo Bueno, Winebarger, et al., The Astrophysical Journal Letters, **839**, L10 (2017)
[3] Ishikawa, Trujillo Bueno, del Pino Alemán, et al., Science Advances, **7**, 8 (2021)

# I-19

## Testing High Density XSTAR Models with Fe Photoionized Plasma Experiments on the Z Machine

**Patricia Cho**[1], Guillaume Loisel[2], Jim Bailey[2], Dan Mayes[3], Isaac Huegel[4], Taisuke Nagayama[2], Chris Fontes[5], Tim Kallman[6], Javier Garcia[6], Roberto Mancini[7], Stephanie Hansen[2]

[1]Lawrence Livermore National Laboratory, Livermore, CA, USA
[2]Sandia National Laboratories, Albuquerque, NM, USA
[3] University of Texas at Austin, Austin, TX, USA
[4] University of Michigan, Ann Arbor,Michigan, USA
[5]Los Alamos National Laboratories, Los Alamos, NM, USA
[6]NASA Goddard Space Flight Center, Greenbelt, MD, USA
[7] University of Nevada Reno, Reno, NV, USA

The Z-machine at Sandia National Laboratories generates powerful X-ray radiation fluxes. This enables experiments to produce and study macroscopic quantities of matter at extreme conditions. Astronomers use spectra collected with satellite telescopes to construct models for the behavior of accretion powered plasmas around black holes in both active galactic nuclei and X-ray binaries. However, complex models for these radiation dominated non-Local-Thermodynamic-Equilibrium (NLTE) photoionized plasmas are mostly untested with laboratory data. A novel platform developed on the Z-machine for expanding-foil photoionized plasma experiments opens a new regime for benchmark measurements of NLTE photoionized plasmas. The data from these experiments reveal difficulties in modeling both emission intensities and the level of ionization in the plasma. Such data have been a laboratory astrophysics goal for two decades but are even more critical now because of the "Super-Solar" iron abundance problem. Iron abundances inferred from X-ray spectra emitted by photoionized plasma in many accretion disks around black holes appear to contain 5-20 times more iron than the Sun. This contradicts the widely held expectation that most objects in the universe have metallicities that are at most, only slightly larger than Solar. One prevailing theory is that effects of high electron density are not properly accounted for in the models. Reinterpreting astrophysical X-ray spectra with updated high density models resolved some of the discrepancy. However, much of the discrepancy remains along with a key question: do spectral models of photoionized plasmas accurately account for X-ray emission? I will describe my progress in using this dataset to inform the Super-Solar iron abundance problem and discuss the broader potential to evaluate the accuracy of model calculations.

This work was performed under the U.S. Department of Energy LRGF Contract No. DE-NA0003960, WCAPP Contract Nos. DE-NA0003843 & DE-NA0004149, Sandia Contract No. DENA0003525, LANL contract 89233218CNA000001, and LLNL Contract No. DE-AC52-07NA27344.

References
[1] García et al., Mon. Not. R. Astron. Soc. **462**, 751 (2016).
[2] Heeter, et al., Review of Scientific Instruments **72**, 1224 (2001).
[3] Jiang et al Mon. Not. R. Astron. Soc. **484**, 1972 (2019).
[4] Loisel et al., Phys. Rev. Lett. **119**, 075001 (2017).

# I-20

## Large scale computation of atomic data in heavy elements for kilonova modeling

**J. Deprince***

Atomic Physics and Astrophysics, University of Mons, Belgium
(*) Jerome.Deprince@umons.ac.be

The production of elements heavier than iron in the Universe still remains an unsolved mystery. About half of them are thought to be produced by the astrophysical r-process (rapid neutron-capture process) [1], for which one of the most promising production sites are neutron star mergers (NSMs) [2]. In August 2017, gravitational waves produced by a NSM were detected for the first time by the LIGO detectors (event GW170817) [3], and the observation of its electromagnetic counterpart, the kilonova (KN) AT2017gfo, suggested the presence of heavy elements in the KN ejecta [4]. The luminosity and spectra of such KN emission depend significantly on the ejecta opacity, which is thought to be dominated by millions of lines from the heavy elements produced by r-process, in particular f-shell elements, *i.e.* lanthanides and actinides [5]. Atomic data and opacities for these elements are thus sorely needed to model and interpret KN light curves and spectra.

In this context, the present work consists in a large-scale computation of atomic data and opacities for all heavy elements with $Z \geq 20$, with a special effort on lanthanides and actinides, and for a grid of typical KN ejecta conditions (temperature and density) between one day and one week after the merger (corresponding to the photospheric phase of the KN ejecta, for which the local thermodynamical equilibrium -LTE- is thought to be valid). In order to do so, we used the pseudo-relativistic Hartree-Fock (HFR) method as implemented in the Cowan's codes [6], in which the choice of the configuration interaction model is of crucial importance [7].

In this talk, our HFR atomic data and opacities for all heavy elements will be presented (with a special focus on lanthanides and actinides), as well as some comparisons with previous works. Besides, we will also discuss the contribution of each element to the total KN ejecta opacity for several NSM models [8] based on their Planck mean opacities and elemental abundances deduced from NSM simulations. The impact of considering such atomic-physics based opacity data instead of typical approximation formulae [5] for the determination of the total KN ejecta opacity will also be discussed. This work is presented in our recently-accepted paper [9]. A dedicated database with all the atomic data and opacities that we computed in this work has been created and is available online [10].

References

[1] J.J. Cowan, C. Sneden, J.E. Lawler *et al.*, Reviews of Modern Physics **93**, 015002 (2021)
[2] B.D. Metzger, G. Martinez-Pinedo, S. Darbha *et al.*, MNRAS **406**, 2650 (2010)
[3] B.P. Abbott, R. Abbott, T.D. Abbott *et al.*, Phys. Rev. Lett. **119**, 161101 (2017)
[4] D. Kasen, B. Metzger, J. Barnes *et al.*, Nature **551**, 80 (2017)
[5] O. Just, I. Kullmann, S. Goriely *et al.*, MNRAS **510,** 2820 (2022)
[6] R.D. Cowan, The Theory of Atomic Structure and Spectra, California University Press, Berkeley (1981)
[7] A. Flörs, R.F. Silva, J. Deprince *et al.*, MNRAS **524**(2), 3083 (2023)
[8] O. Just, V. Vijayan, Z. Xiong *et al.*, ApJL **951**, L12 (2023)
[9] J. Deprince, G. Wagle, S. Ben Nasr *et al.*, A&A **696**, A32 (2025)
[10] J. Deprince, G. Wagle, S. Ben Nasr *et al.*, https://zenodo.org/records/14017952 (2024)

# MEMORIAL TALKS

**M-01**

# Approaching complexity for atomic data and models

**M G O'Mullane**, C Y Zhang, N Ferguson

Department of Physics, University of Strathclyde, Glasgow, UK

The majority of atomic data needed to explain the emission from, and the evolution of, plasmas is calculated rather than measured in dedicated experiments. The difficulties of performing high precision measurements of atomic quantities, apart from wavelengths, complicates any validation since models of both the atomic system and its environment are intertwined. The complexity increases for ions with configurations involving open *d* and *f* shells. Emission from complex ions have rich spectra but there are sparse validated collision data to fully predict the intensity of their emission features. Such plasmas are not rare and are found in many different scientific and technical environments. Examples are the first few ionized ions of heavy elements seen in kilonovae (La, Ce, Nd, Te etc.); xenon and tin emission used in nanolithography; tungsten emission in fusion plasmas; the effect of iron opacity on stellar models.

AUTOSTRUCTURE [1] is a general purpose code to calculate free-bound electron and photon collision processes. Its atomic structure is based on kappa-averaged relativistic wavefunctions and it has been extended to implement a Breit-Pauli distorted wave approach for electron-impact excitation of atomic ions. The code is optimized for speed and, apart from ionization which is in development, can calculate a self-consistent set of structure and collision data needed for modelling complex emission features. Notable strengths of the code to address complexity are its handling of very many configurations, Rydberg series, per-orbital adjustments of the central potential and means to adjust which configurations are included in the internal minimization algorithm.

We illustrate strategies for optimizing the atomic structure of lowly ionized heavy species when there are observed measurements (Fe VII, La V) and ways to extend these adjustments to cases with no experimental confrontation. There are two principal approaches to uncertainty quantification with AUTOSTRUCTURE. The choice of configurations is key and algorithmic methods are described to optimize the set. Secondly, varying the scaling factors within an envelope that gives results consistent with an experimental metric (structure or emission feature) is applied. This variation is controlled by an external framework and the fast AUTOSTRUCTURE code, with good initial results from its default settings, enables a number of different methods, via classical or Bayesian sampling. The resulting spread in the coefficients of dielectronic and radiative recombination, photoionization and excitation can be considered as a robust *atomic code* error bar.

This talk is also a memorial to Nigel Badnell who passed away for too soon in September 2024. We will continue his legacy by applying AUTOSTRUCTURE to existing and new areas and shall continue to develop the code and make it accessible to a wider audience [2].

References

[1] N. R. Badnell, Computer Physics Communications, **182**, 1528 (2011)
[2] https://git.adas.ac.uk/autostructure

## M-02

# Howard Scott: The scientist, the colleague, the mentor

**John Sheil**[1,2]

[1]Advanced Research Center for Nanolithography, Science Park 106, 1098 XG Amsterdam, The Netherlands
[2]Department of Physics and Astronomy, and LaserLab, Vrije Universiteit Amsterdam, De Boelelaan 1081, 1081 HV Amsterdam, The Netherlands

Howard Allen Scott (1954 – 2024) was a colleague, friend, and mentor to many of us in the APIP community. In this talk, I will give an overview of some of Howard's outstanding work in collisional-radiative modelling [1-3], plasma spectroscopy [4], and EUV source modelling [5]. Howard's knowledge and expertise were simultaneously broad and deep, a unique combination that benefitted a whole generation of scientists working in the field of atomic-plasma processes. This, combined with Howard's kind and genial manner, made interactions with him truly memorable. I had the honour and privilege to work closely with Howard over the past few years, most notably on the establishment of an EUV source code comparison activity [6]. I will detail the joy of working with Howard, as well as the many physics (and non-physics) insights he imparted to me.

References

[1] H. A. Scott, J. Quant. Spectrosc. Rad. Transf. **71**, 689 (2001)
[2] H. A. Scott and S. B. Hansen, High Energy Density Phys. **6**, 39 (2010)
[3] H. A. Scott *et al.* Phys. Plasmas **29**, 082703 (2019)
[4] B. A. Hammel *et al.* Phys. Plasmas **18**, 056310 (2011)
[5] H. A. Scott, S. Langer, and Y. Frank Radiation-Hydrodynamics Modeling of LPP EUV Sources In *Photon Sources for Lithography and Metrology*; Bakshi, V., Ed.; SPIE Press: Washington, DC, USA, 2023; pp. 71–110.
[6] J. Sheil, O. Versolato, V. Bakshi, H. Scott Atoms **11**, 130 (2023)

# ORAL TALKS

O-01

# Simulating the Low Charge State Emissions from Tungsten for Fusion Applications

[1]**Ritu Dey**, [1]Reetesh kumar Gangwar, [2]Deepti Sharma, [2,3]Bharat Hegde, [4]Rajesh Srivastava, [5]Mizanur Rahman, [5]M. Kakati, [2,3]Joydeep Ghosh

[1]Department of Physics, Indian Institute of Technology Tirupati, Yerpedu, India,
[2]Institute for Plasma Research, Gandhinagar 382428, Gujarat, India,
[3]Homi Bhaba National Institute, Training School Complex, Anushakti Nagar, Mumbai 400094, India,
[4]Department of Physics, Indian Institute of Technology Roorkee, Roorkee, India
[5]CIMPLE-PSI Laboratory, Centre of Plasma Physics-Institute for Plasma Research (CPP-IPR), Sonapur, Assam, India

Tungsten (W) is one of the most suitable and widely utilised materials for plasma-facing components in present day tokamaks and future fusion reactors including ITER, primarily due to its exceptional thermophysical properties. Due to its higher atomic number, Z, it enhances the radiative losses when it enters the plasma and hence its radiative emission characteristics from the tokamak plasma require to be precisely known to optimized tokamak-based reactor operations. However, the atomic database for spectral emissions from different tungsten charge-states is limited. Therefore, generating atomic data such, as, energy levels, oscillator strengths, electron-impact cross-section etc. of different line spectral emission from different tungsten charge states along with their experimental validation is one of the frontline research topics in fusion community.
The atomic structure calculations for spectral lines of W, W neutral at 368.2 nm ($5d^4 6s^2$-$5d^4 6s(^6D)6p$) and 365.4 nm ($5d^4 6s^2$-$5d^4 6s(^6D)6p$) are carried out through Flexible atomic code (FAC) [1]. These spectral lines are observed in CIMPLE-PSI device where a tungsten target is irradiated with plasma. The electron impact excitation cross sections for these transitions of neutral and ionized tungsten are calculated. Both of the transitions show a similar trend of decreasing with the incident electron energy, however, the cross-section for the transition line 368.2 nm ($5d^4 6s^2$-$5d^4 6s(^6D)6p$) is higher than the other one. Along with the above, calculations for spectral line W+ at 373.6 nm are done. These calculated electron-impact cross-sections are then used to obtain excitation reaction rate coefficients. Using the calculated rate-coefficients, the emitted photons per unit volume per second, i.e. emissivity of these transitions are estimated through collisional radiative model. The simulated line spectra of these transitions are then compared to the measured emission spectra of W in CIMPLE-PSI device for validating the calculations. The model calculations along with experimental validation will be presented in this paper.

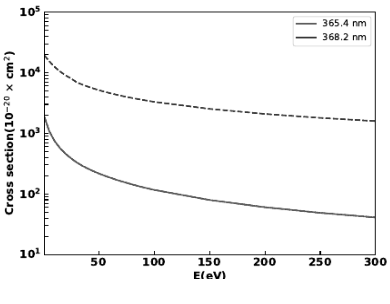


**Fig1.** Simulated electron impact excitation criss-section for neutral W.

References

[1] Ming Feng Gu, Can. J. Phys. **86** 675 (2008).
[2] Trinayan Sarmah et al, Journal of Alloys and Compounds **725,** 606 (2025).

**O-02**

# Hydrogen Stark broadening revisited for magnetic fusion plasma diagnostics

**I. Hannachi**[1], A. Calisti[2], M. Goto[3], J. Rosato[2], Y. Marandet[2] and R. Stamm[2]

[1]University of Batna 1, Department of Physics, Batna, Algeria
[2]Aix-Marseille University and CNRS, PIIM, 13397 Marseille, France
[3]National Institute for Fusion Science, Toki, Japan

Stark effect was discovered more than a century ago [1], soon after the introduction by H. Lorentz [2] of a line shape model assuming that the lifetime of the upper level of a radiative transition is shortened by the impact of perturbers and thereby increases the width of the emitted line. Following the Lorentzian model, impact theories of Stark broadening were developed during the $20^{th}$ century and resulted in a standard model for hydrogen lines [3], where an impact approximation is used for electrons, and a quasistatic model for the ions. Such an approach provides a good accuracy for the diagnostic of dense plasmas like those of arcs, but becomes problematic in the case of magnetic fusion plasmas. In most fusion devices, the low density implies that ion dynamics affects the first lines of the main hydrogen series. Several models for retaining ion dynamics have been developed in the last decades [4,5]. In the present work, we use a numerical simulation of the charged particle coupled to a numerical solution of the hydrogen emitter. During the emission time, the atom is submitted to the sum of the electric fields of the charged particles, which all contribute to the decorrelation of the atomic dipole and thereby increase the line width. An interesting feature of this approach is that one can add the simultaneous effect of a collective field created by a plasma instability, or an externally driven radio-frequency field. We here report about the possibility of a spectroscopic diagnostic using Balmer lines in a plasma submitted to a wave generated by runaway electrons at the upper hybrid frequency. We are also interested by a spectroscopic diagnostic of the coupling of radio-frequency waves to the edge plasma. In this framework, we apply our model to the Paschen beta line of hydrogen in the experimental conditions of the spherical tokamak QUEST in Kyushu (Japan), in presence of an electron cyclotron microwave beam produced by a gyrotron at 28 GHz with a power of 250 kW. Additionally, the Paschen beta line of deuterium will be calculated for the conditions in the Heliotron J at Kyoto University, in the presence of a radio frequency wave at 70 GHz with a power of 290 kW.

References

[1] J. Stark, Ann. Physik **43**, 965 (1914)
[2] H. Lorentz, Proc. Amsterdam Acad. Sci. **8**, 591 (1906)
[3] H. Griem, A. Kolb, K. Shen, Phys. Rev. **116**, 4 (1959)
[4] A. Calisti *et al*., Phys. Rev. E **81**, 016406 (2010)
[5] T. A. Gomez *et al*., J. Phys. B : At. Mol. Opt. Phys. **55**, 034002 (2022)

**O-03**

# Dynamic response of atomic processes in recombining helium plasmas to high-density pulse in Magnum-PSI

**Yuki Hayashi**[1]*, Hirohiko Tanaka[2], Shin Kajita[1], Noriyasu Ohno[3], Dogyun Hwangbo[4, 5], Jordy Vernimmen[6], John Scholten[6], Hennie van der Meiden[6], Ivo Classen[6] and Thomas Morgan[6]

[1]Graduate School of Frontier Sciences, The University of Tokyo, Kashiwa 277-8561, Japan
[2]Institute of Materials and Systems for Sustainability, Nagoya University, Nagoya 464-8603, Japan
[3]Graduate School of Engineering, Nagoya University, Nagoya 464-8603, Japan
[4]Institute of Pure and Applied Sciences, University of Tsukuba, Tsukuba 305-8577, Japan
[5]Plasma Research Center, University of Tsukuba, Tsukuba 305-8577, Japan
[6]DIFFER - Dutch Institute for Fundamental Energy Research, Eindhoven 5612 AJ, The Netherlands
*hayashi.yuki@k.u-tokyo.ac.jp

Plasma detachment is crucial for reducing steady-state heat flux to the divertor in fusion reactors. In addition, intermittent high heat flux caused by Edge Localized Modes (ELMs) also reaches the divertor. To support future reactor design, pulsed plasma experiments under ITER-relevant divertor conditions are needed. This study investigates the dynamic response of detached plasmas to pulsed heat flux, with a focus on atomic processes in a high density environment.

The experiments were performed in the Magnum-PSI device. Figure 1 shows a schematic of the experimental setup. The steady-state plasmas were produced by pure He discharges. In parallel, the capacitor bank was used to transiently enahnce discharge power to generate the pulse. The dynamic responses of recombining He plasmas to the pulsed plasma in front of the target plate were observed through time-resolved laser Thomson scattering (TS) and optical emission spectroscopy (OES).

Figures 2(a) and (b) show the transient increase in the electron density, $n_e$, and temperature, $T_e$, by pulsed plasma input. At the same time, figures 2(c) shows the suppression of the He I population density at highly excited level. Before the pulse, when $T_e$ < 1eV, recombination processes dominate, and the observed decay indicates suppression of recombination. Because the plasma pressure exceeds the background pressure by two orders of magnitude, and the charge exchange mean-free-path is shorter than the plasma diameter, He atom penetration was limited during the pulse. Consequently, both the increase in $T_e$ and neutral depletion reduce plasma-neutral interactions, strongly suppressing recombination. Figure 2(d) shows the He II emission. The timing of the He II emission peak, occurring as $T_e$ decreases, indicates that the excited $He^+$ was generated through the recombination processes of $He^{2+}$. The emission peaks of He II and He I occur with a time delay, indicating the sequential recombination: $He^{2+}$ first recombines into $He^+$, followed by that of $He^+$ into He atoms during pulse passage. It is important to recognize that $He^{2+}$ must first recombine into $He^+$ before they can be neutralized, significantly increasing the time required for He ash removal in divertor region.

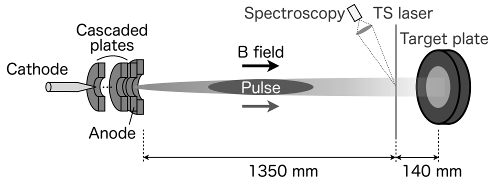


Figure 1. Experimental setup in Magnum-PSI.

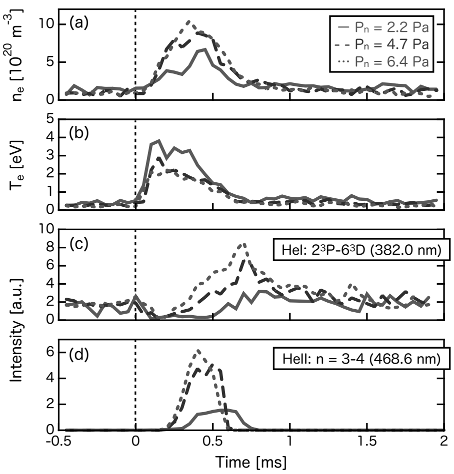


Figure 2. Dynamic responses of (a) $n_e$, (b) $T_e$, and (c) He I and (d) He II emissions by pulse.

# O-04

# A numerical study on the feasibility of the recombination front measurements by analyzing the Zeeman effect on the chord integrated deuterium Paschen α line spectrum in JT-60SA

**T. Morita**[1], T. Shikama[1], T. Nakano[2], R. Sano[2], T. Kawate[2], M. Xu[1], M. Hasuo[1]

[1]*Graduate School of Engineering, Kyoto University, Kyoto, Japan*
[2]*National Institutes for Quantum Science and Technology, Naka, Japan*

morita.tsunehiro.75n@st.kyoto-u.ac.jp

In the operation of fusion reactors, monitoring the deuterium recombination front location in the outer divertor is crucial for maintaining the detached plasma. This location has been measured by identifying the Dα emissivity peak using multiple chords spectroscopy [1]. However, in fusion reactors, the use of multiple chords is challenging due to the limited availability of diagnostic ports [2], prompting the need for methods that use fewer chords. In this study, we propose a method that utilizes the Zeeman effect on the Paα emission line spectrum. Given a known magnetic field profile, the emissivity peak along a chord can be estimated based on the magnetic field strength derived from the Zeeman effect [3], which is more pronounced for Paα than Dα.

We investigated the method using the numerical data computed by the integrated divertor code SONIC [4] in JT-60SA. The dataset including one attached and three detached plasmas, with varying the injection amounts of Ar and Ne. First, the ground truth recombination front location was determined as the point where the recombination flux, calculated using the collisional-radiative model [5], reaches its maximum. The front was found to exist only in the detached plasmas and its locations within 1.5 mm of the Paα emissivity peaks.

Next, we examined whether the front location could be determined using the Zeeman effect on the chord-integrated Paα emission line spectrum. We assumed multiple chords passing near the front from the tangential port and calculated the chord-integrated spectra, considering the Zeeman effect, Stark and Doppler broadening, the instrumental function, bremsstrahlung, and blackbody radiation from the target plate. The spectra were fitted using a model that assumes emission originates from a single point on the chord, with fitting parameters including Paα emissivity, magnetic field strength, electron density, and baseline intensity.

For the chord represented by the red line in Fig. 1, the recombination front location can be determined with high accuracy. However, due to the ionization emission occurring at the same location in attached plasma, it was not possible to monitor the transition between attached and detached plasma. To address this issue, we propose using an additional chord parallel to the separatrix (yellow line), which allows monitoring changes in the emission region of the attached and detached plasma. Using these two chords enables effective monitoring of the recombination front.

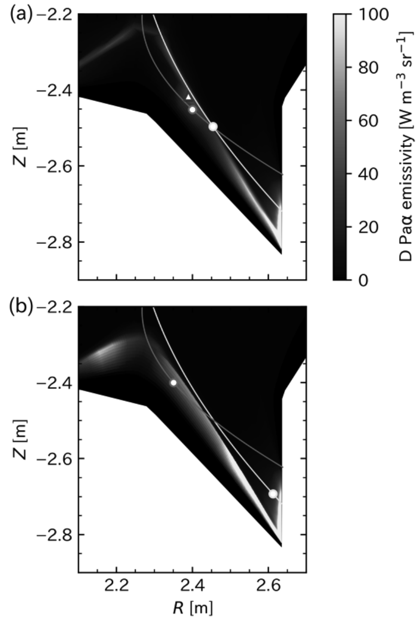


Fig. 1 Distribution of D Paα emissivity ((a)detached and (b)attached plasma). The blue marker indicates the recombination front location, and the red and yellow markers indicate the emissivity peak locations on the chords determined by the fitting.

[1] J. Karhunen, *et al.*, *Plasma Phys. Control. Fusion* **63**, 085018 (2021).
[2] W. Biel, *et al.*, *Fusion Eng. Des.* **146**, 465 (2019).
[3] J. L. Weaver, *et al.*, *Rev. Sci. Instrum.* **71**, 1664 (2000).
[4] K. Shimizu, *et al.*, *Nucl. Fusion* **49**, 065028 (2009).
[5] T. Fujimoto, *et al.*, *J. Appl. Phys.* **66**, 2315 (1989).

**O-05**

# Analytic Scaling of Neutral Transport in High-Temperature Plasma Edges through Repetitive Charge Exchange Collisions

**Keisuke Fujii**[1], Masahiro Hasuo[2], Motoshi Goto[3], Gilson Ronchi[1],
Quinn Pratt[4], Shaun R. Haskey[4], Jeremy D. Lore[1]

[1]Oak Ridge National Laboratory, Oak Ridge, TN 37831-6305, USA
[2]Graduate School of Engineering, Kyoto University Kyoto 615-8540, Japan
[3]National Institute for Fusion Science, Toki, Gifu, 5909-5292, Japan
[4]Princeton Plasma Physics Laboratory, P.O. Box 451, Princeton, New Jersey 08543, USA

Neutral particle transport in magnetically confined plasmas critically impacts the edge plasma performance through its influence on particle, heat, and momentum balance [1]. In this work, we derive an analytic scaling law that quantifies the penetration length scale of neutral atoms into high-temperature plasma edges by incorporating both electron-impact ionization and successive charge-exchange collisions. Under the assumption of steep spatial gradients, the neutral density decays exponentially as $n_n \propto e^{-x/L_\mathrm{H}}$ with the penetration length scale $L_\mathrm{H}$ expressed by electron density $n_\mathrm{e}$, ion temperature $T_\mathrm{i}$, and their decay length $L_n$ and $L_T$ at the edge.
As neutrals are heated by charge-exchange collisions during their transport, the resulting Balmer-α emission spectrum becomes a superposition of Doppler-broadened components from different temperature regions [2, 3]. From our analysis, the spectral wing is shown to follow a power-law distribution, $f(\Delta\lambda) \approx |\Delta\lambda|^{-2\alpha-1}$, where the exponent α is given analytically by $\alpha = (L_\mathrm{H}^{-1} + L_n^{-1})L_T$.
A Monte-Carlo simulations for simplified plasma geometry and the experimental observations of the Balmer-α spectrum from LHD are compared with our scaling law, showing a good agreement.
Notably, while previous neutral density measurements have heavily relied on precise edge parameter profiles and numerical inversion techniques, the proposed scaling law provides a more robust method for extracting the neutral density directly from the spectrum. Furthermore, this analytic framework also facilitates comparisons between observed spectral shapes and predictions from numerical edge transport models (e.g., SOLPS-ITER).

References

[1] K. Fujii, M. Hasuo, M. Goto, J. D. Lore, “A scaling law of the neutral opacity and Balmer-α wing shape in high-temperature plasmas” https://arxiv.org/abs/2409.18064 2024
[2] M. Goto, K. Sawada, K. Fujii, M. Hasuo, and S. Morita. “Evaluation of Hydrogen Atom Density in the Plasma Core Region Based on the Balmer-α Line Profile.” *Nuclear Fusion* **51** 023005, 2011
[3] K. Fujii, M. Goto, et al., “Study of Neutral Hydrogen Transport in LHD Core Plasmas Based on High Dynamic-Range Balmer- α Spectroscopy.” *Nuclear Fusion* **55** 063029, 2015

**O-06**

# Influences on the continuum atomic processes in hot and dense plasmas due to IPD and changes of continuum electron wavefunctions

**Jianmin Yuan**, Jiaolong Zeng *

Institute of atomic and molecular physics, Jilin University, Changchun 130012, China
(*) College of Science, Zhejiang University of Technology, Hangzhou 310023, China

In comparison to free space, ionization potential depression (IPD) of ions and continuum electron wavefunction changes are made by the collisions among the charged particles in plasmas. For the continuum atomic processes initiated by photons and electrons occurring in a plasma, IPD will change the threshold and reaction energy of the electrons, and continuum electron wavefunction changes will change the transition matrix elements. Here we propose that transient space localization of continuum electron wavefunction in hot and dense plasmas can significantly modify the cross sections of ionization and excitation processes caused by electron and x-ray photon impact on ions [1-4]. A theoretical formalism is developed to study the wave functions of the continuum electrons that takes into considering the momentum broadening by coupling with the plasma environment. The method is applied to the photoionization of Fe ions embedded in hot dense plasmas. We find that the cross section is considerably enhanced compared with the predictions of the existing free-atom model, and thereby partly explains the big difference between the measured opacity of Fe plasma [5] and the existing standard models for short wavelengths.

We also proposed that application to study the electron-ion collision processes embedded in a solid-density magnesium plasma. The results show that not only the collision dynamics and the energy correlation of the two continuum electrons are greatly modified, but also the integrated cross sections and transition rates are dramatically increased in hot dense plasmas. Compared with the results obtained by the isolated ion model, the integrated cross section can be increased by one order of magnitude and the transition rate by two orders of magnitude, which supports the recent experimental evidences that the state-of-the-art theories with the results of isolated atom model underestimate the electron impact ionization cross sections and collision rates in the solid-density Al [6] plasmas produced using X-ray free electron lasers (FEL) by more than one order of magnitude.

References

[1] Liu, P., Gao, C., Hou, Y. *et al*. Transient space localization of electrons ejected from continuum atomic processes in hot dense plasma. Commun Phys **1**, 95 (2018).
[2] Zeng, J., Gao, C., Liu, P. *et al*. Electron localization enhanced photon absorption for the missing opacity in solar interior. Sci. China Phys. Mech. Astron. **65**, 233011 (2022).
[3] Zeng J., Ye C., Liu P. *et al*. The Strong Enhancement of Electron-Impact Ionization Processes in Dense Plasma by Transient Spatial Localization, Int. J. Mol. Sci. **23**, 6033(2022).
[4] Zhang P., Jin Y., Zan X. *et al*. Enhancement of electron-impact ionization induced by the warm-dense environments, Physical Review E **104**,035204（2021）
[5] Bailey, J., Nagayama, T., Loisel, G. *et al*. A higher-than-predicted measurement of iron opacity at solar interior temperatures. Nature **517**, 56–59 (2015)
[6] Vinko, S., Ciricosta, O., Preston, T. *et al*. Investigation of femtosecond collisional ionization rates in a solid-density aluminium plasma. Nat Commun **6**, 6397 (2015).

# O-07

# Theoretical Investigation of Electron Impact Excitation and Radiative Processes in Highly Charged Tin Ions Using a Collisional-Radiative Model

**Shivam Gupta**[1], Chun-Tse Wu[2], Yao-Li Liu[1], Shih-Hung Chen[2]

[1]Institute of Space and Plasma Sciences, National Cheng Kung University, Tainan-70101, Taiwan
[2]Department of Physics, National Central University, Zhongli-32001, Taiwan

Extreme ultraviolet (EUV) light at 13.5 nm has emerged as a critical radiation source for advanced lithography applications, driving the continual evolution of semiconductor manufacturing. Among the candidate elements for EUV generation, tin (Sn) has proven to be the most effective, as its highly charged ions exhibiting strong resonance transitions within the required 13.5 nm wavelength range [1-2]. Sn-based plasma sources generally achieve higher conversion efficiencies, making Sn the preferred choice for industrial EUV sources. Laser-produced tin plasmas (LPPs) are particularly advantageous because of their high efficiency in the 13.5 nm wavelength range. The emission spectrum of these plasmas is predominantly governed by highly charged tin ions, specifically those in charge states from $Sn^{5+}$ to $Sn^{15+}$. This emission primarily from $Sn^{5+}$ to $Sn^{15+}$ ions, appears in unresolved transition arrays (UTAs) due to spectral line blending from adjacent charge states, complicating spectroscopic investigations. The calculation of conversion efficiency (CE) of an LPP-EUV light source is sensitive to the precision of the radiative data, including line positions and intensities, used in the simulations. Comprehensive benchmarking of the atomic structure, and electron collision parameters is necessary for the development of a theoretical plasma model. In light of this, the EUV emission spectra from different tin ions is theoretically computed through detailed atomic structure and collisional-radiative (CR) model calculations.

To address this gap, we present the calculation of atomic-ion structure parameters and fine-structure-resolved electron impact excitation cross-sections for multiple tin ions, providing essential data for precise plasma diagnostics and linked spectroscopic modeling of extreme ultraviolet emissions from laser-produced tin plasma. The methodologies, including the relativistic multiconfiguration Dirac-Hartree-Fock method, relativistic configuration interaction and relativistic many-body perturbation theory, are implemented through the general relativistic atomic structure package-2018 [3] and the flexible atomic code [4], facilitating the calculation of bound-state wave functions, excitation energies, and transition parameters, such as oscillator strengths and transition probabilities for the bound states of the tin ions. Electron impact excitation processes from the ground state to higher configurations are systematically analyzed. Cross-sections of various fine structure transitions are computed using the relativistic distorted wave method. These results are integrated into a collisional-radiative plasma model, accounting for processes such as electron impact excitation, ionization, radiative decay, de-excitation, and three-body recombination. The theoretical emission spectra within the 10-25 nm wavelength range are generated. The detailed results on electron impact excitation and plasma modeling will be presented and discussed at the conference.
participant.

References

[1] J. Scheers et al, Physical Review A, **101**, 062511 (2020).
[2] O. O. Versolato, J. Opt., **24**, 054014 (12pp) (2022).
[3] C. F. Fischer et al, Computer Physics Communications, **237**, 184-187 (2019)
[4] M. F. Gu, Can. J. Phys. **86**, 675 (2008).

**O-08**

# Cooling and recombination dynamics of an Al plasma in AlTi or AlAu mixtures heated by an ultraintense laser pulse

**P. Renaudin** *, L. Lecherbourg *, S. Baton **, Ch. Blancard *, Ph. Cossé *, G. Faussurier *, L. Gremillet *, J.-Ch. Pain *, F. Pérez **, O. Poujade *, C Reverdin *

CEA, DAM, DIF, F-91297 Arpajon, France
(*) also at Université Paris-Saclay, CEA, LMCE, 91680 Bruyères-le-Châtel, France
(**) LULI, CNRS, Ecole Polytechnique, CEA, Sorbonne Université, 91120 Palaiseau, France

The rapid cooling dynamics of thin solid foils heated by an ultraintense ($\sim 10^{18}\,\mathrm{Wcm}^{-2}$) picosecond laser pulse is experimentally studied through time-integrated and time-resolved x-ray emission spectroscopy as well as 2D x-ray imaging. Targets consist of plastic foils with buried Al, $Al_{42}Ti_{58}$, or $Al_{85}Au_{15}$ layers, where Al is used to infer the plasma conditions. Our measurements indicate that the Al $K$-shell emission occurs over a shorter duration and from a narrower region in AlTi or AlAu mixtures compared to pure Al samples, and that the average temperature is lower when increasing the atomic number of the high-Z element in the mixture. Our measurements are satisfactorily reproduced by 2D radiative hydrodynamic simulations performed with the TROLL code using an ad hoc spatio-temporal law for the absorbed power in the plasma and coupled with the non-stationary collisional radiative SAPHyR model. This specified energy deposition law serves as a proxy for the fast collisional and resistive heating induced by the laser-driven fast electrons. Our results show that the heating mechanism is compatible with a collisional heating as the main processes for such ”long” laser pulse ($> 1$ ps). The consideration of a spatiotemporal heating distribution similar to the laser intensity profile proved to be necessary to achieve a good agreement with the experimental observations. The use of mixed targets with different atomic numbers revealed different plasma behaviors. Because three-body recombination is the dominant process during the plasma recombination, accurate NLTE atomic physics calculations are essential to account for small variations in electron density and temperature. In addition, our calculations show that important radiative power losses strongly affect the cooling phase of the AlAu plasma. This study opens an avenue for studying radiative cooling rates in high energy density plasmas and for benchmarking atomic physics calculations of non-LTE radiative processes in such systems [L. Lecherbourg et *al.*, submitted to Phys. Plasmas (2025)].

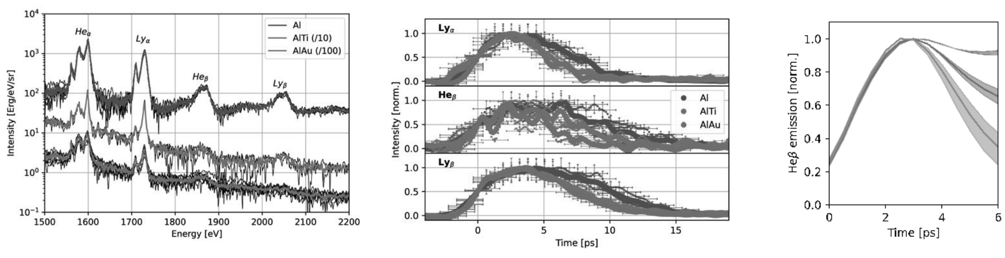


Figure 1: (left) Measured time-integrated Al K-shell spectra from Al, AlTi, and AlAu samples, (center) Measured time-resolved $Ly_\alpha$, $He_\beta$ and $Ly_\beta$ emission from the three target types. Scatter plots with error bars represent data from all shots, with thick curves showing their averages. (right) Calculated Al $He_\beta$ intensity as a function of time, for the three targets.

## O-09

# Enhanced x-ray absorption and heating in medium-Z-doped CHO foams under laser-driven hohlraum radiation

**Xing Wang**[1,*], Shaoyi Wang[2], Yitong Liu[1], Jinrui Qin[1], Jindou Shen[1], Yuchao Su[1], Zhongfeng Xu[1], Jieru Ren[1], Bubo Ma[1],Bo Cui[2], Lai Wei[2], Xingsen Che[2], Zhigang Deng[2], Yongtao Zhao[1]

[1]School of Physics, Xi'an Jiaotong University, Xi'an 710049, China
[2]Laser Fusion Research Center, China Academy of Engineering Physics, Mianyang 621900, China
(*) wangxingcn@xjtu.edu.cn

Near-critical density (NCD) plasmas are produced indirectly by irradiating gold hohlraums with nanosecond lasers ($E_{\text{laser}}$ = 141–172 J, $\tau = 2$–3 ns), generating X-ray radiation temperatures ($T_r \approx 50$ eV) measured via X-ray diodes. The X-rays uniformly heated tri-cellulose acetate (TCA) foam targets doped with controlled concentrations of Mg, Al, Fe, and Mo, respectively.

Plasma emission spectra in the soft X-ray/EUV range are acquired using a high-resolution flat-field grating spectrometer [1]. Under the Local Thermodynamic Equilibrium (LTE) assumption, the Boltzmann plot method yields an electron temperature of $T_e \approx$ 34–41 eV. Metal dopants enhance energy absorption through K- and L-shell edges, significantly increasing plasma temperatures compared to undoped foams. From the measured mass densities and plasma temperatures, we derive ion charge state distributions, obtaining a free electron density of $n_e \approx 10^{21}$ cm$^{-3}$. These results provide quantitative benchmarks for NCD plasma generation under laboratory conditions relevant to high-energy-density physics and astrophysical studies.

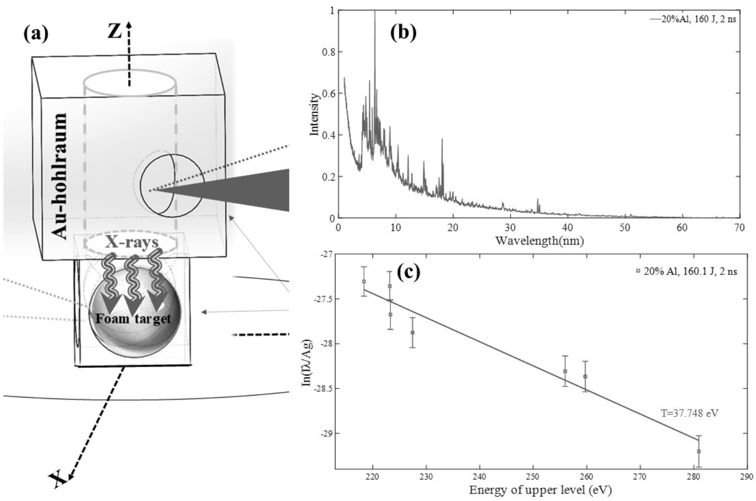


Figure 1: Generation and Diagnostics of plasma generated by indirect heating of doped foam target. (a) Schematic diagram of plasma generation. (b) Spontaneous emission spectrum of the plasma with laser energy of 160 J and pulse width of 2 ns. (c) Plasma temperature is diagnosed with the Boltzmann plot method and derived to be 37.748 eV.

References

[1] J. Ren, B. Ma, L. Liu et al., Phys. Rev. Lett. **130**, 095101 (2023)

**O-10**

# Impact of super-Gaussian electron distributions on plasma K-shell emission

**H.P. Le**, E.V. Marley, H.A. Scott

Lawrence Livermore National Laboratory, Livermore, California 94550, USA

Electron distributions in laser-produced plasmas will be driven toward a super-Gaussian distribution due to inverse bremsstrahlung absorption [1]. Both theoretical and experimental evidence suggest that fundamental plasma properties are altered by the super-Gaussian distribution [2-5]. This work examines how the super-Gaussian distribution affects the ionization balance and K-shell emission of atomic plasmas, utilizing approximate formulas and detailed collisional-radiative simulations [6]. While the impact on plasma ionization is small, K-shell spectra can be significantly modified. Based on these findings, we demonstrate that K-shell spectroscopy can be used to infer super-Gaussian or other similar non-equilibrium electron distributions.

This work was performed under the auspices of the U.S. Department of Energy by Lawrence Livermore National Laboratory under Contract DE-AC52-07NA27344.

References

[1] A.B. Langdon, Phys. Rev. Lett. **44**, 575 (1980)

[2] P. Mora, H. Yahi, Phys. Rev. A **26**, 2259 (1982)

[3] J.P Matte et al., Plasma Physics and Controlled Fusion **30**, 1665 (1988)

[4] D. Turnbull et al., Nature Physics **16**, 181 (2020)

[5] M. Sherlock et al., Phys. Rev. E **109**, 055201 (2024)

[6] H.A. Scott, Journal of Quantitative Spectroscopy and Radiative Transfer **71**, 689 (2021)

**O-11**

# Nonlinear response of highly charged ions to ultraintense XFEL radiation

**Moto Togawa**[1], José R. Crespo López-Urrutia[2], Michael Meyer[1], Thomas M. Baumann[1] et al.

[1] European XFEL, Holzkoppel 4, 22869 Schenefeld, Germany
[2] Max-Planck-Institut für Kernphysik, Saupfercheckweg 1, 69117 Heidelberg, Germany

Highly charged ions (HCI) allow for stringent tests of predictions involving relativistic effects, quantum electrodynamics (QED), and nuclear effects. Monochromatic X-rays are an ideal tool for probing their core electrons [1,2]. However, such studies have so far been limited to states accessible by single-photon absorption.

X-ray free-electron lasers (XFELs) can trigger femtosecond-scale responses in all kinds of matter by inducing rapid multiple ionization of inner-shell electrons [3,4]. However, structural and dynamical information on such transient, multiply excited states of inner-shell electrons is often obscured by complex ionization pathways during the evolution from neutral atoms to highly charged ions.

Here, we solve this problem by employing an electron-beam ion trap (EBIT) to prepare and confine highly charged ions, enabling direct exploration of multiply excited states, in particular the interplay between relativistic and electron correlation effects beyond the well-known resonance-enhanced X-ray multiphoton ionization process (REXMI) [3,4]. Specifically, we highlight the prominent 2p – 3d transitions neon-like krypton ($Kr^{26+}$), lines where relativistic and correlation-induced energy shifts nearly cancel out for specific states. This quasi-degeneracy causes a resonant condition that enables a novel, highly efficient nonlinear two-photon ionization mechanism, and facilitates state-selective two-color pump-probe schemes.

References

[1] **M. Togawa** et al., Phys. Rev. Lett. **133**, 163202 (2024)

[2] S. Kuehn et al., Phys. Rev. Lett. **129**, 245001, (2022)

[3] L. Young, et al., Nature **466**, 56 (2010).

[4] A. Roerig et al., Nat. Commun. **14** 5738 (2023)

# O-12

## Understanding of hot dense plasmas isochorically heated by XFEL using X-ray emission spectroscopy

**Hae Ja Lee**[1 *], S. M. Vinko[2,3], O. Humphries[4], C. Prestwood[4], E. Galtier[1], R. Royle[2], M. F. Kasim[2], Y. Shi[2], S. Ren[5], R. Alonso-Mori[1], P. Heimann[1], D. Khaghani[1], M. Liang[1], M. Seaberg[1], S. Boutet[1], A. Aquila[1], S. Brown[1], A. Hashim[7], D. Ranjan[6], M. Makita[4], J. P. Schwinkendorf[6], T. Preston[4], M Mishchenko[4], U. Zastrau[4], O Karnbach[2], C. David[8], G. Seniutinas[8], F. Seiboth[9], H-K. Chung[10], R. Falcone[7], G. Dyer[1], J. S. Wark[2], and B. Nagler[1]

[1]SLAC National Accelerator Laboratory, Menlo Park, USA
[2]Department of Physics, Clarendon Laboratory, University of Oxford, Oxford, UK
[3]Central Laser Facility, STFC Rutherford Appleton Laboratory, Didcot, UK
[4]European XFEL, Schenefeld, Germany
[5]Beijing Jiaotong University, Beijing, China
[6]HZDR, Dresden, Germany
[7]University of California, Berkeley, USA
[8]Paul Scherrer Institute, Villigen PSI, Switzerland
[9]DESY, Hamburg, Germany
[10]Korea Institute of Fusion Energy, Daejeon, Republic of Korea

The characteristics of solid-density plasma in the hot dense matter regime is important for the study of stellar matter and inertial confinement fusion, yet many phenomena, such as nonlinear transport, partial ionization, strong coupling, and atomic processes, are poorly understood under such conditions. With the advent of the X-ray free-electron lasers (XFEL), intense x-ray radiation, in excess of $10^{17}$ W/cm$^2$ at hard X-ray photon energies, can be applied to samples to create and probe such hot dense plasma under well-defined conditions. We applied intense XFEL beam to 2 or 10 mm thick metal foils and investigated K-shell emissions from the various charge states produced, all the way from cold Fe to hydrogenic (Fe XXV). Satellite K$\alpha$ emissions will be compared with CCFLY calculations and discussed for different charge states and Z.

**O-13**

# Development of Ar and N2 Plasma Spectroscopy Reference Data for Plasma Characterization using Collision-Radiation Models and Machine Learning

[1]Mi-Young Song*, [1]Swati Bharti, [1]Yong-Hyun Kim, [1]Jong-Sik Kim, [1]Dae-Chul Kim

[1]37 Dongjangsan- ro, Gunsan, Jeollabuk-do 54004, South Korea
(*) mysong@kfe.re.kr

In this study, we quantified the spectral emissions produced during inductively coupled plasma (ICP) generation in order to monitor key plasma parameters—electron temperature and density—in real time. We combined non-invasive optical emission spectroscopy (OES) with collisional–radiative (CR) modeling, validating the CR approach against experimental measurements for pure argon plasmas. Despite its success with argon, CR modeling alone proved insufficient for nitrogen and argon–nitrogen mixtures due to a lack of reliable molecular input data such as accurate cross-sections and detailed population distributions across vibrational and rotational levels.

To address these limitations, we constructed a comprehensive training dataset by measuring spectral signals under controlled variations of pressure (10–70 mTorr), RF power (100–3,000 W), and gas flow rates for pure Ar, pure $N_2$, and Ar–$N_2$ mixed plasmas. Electron temperature and density were simultaneously determined using a Langmuir probe, and standardized experimental protocols with cross-validation ensured the reliability of our data. We then applied machine learning algorithms to this dataset: for argon plasmas, we compared CR model predictions with measured spectra to identify the 750 nm/763 nm line ratio as the most sensitive indicator of plasma condition changes; for nitrogen plasmas, the AI model autonomously selected the optimal spectral feature that best reflected $N_2$ plasma behavior.

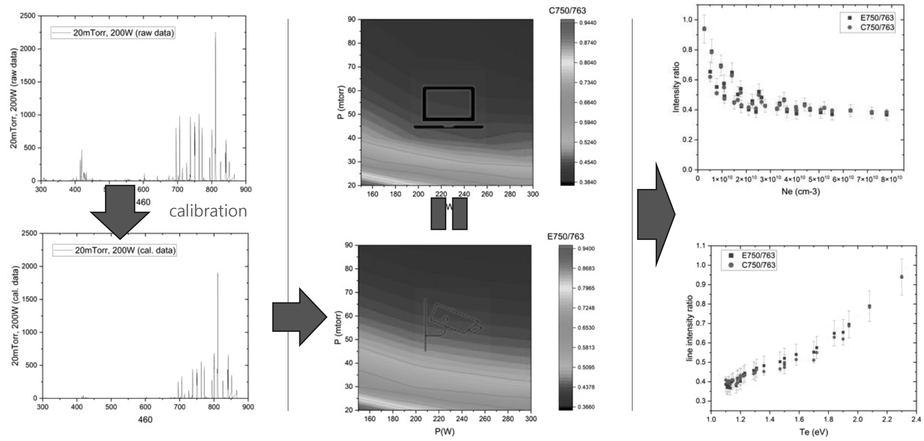


Figure 1: , the 750 nm/763 nm line ratio is optimized for electron temperature prediction.

**Acknowledgments**

This research was supported by the R & D Program Plasma Big Data ICT Convergence Technology Research Project through the Korea Institute of Fusion Energy (KFE) funded by the Ministry of Science and Technology Information and Communication, Republic of Korea (EN2442).

References

[1] H-K. Chung, M-Y. Song, J-W. Kwon, M-G. Lee, J. Park, N. Bae, J. Song, G-H. Kim, Dipti and Y. Ralchenko, Atoms, 9, 100 (2021).

O-14

# Probing dense plasmas with high harmonics*

P. Velarde[1] *, L. Ansia[1,2], A.G de la Varga[1],
A. González[1], G. Williams[2], and M. Fajardo[2]

[1] Instituto de Fusión Nuclear, Universidad Politécnica de Madrid, José G. Abascal 2, 28006 Madrid, Spain.
[2] GoLP/Instituto de Plasmas e Fusão Nuclear, Universidade de Lisboa, 1049-001 Lisboa, Portugal.

The advent of X-ray free electrons laser opened up new opportunities in the study of warm dense matter. With intensities previously achievable only by infrared and visible lasers, XFELs facilitate the creation of matter with precisely better defined properties, such as temperature and density. Recently, there has been a particular focus on the generation of dense plasmas from mid-Z materials, especially transition metals.

These experiments are typically complemented by collisional radiative models (CRM), which have proven to be useful tools for understanding the temporal evolution of the sample. Recently, the non-thermal CRM BigBarT [1, 2] code has been extended to simulate arbitrary materials while maintaining a self-consistent approach for evolving non-thermal electron distributions in 1D and incorporating degeneracy effects. Additionally, time-dependent indexes of refraction have been derived using the Kronig-Kramers relations, allowing for the investigation of electromagnetic wave propagation in the plasmas.

The dielectric function is used to calculate the polarization using frequency domain decomposition in the polarization equation. This polarization is used to calculate the propagation of a harmonic HHG beam in a target which has been isochorically heated by the XFEL. For this calculation, Maxwell's equations are solved numerically with a Godunov method with adaptive mesh refinement [3], which allows to simulate the complete physical system during the whole HHG pulse. The phase differences of the outgoing HHG beam can be measured on a wavefront detector and the spatial variation of the sheet electron density can be derived. By comparing the HHG pulses at the exit of the foil with the database of the simulations for different pulse intensities and pulse times, we can determine the spatial profile of electron densities and temperatures.

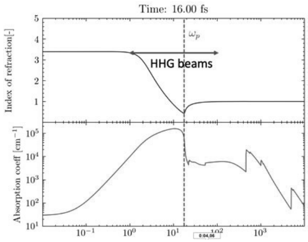


Refractive index and absorption coefficient for Ti illuminated by a XFEL pulse of I=$10^{17}$ W/cm$^2$, FWHM=30 fs and h$\nu$=6 keV

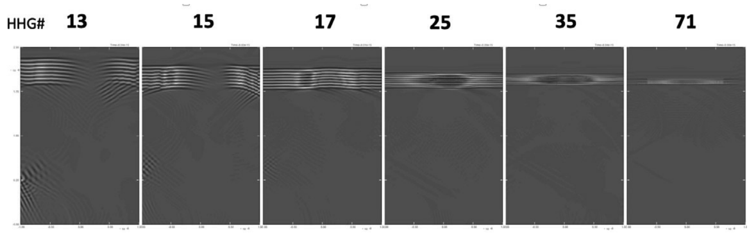


Electromagnetic field of the HHG pulse (Bz in the figure) after interacting with the isochorically heated foil by the XFEL. The spatial and temporal profile of the absorption and refraction coefficient as well as the electron density is calculated with the BigBarT code.

## References

[1] A. G. de la Varga et al, HEDP **9**, 542-547 (2013).

[2] Van Den Berg Q. Y. et al., Phys Rev Lett **120**, 055002 (2018).

[3] J.A. Moreno et al, Comp Phys Comm **260**, 107268 (2021)

*E-mail: pedro.velarde@upm.es

# Shake-off in XFEL Heated Solid-Density Plasma

L. Ansia[1]*, G. O. Williams[1], M. Makita[2], P. Estrela[1], M. Hussain[1], T. R. Preston[2], J. Chalupský[3], V. Hajkova[3], T. Burian[3], M. Nakatsutsumi[2], J. Kaa[2], Z. Konopkova[2], N. Kujala[2], K. Appel[2], S. Göde[2], V. Cerantola[2], L. Wollenweber[2], E. Brambrink[2], C. Baehtz[4], J.-P. Schwinkendorf[2], V. Vozda[3], L. Juha[3], H.-K. Chung[5], P. Vagovic[6], H. Scott[7], P. Velarde[8], U. Zastrau[2], M. Fajardo[1]

[1]GoLP/Instituto de Plasmas e Fusão Nuclear, Instituto Superior Técnico, Universidade de Lisboa, Portugal.
[2]European XFEL, Schenefeld, Germany.
[3]Institute of Physics, Czech Academy of Sciences, Prague, Czech Republic.
[4]Helmholtz-Zentrum Dresden-Rossendorf, Dresden, Germany.
[5]Korea Institute of Fusion Energy, Daejeon, Republic of Korea.
[6]Center for Free-Electron Laser Science, DESY, Hamburg, Germany.
[7]Lawrence Livermore National Laboratory, Livermore, California, USA.
[8]Instituto de Fusión Nuclear, Universidad Politécnica de Madrid, Spain.

Over the past two decades, X-ray free-electron lasers (XFELs) have made significant progress, achieving peak brightness in the XUV and X-ray regions that were previously only attainable in the optical and infrared ranges. This advancement has opened up new possibilities in high-energy density science. It enables the creation of solid-density plasmas with larger volumes, greater uniformity, and well-defined properties, including temperature and density. The ability to deposit energy on femtosecond timescales has also enabled spectroscopic studies of ionisation dynamics in previously inaccessible regimes.

In this work, we report the observation of the shake-off process in a solid-density XFEL created plasmas. Titanium foils were irradiated with XFEL pulses at photon energies of 5.1 keV and 6 keV. Emission spectra display satellite features that emerge only at the higher photon energy, consistent with the threshold required for simultaneous K- and L-shell ionisation. These signatures are absent at lower photon energies and cannot be accounted for by standard collisional or Auger ionisation processes.

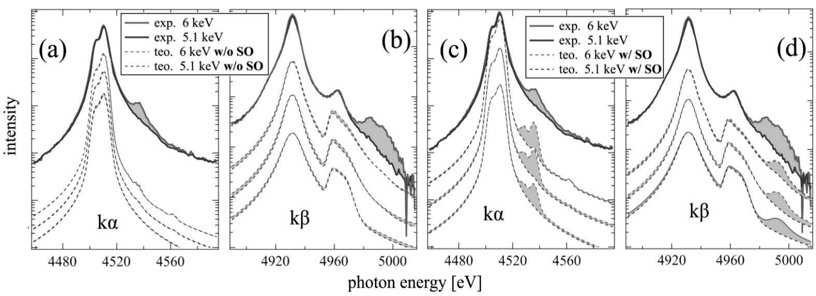


Figure 1: Experimental data obtained at full intensity for XFEL photon energies of 5.1 keV and 6 keV compared to models without shake-off (a and b), and with shake-off (c and d). The calculations were done for three XFEL intensities (0.1, 0.5 and $1 \times 10^{16}$ W/cm$^2$) increasing vertically. The shaded areas highlight the difference between the 6 and 5.1 keV XFEL photon energy.

To interpret the experimental results, we used the collisional-radiative model BigBarT, suited for the self-consistent evolution of the electron continuum, including degeneracy effects [1, 2, 3]. The resulting spectra show good agreement with the measurements (Fig. 1). These results demonstrate that shake-off persists in solid-density plasmas and must be considered in the analysis of emission spectra under XFEL irradiation [4].

## References

[1] A. G. de la Varga, P. Velarde, High Energy Density Physics **7**, 163-168 (2011).

[2] A. G. de la Varga, P. Velarde, High Energy Density Physics **9**, 542-547 (2013).

[3] Ansia L. et al., arXiv, 2501.17000 (2025).

[4] G. O. Williams et al., arXiv, 2501.16970 (2025).

*E-mail: lucas.ansia.fernandez@tecnico.ulisboa.pt

O-16

# A Laboratory plasma experiment for X-ray astronomy using a compact electron beam ion trap (EBIT)

**Yuki Amano**[1)], Leo Hirata[1),2)], Hiromasa Suzuki[3)], Moto Togawa[4)], Hiroyuki A. Sakaue[5)], Nobuyuki Nakamura[6)], Makoto Sawada[7)], Naoki Kimura[5)], Hiroya Yamaguchi[1),2)]

[1)] The Institute of Space and Astronautical Science (ISAS), Japan Aerospace and Exploration Agency (JAXA), 3-1-1 Yoshinodai, Chuo-ku, Sagamihara, Kanagawa 252-5210, Japan
[2)] Department of Physics, The University of Tokyo, 7-3-1 Hongo, Bunkyo-ku, Tokyo 113-0033, Japan
[3)] Faculty of Engineering, University of Miyazaki, Miyazaki 889-2192, Japan
[4)] Max-Planck-Institut für Kernphysik, Saupfercheckweg 1, 69117 Heidelberg, Germany
[5)] National Institute for Fusion Science,Toki, Gifu 509-5292, Japan
[6)]Institute for Laser Science, The University of Electro-Communications, Chofu, Tokyo 182-8585, Japan
[7)]Department of Physics, Rikkyo University, 3-34-1 Nishi-ikebukuro, Toshima-ku, Tokyo 171-8501, Japan

X-ray observations of astronomical objects play a critical role in understanding the processes of structural formation and chemical evolution of the Universe. The X-ray astronomy satellite XRISM, launched in September 2023, is equipped with a microcalorimeter, which provides high-resolution X-ray spectroscopy in the soft X-ray bandpass up to 12 keV with an energy resolution of $E/\Delta E \approx 1300$ at 6 keV. This spectral resolution enables precise diagnostics of astrophysical plasmas, including measurements of velocity structures and elemental abundances of objects. However, more accurate atomic data is required to analyze the high-resolution X-ray spectra. We have introduced an electron beam ion trap (EBIT) to the Japanese astronomical community in collaboration with Japan Aerospace and Exploration Agency and Max-Planck-Institut für Kernphysik. The EBIT produces highly-charged ions in arbitrary charge states using a monochromatic electron beam (Figure 1), providing an experimental benchmark for atomic data. In this presentation, we review the outcomes and future prospects of our EBIT experiment. In June 2024, we performed high-resolution photoexcitation spectroscopy of highly charged ions at the synchrotron radiation facility SPring-8. As a result, we successfully measured the resonance transition of the L-shell of Ne-like Fe. Meanwhile, XRISM has observed various high-energy astrophysical phenomena, including supernova remnants, active galactic nuclei, and X-ray binaries, producing pioneering results. These observations have also highlighted the urgent need for new atomic data. For example, the wavelengths and transition rates of inner shell transitions such as $1s$–$3p$ transitions of Li-like ions are needed to analyze observational data of X-ray binaries and supernova remnants. We will also present the current status of updating the EBIT toward the measurement of these atomic data.

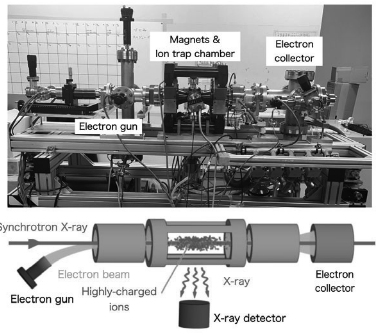


Figure 1: Photograph and schematic view of the EBIT [2, 3].

References

[1] M. Tashiro, et al., Proc. SPIE 10699, 1069922 (2018).

[2] P. Micke, et al., Rev. Sci. Instrum. **89**, 063109 (2018).

[3] S. Kühn, et al., Phys. Rev. Lett. **124**, 225001 (2020).

**O-17**

# X-ray Microcalorimeter Spectroscopy & Radiative Transfer Modeling of Astrophysical Plasmas around Neutron Stars and Black Holes

**Masahiro Tsujimoto**[1], Chamani M. Gunasekera[2], Peter A. M. van Hoof[3], Priyanka Chakraborty[4], Gargi Shaw[5], Stefano Bianchi[6], Marios Chatzikos,[7] Maryam Dehghanian[8], and Gary J. Ferland[7]

[1]JAXA ISAS, Sagamihara, Kanagawa, 252-5210, Japan, [2]STSci, Baltimore, MD, USA, [3]Royal Observatory of Belgium, Brussels, Belgium, [4]CfA, Harvard & Smithsonian, Cambridge, MA, USA, [5]Tata Institute of Fundamental Research, Mumbai, India, [6]Università degli Studi Roma Tre, Roma, Italy, [7]University of Kentucky, Lexington KY, USA, [8]Virginia Tech, Blacksburg, VA, USA

Compact objects, such as neutron stars and black holes, are copious X-ray emitters when they accrete matter from a companion star in a binary system. The released gravitational energy is converted to heat, which is cooled by X-ray radiation. Matter surrounding these objects is radiatively ionized and driven outward forming an outflow. This is one of the most ubiquitous mechanisms of mass and energy circulation in the Universe. X-ray plasma spectroscopy is a key to understanding its physics.

The XRISM space telescope was launched in September 2023. It carries an X-ray microcalorimeter spectrometer. Its unprecedented spectroscopic capability in the 2–12 keV band enables us to detect many atomic spectral features, which include the $n \to 1$ ($n \geq 2$) transitions of H-like and He-like elements of cosmic abundant elements such as Si, S, Ca, Ar, Fe, and Ni as well as K$\alpha$ and K$\beta$ inner-shell transitions of Li-like to F-like Fe[2]. The fine-structure levels[3] and dielectronic satellite lines[4] were resolved for the first time from astrophysical plasmas besides the Sun (figure 1).

These lines from compact object binaries are formed in non-local thermal equilibrium (NLTE) conditions. Radiative transfer (RT) calculations are thus a requisite to interpret the observed spectra. `Cloudy` is one of the most widely used numerical RT codes in astrophysics. We present the result of the code being applied to actual data with XRISM. We found that some new atomic processes need to be implemented such as inner-shell photoionization/excitation and proton/electron collision excitation and call for contributions by atomic physicists to make the best use of the observed spectra.

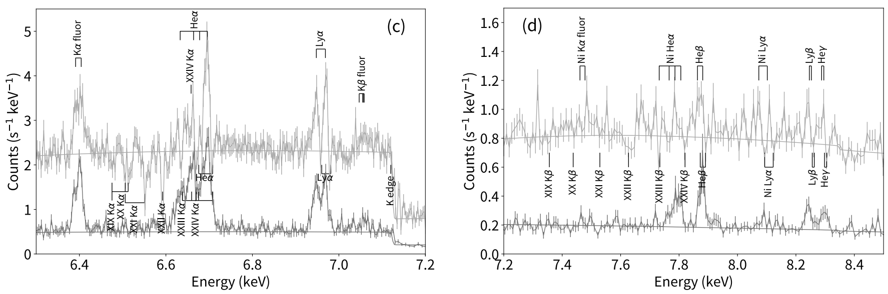


Figure 1: Parts of the XRISM spectrum of a neutron star binary Circinus X-1[1].

References

[1] M. Tsujimoto, T. Enoto, M. Diaz-Trigo, et al. PASJ, in press (2025)
[2] C. Gunasekera, P. A. M. van Hoof, M. Tsujimoto, G. J. Ferland, A&A, **694**, L13 (2024)
[3] M. Kurihara, M. Tsujimoto, M. Audard, et al. PASJ, submitted (2025)
[4] P. Chakraborty, G. J. Ferland, M. Chatzikos, et al. ApJ, **901**, 68 (2020)

**O-18**

# The structure of the AGN narrow-line region as probed by emission line ratios

**Roi Rahin**[1], Gabriel Grell[1], Maurice Leutenegger[1], Ehud Behar[2]

[1]NASA Goddard Space Flight Center 8800 Greenbelt Road, Greenbelt, Maryland 20771, USA
[2]Physics Department, Technion, Haifa 32000, Israel

Active Galactic Nuclei (AGN) are galactic cores hosting a supermassive blackhole and emitting bright radiation across multiple wavelengths, from radio to X-ray. Type II AGN are thought to have a sufficiently side-on viewing angle to obscure direct observation of the central source. They show emission from a wide range of ion species thought to originate in the so-called narrow line region (NLR). The wide range of ion species observed in AGN NLR cannot be explained by a homogeneous outflow with $1/r^2$ density profile, as that produces a narrow ionization range [1]. It requires either a different radial density profile, resulting in stratification of the ionization parameter, or a clumpy outflow, so that a distribution of densities is present at each radius. Here, we present an observational method to differentiate an inhomogeneous wind from a radially stratified wind using the helium-like K$\alpha$ line emission complex.

The helium-like K$\alpha$ line complex strength ratios, denoted $\mathcal{R} = z/(x+y)$ and $\mathcal{G} = (z+x+y)/w$, are valuable quantities for plasma diagnostics in astrophysical plasma. In type II AGN, the observed $\mathcal{R}$ ratios of various elements are often higher than can be explained by atomic processes in He-like ions [2]. We consider the influence of Li-like ions on $\mathcal{R}$ and find that they can explain the apparent discrepancy with theory. Li-like ions can change the observed He-like line ratios by both suppressing the intercombination lines through resonant Auger-Meitner destruction [3] and enhancing the forbidden line through inner-shell ionization. The predicted effect depends on the degree of stratification of Li-like, He-like, and H-like ions in the emitting plasma. In a stratified plasma, Li-like ions enhance the forbidden line but do no suppress the intercombination lines. We present an analysis of He-like complexes in AGN such as NGC 1068 and draw conclusions about the ionized wind structure.

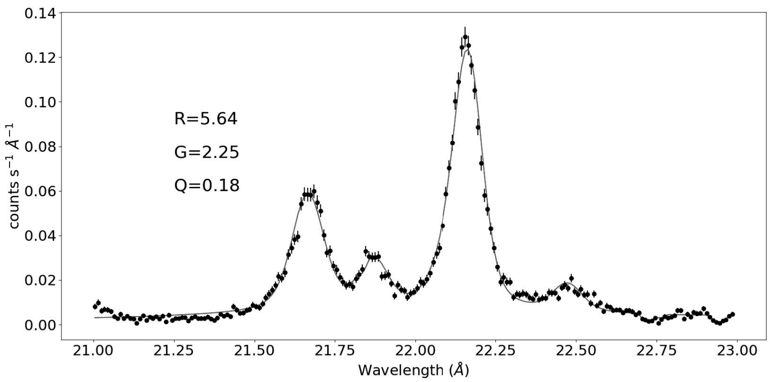


Figure 1: The He-like oxygen complex in NGC 1068 as observed by XMM/RGS. The $\mathcal{R}$ value of oxygen is expected to be $\sim 4$, but the presence of Li-like ions enhances the $\mathcal{R}$ value.

References

[1] Behar, E., The Astrophysical Journal, 703(2), 1346. (2009)

[2] Kinkhabwala, A., Sako, M., Behar, E., et al. , The Astrophysical Journal, 575, 732. (2002)

[3] Mehdipour, M., Kaastra, J. S., & Raassen, A. J. J., A&A, **579**, A87 (2015)

**O-19**

# Dielectronic Recombination of Fe $3d^k$ Ions

Chunyu Zhang*, Nigel Badnell

Department of Physics, University of Strathclyde, Glasgow G4 0NG, UK

*Chandra* and *XMM-Newton* spectroscopy of active galactic nuclei (AGNs) shows a rich spectrum of X-ray absorption lines due to $n = 2 - 3$ inner shell transitions of Fe I - Fe XVI (so-called iron M-shell ions). However, the iron M-shell UTA feature at 16 – 16.5Å presents the only real discrepancy between the modelling of AGN spectra and the observations. Netzer [1] has suggested the reason for these discrepancies is the underestimation of the low-temperature $\Delta n = 0$ dielectronic recombination (DR) rates for the iron M-shell ions. The multiconfiguration Breit-Pauli (MCBP) AUTOSTRUCTURE (AS) calculations for DR rates of Fe $3p^q(q = 1 - 6)$ have been carried-out by Badnell [3, 4]. In this work, also using the MCBP approximation implemented in AS [5], we continue to explore the theoretical calculation of DR rates for lower-charged iron ions, i.e. Fe $3d^k(k = 1 - 6)$. Fig. 1 shows the comparison of the DR rate coefficients for $Fe^{7+}$ from the previous AS calculation [6], recommended data in [2], the present 7CF and 8CF calculations as well as the experimentally derived values [6].

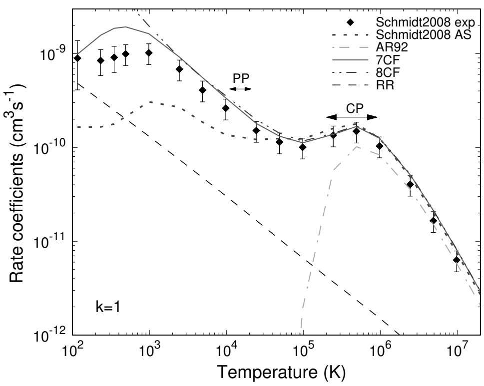


Figure 1: DR rate coefficients for $Fe^{7+}$.

We will report the DR data for Fe $3d^k(k = 1 - 6)$ at the meeting. This work was supported by grant from the UK APAP Network by the UK STFC (ST/V000683/1)

References

[1] H. Netzer 2004 *Astrophy. J.* **604** 551.

[2] Arnaud, M. and Raymond, J. 1992 *Astrophy. J.* **398** 394.

[3] N. R. Badnell 2006 *J. Phys. B: At., Mol. Opt. Phys.* **39** 4825.

[4] N. R. Badnell 2006 *Astrophy. J.* **651** 73.

[5] N. R. Badnell 2011 *Comput. Phys. Commun.* **182** 1528.

[6] E. W. Schmidt, S. Schippers, D. Bernhardt, et al. 2008 *Astron. & Astrophys.* **492** 265.

*E-mail: chunyu.zhang@strath.ac.uk

**O-20**

# Molecular Dynamics Study of Amino Acid Precursor Formation under Space-like Conditions

**Hiroaki Nakamura**[1,2], Masayuki Murai[2], Kensei Kobayashi[3], Masahiro Kobayashi[1,4], Seiki Saito[5]
[1] National Institute for Fusion Science, [2]Nagoya University, [3]Yokohama National University, [4]The University of Tokyo, [5]Yamagata University

Proteins, essential components of terrestrial life, are formed through condensation polymerization of amino acids. In the study of the origin of life, there is a theory that organic molecules such as amino acids were synthesized in inanimate environments [1]. This concept underpins the theory of chemical evolution, where simple molecules transform into complex molecules via chemical reactions, eventually leading to life. Meteorite analyses have revealed amino acids and high-molecular-weight organics, suggesting that organic compounds could have been synthesized in space.

In this study, we conducted reactive molecular dynamics simulations to investigate the formation of polymeric organic molecules under conditions mimicking interstellar environments. Molecular clouds, characterized by high matter concentration and extremely low temperatures, are shielded from stellar radiation and host dust grains covered by ice mantles composed of water, carbon monoxide, ammonia, and other simple molecules. Cosmic ray irradiation of these ice mantles is thought to trigger chemical reactions leading to complex organic matter.

Our simulations placed small molecules (water, carbon monoxide, ammonia) within a simulation box and modeled the energy input from cosmic ray irradiation. A temperature control process was applied, heating the system to 10,000 K and then cooling it to 10 K, representing conditions in molecular clouds. We employed reactive force fields to model bond formation and cleavage accurately.

Two types of simulations [2,3] were performed: canonical ensemble simulations, controlling system energy with an external heat bath, and microcanonical ensemble simulations, treating isolated systems without energy exchange. Canonical simulations analysed the effects of molecular density and initial composition. Results showed that higher density promotes bond breaking and carbon atom chaining, leading to larger molecule formation. Configurations with higher carbon and nitrogen content in the initial mixture favored the synthesis of larger molecules. Microcanonical simulations reproduced the gradual cooling process of sparse materials, showing enhanced formation of larger molecules during cooling.

These findings suggest that cosmic ray irradiation of ice mantles rich in carbon and nitrogen atoms likely promotes the synthesis of high-molecular-weight organic materials, potentially contributing to the origin of life.

Acknowledgements: The computation was performed using Research Center for Computational Science, Okazaki, Japan (Project: 24-IMS-C099) and Plasma Simulator of NIFS. The research was supported by KAKENHI (Nos. 21H04456, 22H05131, 23H04609, 22K18272, 23K03362), by the NINS program of Promoting Research by Networking among Institutions (01422301) by the NIFS Collaborative Research Programs (NIFS22KIIP003, NIFS24KIIT 009, NIFS24KIPT013, NIFS22KIGS002, NIFS22KISS021) and by the ExCELLS Special Collaboration Program of Exploratory Research Center on Life and Living Systems(24-S5).

References

[1]K. Kobayashi et al., Astrobiology: Emergence, Search, and Detection of Life (Ed.: Basiuk, V. A.), p. 175, American Scientific Publishers, Stevenson Ranch, CA, USA (2010).
[2]H. Nakamura et al., Conference Proc. of JSST2023, Aug. 29th-31st, 2023, Niigata Univ., Niigata, Japan.
[3]H. Nakamura et al., Conference Proc. of JSST2024, Sept. 17th-20th, 2024, Univ. of Hyogo, Kobe, Japan.

**O-21**

# Visible-Near Infrared Photo-absorption in Zirconium Plasmas for Kilonova Studies

**K Dowd**[1], P Dunne[1], H Dannar[3], L Mullholland[2], C Ballance[2], C Ramsbottom[2], J Jones[3] and M McCann[2]

[1]School of Physics, University College, Belfield, Dublin 4, Ireland, D04 V1W8
[2]Astrophysics Research Centre,School of Mathematics and Physics, Queens University Belfast, Northern Ireland, BT7 1NN
[3]College of Optical Sciences, University of Arizona, 1630 E University Blvd, Tucson, AZ 85721

Approximately half of the elements with Z $>$ 26 are believed to be synthesised via rapid neutron capture (r-process). Binary neutron star (BNS) mergers are favoured as a significant site for the r-process, due to their neutron rich and explosive environmental conditions [1]. Electromagnetic radiation is thermally emitted from the neutron rich ejecta of these events mainly in the ultraviolet (UV), optical and infra-red spectral regions [2]. The first detailed photometric and spectroscopic observations were of a kilonova event AT170817gfo, which occurred in August 2017. Currently, there is a lack of a set of complete atomic data for elements present in the visible and NIR spectra of AT2017gfo, and more generally those theorised to be formed in BNS mergers. Therefore, accurate kilonova models are extremely difficult to produce [3].

We present a novel visible-near infrared (NIR) photo-absorption experiment, which uses laser produced plasmas (LPP) to obtain atomic and near neutral ionic species. This novel experimental set up consists of a supercontinuum fibre laser, a neodymium-doped yttrium aluminium garnet (Nd:YAG) laser, fibre optic beam delivery systems, and a 0.750-m Czerny-Turner spectrometer. The spectrometer is equipped with 300 groove/mm gratings and an InGaAs complementary metal oxide semiconductor (CMOS) camera. The wavelength range covered by the experiment is 450 – 1700 nm. The Nd:YAG laser pulses (500 mJ, 5.5 ns) generate an absorbing plasma. This is probed by supercontinuum laser pulses in a range of controlled time delays between 10 and 2000 ns. There are two optical paths: the I path where the continuum passes through the plasma; and the $I_0$ path which is incident directly on the spectrometer.

The $\log_{10}[\frac{I}{I_0}]$ is taken to obtain an absorption spectrum. Absorption spectra of neutral to three-times ionised yttrium, zirconium and niobium have been recorded. A high-resolution dual comb spectroscopy experiment is used to cross reference atomic absorption lines [4]. Atomic structure calculations, using the GRASP code [5] and the Cowan suite of codes [6], along isoelectronic and isonuclear sequences, aided the analysis and identification of lines.

References

[1] D. Watson et al., Nature **574(7779)** 497 (2019)

[2] S. Smartt et al., Nature **551(7678)** 75 (2017)

[3] J.H. Gillanders et al., Mon. Not. R. Astron. Soc. **529(3)** 2918 (2024).

[4] J. Bergevin et al., Nat. Commun. **9(1)** 1273 (2018)

[5] F.A. Parpia et al., Comput. Phys. Commun. **94(2-3)** 249 (1996)

[6] R.D. Cowan, The Theory of Atomic Structure and Spectra, University of California Press (1981)

**O-22**

# Mapping Rydberg states of $H_2$ with the Halfium R-matrix method

**Mourad Telmini**, Rawand Mezlini*, Soumaya Bezzaouia

LSAMA, Department of Physics, Faculty of Science of Tunis, University of Tunis El Manar, 2092, Tunis, Tunisia

Molecular Rydberg states play an important role in electron-cation collisions that are relevant in plasma physics, particularly in cool plasma and discharges where these collisions are the dominant process [1]. In this contribution lecture, the main processes occurring when an electron collides with a molecule, or a molecular ion, will be briefly introduced. Then, the case of ($e{+}H_2^+$) will be presented in detail, not only because of its simplicity as a prototype, but also in relation with its importance in plasma fusion physics.

A key point in modelling the collision, is the formation of an intermediate neutral super-excited compound ($H_2^{**}$ in the prototype case), which governs the various outcome channels and gives rise to sharp complex variations in the cross sections at low-energy, especially in the important case of dissociative recombination.

The main theoretical approaches for studying this problem will be introduced, with an emphasis on the method that combines the eigenchannel $R-$matrix formalism with Generalized Quantum Defect Theory [2]. We will show how this approach, so-called Halfium $R$-matrix [3], is able to take into account simultaneously the bound spectrum and the fragmentation channels, leading to the key quantities needed for the calculation of the electron-molecule collisions cross-sections and rates of the various processes.

References

[1] D. Hvizdos, C. Greene, C. Jungen, M. Telmini, R. Curik, Bull. Am. Phys. Soc. (Proccedings of 55th DAMOP meeting) R4.003 (2024)

[2] O. Motapon, N. Pop, F. Argoubi, J. Zs Mezei, M. D. Epee Epee, A. Faure, M. Telmini, J. Tennyson, and I. F. Schneider, Phys Rev. A **90** 012706 (2014)

[3] M. Aymar, C.H. Greene and E. Luc-Koenig, Rev. Mod. Phys. **68** 1015 (1996)

[4] M. Telmini and Ch. Jungen, Phys Rev. A **68** 062704 (2003)

## O-23

# Detailed Collisional-Radiative Analysis of Iodine Plasma for Plasma Diagnostics

**Ayushi Agrawal**, Shivam Gupta*, Lalita Sharma and Rajesh Srivastava

Indian Institute of Technology Roorkee, Roorkee, India
(*)Institute of Space and Plasma Sciences, National Cheng Kung University, Tainan, Taiwan

The increasing demand for alternative propellants in electric propulsion systems—such as Hall and ion thrusters—has heightened interest in iodine (I) as a substitute for xenon, due to iodine's advantageous properties, including its lower atomic mass and compatibility with existing spacecraft systems [1]. In addition to propulsion, iodine plasma plays an essential role in various fields, including low-temperature plasma diagnostics, lasers, light sources, and fusion plasma research.

This study addresses a significant gap in the spectroscopic characterization of singly ionized iodine plasma. We have calculated fine-structure-resolved electron impact excitation (EIE) cross-sections for singly ionized iodine, considering transitions from the ground state and seven metastable states. These calculations were performed using the fully relativistic multiconfiguration Dirac-Fock (MCDF) method in conjunction with the relativistic distorted wave (RDW) approach. The resulting cross-sections are incorporated into a comprehensive collisional-radiative (CR) model comprising 92 fine-structure energy levels. This model accounts for critical kinetic processes, including electron impact ionization, two- and three-body recombination, collisional de-excitation, and radiative decay.

To validate our CR model, computed theoretical synthetic emission intensities and derived plasma parameters (electron temperature and density) were compared with experimental measurements obtained from inductively coupled iodine plasma by Maramuse [2]. The strong agreement between our theoretical results and the experimental data confirms the accuracy and reliability of the iodine atomic structure and electron-atom collision data provided by this study.

These results offer robust atomic data essential for iodine plasma diagnostics and modeling, improving plasma control capabilities in space propulsion systems and magnetic fusion reactors. Furthermore, the comprehensive electron collision data and atomic structure parameters generated through this research can facilitate future plasma experiments, refine diagnostic techniques, and enhance the accuracy of plasma performance predictions. Additionally, this work lays the foundation for extending similar CR models to other noble gas plasmas, thereby advancing diagnostic tools and simulation accuracy in fusion energy research. Ultimately, our study underscores the importance of integrating theoretical calculations with experimental data for reliable and accurate predictions of plasma behavior.

References

[1] M A Lieberman and A J Lichtenberg, Principles of Plasma Discharges and Materials Processing (New York: Wiley) (2004).

[2] F. Marmuse 2020 Iodine plasmas: Application to electric propulsion (PhD Thesis)Thèse de doctorat dirigée par Drag, Cyril et Aanesland, AnePhysique des plasmas Sorbonne université

[3] A Agrawal, S Gupta, L Sharma and R Srivastava, PSST **33**, 11 (2024)

# POSTERS A

**A-01**

# Spatially resolved Au L-shell emission spectroscopy of laser-produced NLTE coronal plasmas

**N. Aybar[1 *], W. Farmer[1], D. Liedahl[1], E. Marley[1], O. Landen[1], and J. S. Ross[1]**

[1]Lawrence Livermore National Laboratory, Livermore, USA

Emission and conditions of plasmas out of local thermodynamic equilibrium (LTE) are an important part of high energy density physics, especially in laser-produced plasmas relevant to inertial confinement fusion (ICF). Accurate modeling of non-LTE plasmas remains a challenge. Recent work has shown that shortcomings in this area are largely responsible for hohlraum drive deficits in radiation hydrodynamic modeling[1]. High quality experimental data of non-LTE plasma conditions are necessary to inform and constrain atomic kinetics models. Here, we present spatially resolved spectra of gold L-shell emission from a directly driven gold sphere target. The experiment used the National Ignition Facility (NIF) polar direct drive laser pointing to nearly uniformly illuminate the sphere with ~1e15 W/cm$^2$ of laser intensity, creating a soft X-ray drive and coronal plasma conditions similar to those found in NIF hohlraums. An imaging spectrometer collected emission spectra from the gold L-shell in the 8-12 keV photon energy range across the entire diameter of the sphere. Analysis of this data yields inferences of the charge state distribution and radial electron temperature profile, which are compared with a variety of rad-hydro simulations with modifications to the in-line atomic kinetics. Implications of the measured data compared with simulated data are discussed.

This work was performed under the auspices of the U.S. Department of Energy by Lawrence Livermore National Laboratory under Contract No. DE-AC52-07NA27344.

LLNL-ABS-2004877

**References**

[1] H. Chen, D. T. Woods, et al. Phys. Rev. E. **110**, L013201 (2024)

* E-mail: aybar1@llnl.gov

A-02

# Collision-enhanced EUV spectrum of laser-produced Al plasma collisions

X. B. Liu[1], Q. Min[1, *], S. Q. Cao[1],M. G. Su[1], and **C. Z. Dong[1, †]**

[1] Key Laboratory of Atomic and Molecular Physics & Functional Material of Gansu Province, College of Physics and Electronic Engineering, Northwest Normal University, Lanzhou 730070, China

Laser-produced colliding plasmas have been the focus of strong fundamental research interest and have spawned a wide range of applications including x-ray lasers, pulsed-laser deposition, fusion science, laser ion sources, plasma light sources and in the generation of astrophysical objects in the laboratory frame[1]. LPP contains highly charged ions with multiple ionization states. Under appropriate conditions, the plasma plumes generated by dual-pulse lasers inter-act and collide with each other and different particles transfer energy during the collision process. By increasing the frequency of interactions between particles, the excitation efficiency is enhanced. Therefore, we investigated the emission spectra of laser-induced Al collision plasmas and explored the influence of plasma spatial spacing on the enhancement of spectral signals.

Figure (a) shows the experimental equipment. Figure (b) shows the transient state of the colliding plasma, where two parallel short-pulse Nd:YAG laser beams (1064nm, FWHM:10ns, $3\times10^{10}$ W/cm$^2$, Spot size:150μm, 90mJ) with equal intensity are focused onto a 90° V-shaped aluminum target. Plasma emission through a 50 μm slit and captured by a grazing incidence EUV spectrometer. By adjusting the angle of focus lens and reflecting mirror, the relative distance between the two plasma beams is controlled to achieve a stronger interaction. The enhanced CCD camera can quickly im-age the plasma plume.

Figure (c) shows the experimental spectra of single pulse and Al plasmas collisions in the range of 8-14 nm. Different peaks from spectra are mainly from the 2p-3s, 3d, 4s, 4d and 5d transitions of $Al^{3+}$-$Al^{6+}$ ions. Compared with the case of single plasma, when the interval is large, the two plasmas do not interact with each other and the spectra are simply superimposed. The spectral intensity is higher and EUV light source duration extends when the spatial interval is smaller. This phenome-non is due to higher temperatures and a higher frequency of particle collisions. A more detailed explanation will be provided in the upcoming presentation.

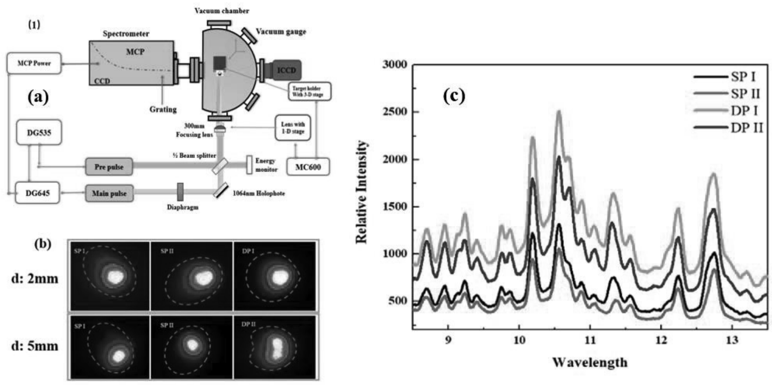


Figure 1 (a) shows the experimental equipment, (b) shows the transient state of the colliding plasma under different conditions, (c) shows the emission spectrum in Al plasma collisions.

References

[1] Hough P, et al 2011 J. Phys. D: Appl. Phys. 44 355203

† E-mail: dongcz@nwnu.edu.cn

## A-03

# Improvements in non-LTE atomic kinetics modeling for ICF hohlraums

**Mehul V. Patel**, Hai P. Le, Holden L. Parks

Lawrence Livermore National Laboratory, Livermore, California 94550, USA

Predicting the X-ray drive in hohlraums at the National Ignition Facility (NIF) is challenging for radiation-hydrodynamics simulations because of the complex interplay between a myriad of physical processes. Uncertainties in modeling the non-local thermodynamic equilibrium (non-LTE) state of the high-Z wall plasma can explain a significant fraction of the modeled drive discrepancy. We review how improved hohlraum energetics predictions have been achieved by successive improvements to the non-LTE atomic models including employing more complete models for the underlying atomic structure and transitions. Because of their computational expense (both in operations and memory), using our most complete atomic models for inline radiation hydrodynamics calculations has required using GPUs and the latest generation of supercomputers (Sierra at LLNL). We will demonstrate how these simulations can provide valuable benchmark data for complementary off-line approaches (steady-state non-LTE tables [1]) as well as estimate constraints on the impact of further improvements in non-LTE models.

Prepared by LLNL under Contract DE-AC52-07NA27344.

References

[1] H. A. Scott, J. A. Harte, M. E. Foord and D. T. Woods, Physics of Plasmas 29 (8) (2022)

A-04

# Analysis of soft X-ray spectra from N-shell ions of europium using the Tokyo EBIT

**Chihiro Suzuki**, Nobuyuki Nakamura*, Fumihiro Koike**, Izumi Murakami

National Institute for Fusion Science, 322-6 Oroshi-cho, Toki 509-5292, Japan
(*) The University of Electro-Communications, 1-5-1 Chofugaoka, Chofu, 182-8585, Japan
(**) Sophia University, 7-1 Kioi-cho, Chiyoda-ku, Tokyo 102-8554, Japan

Soft X-ray spectra emitted from highly charged lanthanide ions having outermost $N$-shell electrons ($N$-shell ions) are of particular interest in terms of basic atomic physics issues such as electron correlation and relativistic effects. For example, the atomic number ($Z$) dependence of the transition wavelength of Ga-like lanthanide ions exhibits an irregular behavior due to the energy level crossing at around europium (Eu, $Z$=63) [1]. Accordingly, the unambiguous identifications of spectral lines of Eu ions would be helpful for the comprehensive $Z$ dependence analysis. Regarding the measurements of charge-resolved spectra in electron beam ion traps (EBITs), a part of soft X-ray spectra from $M$-shell ions of Eu has already been observed in the SuperEBIT facility [2]. However, no EBIT data were available for soft X-ray spectra from $N$-shell ions of Eu.

In this study, we have observed a series of charge-resolved soft X-ray spectra from $N$-shell ions of Eu using the Tokyo EBIT facility at the University of Electro-Communications [3]. The electron beam energy was varied in the range of approximately 0.9–2.5 keV so as to cover charge states from Br-like to Cu-like ions. The spectra were recorded by a flat field grazing incidence spectrometer equipped with a grating of 1200 $\text{mm}^{-1}$ groove density [4] in the wavelength range of 5–30 nm. As for Cu-like to Ge-like ions, the measured spectra have been compared with the simulated spectra by the Flexible Atomic Code (FAC) [5], and some of the transition wavelengths are compared with the ones calculated with the GRASP92 code [6]. In addition, the interpolation of the $Z$ dependences of the transition wavelengths has been carried out using the existing experimental data on the other lanthanide elements. Consequently, a number of spectral lines of Eu ions were identified as the first or second order spectrum, including those of Ga-like ions relevant to the aforementioned energy level crossing.

References

[1] F. Koike, C. Suzuki, I. Murakami, D. Kato, N. Tamura, N. Nakamura, Phys. Rev. A **105**, 032802 (2022)

[2] E. Träbert, N. Hell, G. V. Brown, P. Beiersdorfer, J. H. T. Clementson, Can. J. Phys. **102**, 163 (2024)

[3] N. Nakamura, et al., Phys. Scr. **T73**, 362 (1997)

[4] H. Ohashi, J. Yatsurugi, H. A. Sakaue, and N. Nakamura, Rev. Sci. Instrum. **82**, 083103 (2011)

[5] M. F. Gu, Can. J. Phys. **86**, 675 (2008)

[6] F. A. Parpia, C. Froese Fischer, I. P. Grant, Comput. Phys. Commun. **175**, 745 (2006)

## A-05

# Statistical analysis on energy levels and effective line strengths of singly ionized lanthanides for opacity of kilonovae

**Daiji Kato**, Masaomi Tanaka*, Gediminas Gaigalas**, Laima Kitovienė**, Pavel Rynkun**

National Institute for Fusion Science, Toki, Gifu 509-5292, Japan
(*) Astronomical Institute, Tohoku University, Sendai, Miyagi 980-8578, Japan
(**) Institute of Theoretical Physics and Astronomy, Faculty of Physics, Vilnius University, Vilnius LT-10257, Lithuania

Lanthanides play essential roles in opacities for the kilonova, the ultraviolet-optical-infrared emission from the neutron star merger detected by the gravitational wave (GW170817) [1,2]. In the present study, we examined suitable statistical representations for quasi-continuous spectra of singly ionized lanthanides ($Z = 59 - 70$) based on our previous *ab-initio* calculations [3-6] using the multi-configuration Dirac-Hartree-Fock and parametric potential methods.

Using higher order *Gram-Charlier* expansions [7], an improved representation was obtained for the statistical distribution of the energy levels. Systematic features that appear in *mean, variance, skewness*, and *kurtosis* of the distribution are revealed. The *varience* is also evaluated using the semi-relativistic analytical formula [8] and using the trace of fully relativistic Hamiltonian matrices, which agree with the results obtained by the relativistic configuration interaction calculations.

It is shown that a quantitative index for evaluating kilonova opacity can be obtained from the analysis of the probability density distribution of the effective line intensity, that is defined as a product of the line strength and the Boltzmann factor at a given temperature. The single *Porter-Thomas* distribution [9] gives a good representation only at small effective line strengths, and the range of validity extends as temperature increases. On the other hand, we found that the *log-logistic* distribution gives a simple representation that is valid over a wide range of effective line strength. The scaling parameter of the log-logistic distribution gives an indicator on down to which transitions should be included in opacity calculations for neutron star mergers.

Energy levels and transition data in this presentation are available at *Japan-Lithuania Opacity Database for Kilonova (version 2.0)*: `http://dpc.nifs.ac.jp/DB/Opacity-Database/`.

References

[1] B.P. Abbott et al., Phys. Rev. Lett. **119**, 161101 (2017)

[2] B.P. Abbott et al., ApJL **848**, L12 (2017)

[3] G. Gaigalas et al., ApJS **240**, 29 (2019)

[4] L. Radžiūtė et al., ApJS **248**, 17 (2020)

[5] L. Radžiūtė et al., ApJS **257**, 29 (2021)

[6] D. Kato et al., MNRAS **535**, 2670 (2024)

[7] F. Gilleron et al., Phys. Rev. E **77**, 026708 (2008)

[8] C. Bauche-Arnoult, J. Bauche, M. Klapisch, Phys. Rev. A **20**, 2424 (1979)

[9] C. E. Porter, R. G. Thomas, Phys. Rev. **104**, 483 (1956)

**A-06**

# Atomic, Molecular, and Surface Collision Data Working Group in NIFS

**D. Kato**[1], M. Goto[1], T. Hirayama[2], M. Hiyama[3], M. Hoshino[4], Y. Hoshino[5], A. Igarashi[6], A.M. Imai[7], K. Ishii[8], M. Kato[1], T. Kawate[9], N. Kimura[1], M. Kitajima[10], T. Kusakabe[11], K. Moribayashi[12], T. Morishita[13], I. Murakami[1], B. Peterson[1], H.A. Sakaue[1], N. Shimakura[14], K. Soejima[14], H. Tsuchida[7]

(1) National Institute for Fusion Science (NIFS), Gifu 509-5292, Japan
(2) Rikkyo University, Tokyo 171-8501, Japan
(3) Gunma University, Gunma 376-8515, Japan.
(4) Sophia University, Tokyo 102-8554, Japan
(5) Kanagawa University, Kanagawa 221-8686, Japan
(6) Miyazaki University, Miyazaki 889-2192, Japan
(7) Kyoto University, Kyoto 615-8540, Japan
(8) Nara Women's University, Nara, 630-8506, Japan
(9) Naka Fusion Institute, QST, Ibaraki 311-0193, Japan
(10) Institute of Science Tokyo, Tokyo 152-8551, Japan
(11) Kindai University, Osaka 577-8502, Japan
(12) Kansai Institute for Photon Science, QST, Kyoto 619-0215, Japan
(13) The University of Electro-Communications, Tokyo 182-8585, Japan
(14) Niigata University, Niigata 950-2181, Japan

NIFS is promoting collaborative research organizing working groups of domestic experts to update and make more accessible the numerical database of collision cross sections of atoms and molecules in plasmas and ion sputtering yields and reflection coefficients on solid surfaces. The data are relevant not only to fusion plasma research but also industrial applications of plasmas and astronomical observations.

The working group searched and reviewed literatures relevant to cross section data for various processes of electron and ion collisions with molecules of hydrogen, hydrogen isotope, hydrocarbon, nitrogen, oxygen, carbon oxide, and water [1]. New data collected by this working group were added to the NIFS database (https://dbshino.nifs.ac.jp) for molecular target, i.e. AMOL (electron collision) and CMOL (ion collision).
Recently, cross section data for electron collisions and heavy particle collision with atoms and ions of high-Z elements, such as Fe, Ni, Mo, and W, together with Ne, Ar, Kr, Xe have been surveyed and collected [2]. The new data for excitation-, ionization- and total-cross sections for electron collision with atoms and ions of high-Z elements were stored into the NIFS database AMDIS. For the heavy particle impact cross section data, new data were stored into the NIFS database CHART.

From 2019, we started the new data working group for ion-sputtering of solid surfaces. In this working group, in addition to literature survey for ion-sputtering yield of tungsten by hydrogen isotopes, 3He, He, Be, C, N, O, Ne, Ar, K, Kr, Cd, Xe, Cs, W, Hg, and Pb ions, new measurements of self-sputtering yield were also conducted at 300 keV and 1 MeV energies using the electrostatic accelerator at Kyoto University. Empirical formula by Eckstein and Yamamura were examined with the data set including the new measurements. Based on these results, a novel neural network taking into account the empirical laws is being constructed to make a reliable prediction possible.

References

[1] M. Kimura et al., NIFS-DATA **98**, 1-38 (2006)
[2] M. Kitajima et al., NIFS-DATA, in preparation.

**A-07**

# Corrections to radiative rates between atomic configurations

**Jean-Christophe Pain**[1,2], Djamel Benredjem[3]

[1]CEA, DAM, DIF, F-91297 Arpajon, France
[2]Université Paris-Saclay, CEA, Laboratoire Matière en Conditions Extrêmes, F-91680 Bruyères-le-Châtel, France
[3]Université Paris-Saclay, CNRS, Laboratoire Aimé Cotton, F-91405 Orsay, France

The computation of radiative opacity or emissivity of hot dense matter is a challenging task. It requires accounting for an immense number of energy levels and lines across various excitation and ionization states. Whether in local thermodynamic equilibrium (LTE) [1] or non-LTE plasmas [2], statistical methods provide significant assistance [3]. Many computational codes are based on the Detailed Configuration Accounting approximation, which involves averaged rates between configurations. In that approach, only the mean energies of the configurations are considered, and the effect of the energy distribution of the levels within the initial and final configurations is typically neglected. In 1993, Klapisch introduced a method to correct the rates up to the second order [4]. These corrections include the shift and variance of the UTA (unresolved transition array), as well as the average energies of the configurations. We extend this formalism and investigate its impact on opacity calculations in two specific cases: the iron experiment conducted at Sandia under conditions similar to those at the base of the Sun's convective zone ($T$ = 182 eV and $\rho$ = 0.17 g/cm$^3$), dominated by 2p-$n$d transitions [5], and $T$ = 22 eV and $\rho$ = 0.01 g/cm$^3$, conditions typical of laser opacity measurements performed over the past decades [6] and likely to bring, to a certain extent, useful information about the envelopes of beta-Cephei-type stars [7]. The issue of ensuring the validity of Kirchhoff's law when plasmas approach LTE is also addressed, and a prescription is proposed. This prescription applies both to the standard configuration-to-configuration case and to the new corrections, which account for the energy distribution of the levels within a configuration.

<u>References</u>

[1] J.-Ch. Pain, F. Gilleron, J. Bauche and C. Bauche-Arnoult, High Energy Density Phys. **5**, 294 (2009)

[2] O. Peyrusse, J. Phys. B: At. Mol. Opt. Phys. **32**, 683 (1999)

[3] C. Bauche-Arnoult, J. Bauche and M. Klapisch, J. Opt. Soc. Am. **68**, 1136 (1978)

[4] M. Klapisch, A UTA approach to the collisional radiative model for ionization balance, In Proceedings of The Tenth International Colloquium on UV and X-Ray Spectroscopy of Astrophysical and Laboratory Plasmas, Berkeley, February 1992 (1993)

[5] J. E. Bailey *et al.*, Nature **517**, 56 (2015)

[6] G. Winhart, K. Eidmann, C. A. Iglesias and A. Bar-Shalom, Phys. Rev. E **53**, R1332 (1996)

[7] S. Turck-Chièze, M. Le Pennec, J. E. Ducret, J. Colgan, D. P. Kilcrease, C. J. Fontes, F. Gilleron, J.-C. Pain and N. Magee, Astrophys. J. **823**, 78 (2016)

## A-08

# Configuration- and superconfiguration-averaged excitation and ionization by electron impact in hot plasmas

**Djamel Benredjem**[1], Jean-Christophe Pain[2,3]

[1]Université Paris-Saclay, CNRS, Laboratoire Aimé Cotton, F-91405 Orsay, France
[2]CEA, DAM, DIF, F-91297 Arpajon, France
[3]Université Paris-Saclay, CEA, Laboratoire Matière en Conditions Extrêmes, F-91680 Bruyères-le-Châtel, France

This study investigates ionization and excitation processes induced by electron impact between configurations or superconfigurations, rather than individual energy levels. Transition and super-transition arrays [1, 2] are analyzed, focusing on oxygen-like ions relevant to inertial confinement fusion, specifically silicon, germanium, argon, and krypton. Cross sections are calculated using the Flexible Atomic Code [3] with the distorted-wave method, and rate coefficients are derived over a temperature range of $50-3000$ eV. To enable efficient rate interpolation with respect to both temperature and ion charge, the results are fitted with two-dimensional Chebyshev polynomial expansions [4], yielding a compact set of Chebyshev coefficients. An extension of the Clenshaw algorithm [5] to two dimensions, using the Chebyshev coefficients, is proposed to address numerical challenges and enhance computational efficiency.

References

[1] J. Bauche, C. Bauche-Arnoult, and M. Klapisch (Academic Press, 1988), pp. 131–195

[2] O. Peyrusse, J. Phys. B: At. Mol. Opt. Phys. **32**, 683 (1999)

[3] M. F. Gu, Can. J. Phys. **86**, 675 (2008)

[4] G. Faussurier and C. Blancard, Phys. Rev. E **95**, 053308 (2017)

[5] C. W. Clenshaw, J. Proc. Cambridge Phil. Soc. **53**, 134 (1957)

## A-09

# A new set of radiative decay rates for Os V – VI spectral lines of interest to nuclear fusion plasma analysis

M. Brasseur[1], E. Bokamba Motoumba[2], S. Enzonga Yoca[2,3], P. Palmeri[1], **P. Quinet[1,4]**

[1] Atomic Physics and Astrophysics, University of Mons, B-7000 Mons, Belgium
[2] Faculté des Sciences et Techniques, Université Marien Ngouabi, Brazzaville, Congo
[3] Conseil Africain et Malgache pour l'Enseignement Supérieur, Ouagadougou, Burkina Faso
[4] IPNAS, University of Liège, B-4000 Liège, Belgium

We already know that the ITER Tokamak divertor will be made of tungsten (Z = 74) and some ionic impurities of all possible charge states can be produced, including osmium (Z = 76), by sputtering of neutron flux. On the one hand, these impurities resulting from the transmutation of tungsten will contribute to the radiation losses and, on the other hand, they could allow to diagnose the fusion plasma in terms of temperature and density. Therefore, the knowledge of the radiative parameters corresponding to all charge states of osmium are of great interest for the development of fusion reactors. In the present contribution, we focus on Os V and Os VI ions for which the decay rates (transition probabilities and oscillator strengths) were computed using two independent theoretical approaches, namely the pseudo-relativistic Hartree-Fock including core-polarization corrections (HFR+CPOL) and the fully-relativistic Dirac-Hartree-Fock (MCDHF) methods. This multiplatform approach allowed us to establish a new consistent set of atomic data for a large amount of electric dipole lines in these two specific osmium ions. From cross comparisons between the results obtained in our HFR+CPOL and MCDHF calculations, as well as from comparisons with previously published data, the uncertainty on the computed transition probabilities could be estimated.

**A-10**

# Calculation of M1 and E2 transition probabilities in lanthanide ions for kilonovae nebular-phase analysis

L. Maison[1], J. Deprince[1], P. Palmeri[1], **P. Quinet[1,2]**

[1] Atomic Physics and Astrophysics, University of Mons, B-7000 Mons, Belgium
[2] IPNAS, University of Liège, B-4000 Liège, Belgium

On August 17, 2017, the LIGO/Virgo collaboration detected for the first time a gravitational wave signal (GW170817) associated with a neutron star merger. This event marked a milestone in multi-messenger astronomy. The merger ejected a significant amount of hot and radioactive matter into space, where nuclear reactions synthesized elements heavier than iron, including lanthanides (Z = 57–71). The radioactive decay of these elements powered a transient electromagnetic phenomenon known as a kilonova.

In the early stages, kilonova spectrum is dominated by numerous allowed transitions from heavy elements. However, in the later nebular phase, the temperature and density of the ejecta decrease significantly, limiting the ionization stage to at most doubly charged species. Under these conditions, only low-energy levels, such as metastable states, are populated, resulting in forbidden emission lines such as magnetic dipole (M1) and electric quadrupole (E2) transitions. Observations of kilonova AT2017gfo and more recently of a similar transient event recorded in March 2023 by the James Webb Space Telescope have revealed infrared spectral features in the late-time spectra potentially linked to forbidden transitions of lanthanides and other heavy elements.

To facilitate the analysis of such spectra, new calculations of transition probabilities for M1 and E2 lines between low-lying levels in singly and doubly ionized lanthanide atoms were carried out. The fully relativistic Multi-Configurational-Dirac-Hartree-Fock (MCDHF) method, implemented in the GRASP2018 code, was employed to model the atomic structure and compute radiative parameters. Results were compared to those obtained using the pseudo-relativistic Hartree-Fock (HFR) approach to ensure reliability. This work provides a consistent set of atomic data, highlighting the most intense forbidden lines of lanthanides, which are likely to be observed in the infrared spectra of kilonovae during their nebular phase.

# A-11

## Computation of electron-impact excitation collision strengths in Sr II and Te III in the context of nebular-phase kilonovae

K. Lejeune, **J. Deprince***, L. Maison, P. Palmeri, P. Quinet

Atomic Physics and Astrophysics, University of Mons, Belgium
(*) Jerome.Deprince@umons.ac.be

Gravitational waves emitted following a neutron star merger (NSM) were observed for the first time in 2017 (GW170817) [1]. An electromagnetic signal known as a kilonova (KN) emitted by newly synthesized r-process elements during such an event was also detected (AT2017gfo), suggesting the presence of heavy elements in the KN ejecta [2]. More recently, the spectrum of a new KN was observed by the JWST at late times [3].

NSMs are candidate sites of heavy element production [4], a process that remains incompletely understood so far. KN modeling has thus become a topic of significant scientific interest. During the first few days after the merger, the KN ejecta is in its photospheric phase, and the LTE assumption is valid, simplifying the calculation of atomic energy level populations through Boltzmann and Saha equations. About a week post-merger, the KN ejecta begins its nebular phase, where non-LTE effects become important [5], making the determination of energy level populations extremely complex.

To model nebular-phase KN spectra, it is thus necessary to account for all radiative and collisional processes that can (de)populate the various energy levels of the ejecta ions, such as radiative transitions, electron impact collisions, dielectronic recombinations, photoionization and radiative recombinations. In this work, we model the electron-impact excitation process in heavy ions (potentially) observed in KN spectra, such as Sr II and Te I-III [6,7], by means of two different approaches: the Plane Wave Born approximation as implemented in the pseudo-relativistic Hartree-Fock (HFR) method [8] and a Distorted Waves approach using Autostructure [9]. The resulting collision strengths are compared with values available in the literature that were calculated using the more complex R-matrix method [10,11] to assess the validity of our approximations in the purpose of large-scale calculations in all heavy elements (in particular, lanthanides and actinides) suspected to be present in the KN ejecta. In addition, radiative parameters for allowed and forbidden transitions are also computed using HFR.

References

[1] B.P. Abbott, R. Abbott, T.D. Abbott *et al.*, Phys. Rev. Lett. **119**, 161101 (2017)
[2] D. Kasen, B. Metzger, J. Barnes *et al.*, Nature **551**, 80 (2017)
[3] A. Levan, B. Gompertz, O. Sharan Salafia *et al.*, Nature **626**, 737 (2024)
[4] B.D. Metzger, G. Martinez-Pinedo, S. Darbha *et al.*, MNRAS **406**, 2650 (2010)
[5] Q. Pognan, A. Jerkstrand and J. Grumer, MNRAS **510,** 3806 (2022)
[6] J.H. Gillanders, S.J. Smartt, S.A. Sim *et al.,* MNRAS **515,** 631 (2022)
[7] J.H. Gillanders and S.J. Smartt, MNRAS **538**, 1663 (2025)
[8] R.D. Cowan, The Theory of Atomic Structure and Spectra, California University Press, Berkeley (1981)
[9] N. Badnell, CPC **182**, 1528 (2011)
[10] L.P. Mulholland, N.E. McElroy, F.L. McNeill *et al.*, MNRAS **532**, 2289 (2024)
[11] L.P. Mulholland, N.E. McElroy, F.L. McNeill *et al.*, MNRAS **534**, 3423 (2024)

**A-12**

# Atomic data computations for the identification of heavy elements in hot subdwarfs

S. Beauraind[1], **J. Deprince**[1,2]*, M. Dorsch[3], L. Maison[1] and P. Quinet[1,4]

[1]Atomic Physics and Astrophysics, University of Mons, Belgium
[2]Astronomy and Astrophysics Institute, University of Brussels, Belgium
[3]Institut für Physik und Astronomie, Universität Potsdam, Germany
[4]IPNAS, University of Liège, Belgium
(*) Jerome.Deprince@umons.ac.be

Hot subdwarf stars represent a rare late evolutionary stage of low-mass stars. They are characterized by high temperatures, typically between 20,000 and 60,000 K. Their formation remains poorly understood, but is partly explained by binary interactions on the red giant branch and white dwarf mergers. In particular, the strong overabundances of certain heavy elements detected in several hot subdwarfs have yet to be explained [1-3]. One proposed hypothesis is that such overabundances are caused by radiative diffusion—a competition between radiative levitation and gravity [4]—while an alternative idea involves the i-process, a nucleosynthesis process similar to the s-process but requiring a higher neutron flux, or possibly a combination of both mechanisms [5,6]. However, the reliability of current models is limited due to the lack of atomic data for these heavy elements, which exist in ionization stages III to V under the typical conditions found in hot subdwarf atmospheres.

The goal of this work is to contribute to the study of hot subdwarf stars through the calculation of atomic parameters (energy levels, transition wavelengths, oscillator strengths) for selected lowly-charged (III – V) heavy elements (typically with atomic numbers $70 \leq Z \leq 90$), such as Hf and Tl. These elements were recently identified for the first time in a star, based on the Hubble Space Telescope (HST) spectrum of the hot subdwarf EC22536-5304 [3]. However, the lack of reliable atomic data for these species prevents the identification of many observed spectral lines, and thus leads to inaccurate abundance estimates. A multi-platform approach was used for the atomic calculations, combining the pseudo-relativistic Hartree-Fock (HFR) method as implemented in the Cowan's code [7] and the fully-relativistic Multiconfiguration Dirac-Hartree-Fock (MCDHF) approach using the GRASP2018 package [8]. In this contribution, we present the atomic data that we obtained for Hf IV and Tl IV, as well as new spectra simulations including these data, which are compared to the observed HST spectrum of the hot subdwarf EC22536-5304.

References

[1] M. Dorsch, M. Latour, and U. Heber, A&A **630**, A130 (2019)
[2] M. Dorsch, M. Latour, and U. Heber et al., A&A **643**, A22 (2020)
[3] M. Dorsch, C. S. Jeffery, A. Irrgang et al., A&A **653**, A120 (2021)
[4] G. Michaud, J. Richer and O. Richard, A&A **529**, A60 (2011)
[5] T. Battich, M.M. Miller Bertolami, A. M. Serenelli et al., A&A **680**, L13 (2023)
[6] T. Battich, M.M. Miller Bertolami, A. Weiss et al., A&A, accepted (2025); arXiv:2503.23541 **[astro-ph.SR]**
[7] R.D. Cowan, The Theory of Atomic Structure and Spectra, California University Press, Berkeley (1981)
[8] P. Jönsson, M. Godefroid, G. Gaigalas et al., Atoms **11**, 7 (2023)

# A-13

## Bound-Bound opacity calculations of heavy elements in kilonova ejecta

**Sirine Ben Nasr**, Jerome Deprince, Helena Carvajal Gallego, Patrick Palmeri, Pascal Quinet

Atomic physics and astrophysics, University of Mons, 7000 Mons, Belgium

Neutron star (NS) mergers are at the origin of gravitational waves (GW) detected by LIGO/Virgo interferometers [1]. This collision are cosmic laboratories for heavy-element nucleosynthesis, with kilonovae emissions powered by the radioactive decay of r-process elements.

Among these elements, those belonging to the fifth and sixth rows of the periodic table, are the greatest contributors to the opacity affecting the kilonova spectra, after the lanthanides and actinides. In the present work, new calculations of atomic structures and radiative parameters (wavelengths and oscillator strengths) are reported for a large number of spectral lines in some representative elements belonging to the fifth row, namely Nb (Z = 41) and Ag (Z = 47) [2], and belonging to the sixth row, namely Hf (Z = 72), Os (Z = 76) and Au (Z = 79) [3] from neutral to triply ionized states. The results obtained were used to calculate the expansion opacities characterizing the kilonova signal observed resulting from the collision of two NS, for typical conditions corresponding to time after the merger t = 1 day, the temperature in the ejecta T ≤ 15000 K, and a density of $\rho = 10^{-13}$ g.cm$^{-3}$, corresponding to the local thermodynamical equilibrium photosphere phase of the KN ejecta.

In order to do so, we used the pseudo-relativistic Hartree-Fock (HFR) method as implemented in Cowan's codes, in which the choice of the interaction configuration model is of crucial importance. The results presented in this work are the most complete currently available and are useful for astrophysicists to interpret kilonova spectra.

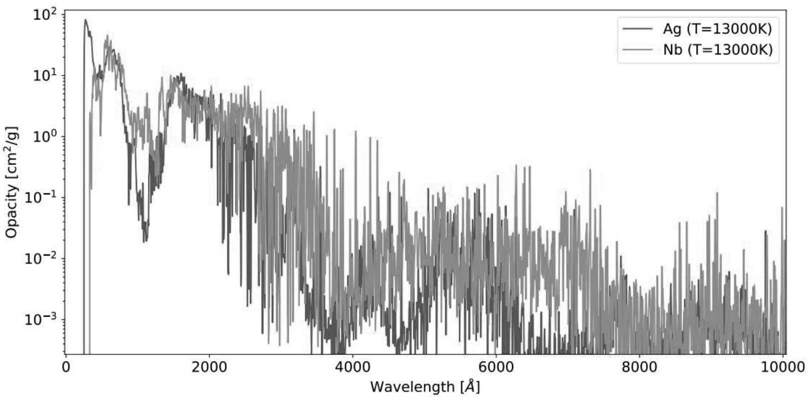


Figure 1: Expansion opacity of Nb and Ag, for T=13000 K, $\rho=10^{-13}$ g.cm$^{-3}$, t=1d and Δλ=10Å.

References

[1] B.P. Abbott, R. Abbott, T. D. Abbott *et al*, Phys. Rev. Lett. **119**, 161101 (2017a)
[2] S. Ben Nasr, H. Carvajal Gallego, J. Deprince, P. Palmeri, P. Quinet, A&A. **678**, A67 (2023)
[3] S. Ben Nasr, H. Carvajal Gallego, J. Deprince, P. Palmeri, P. Quinet, A&A, **687**, A41 (2024)

## A-14

# Experimental Transition Probabilities of Lanthanide elements (La, Ce, and Eu) using Laser-Induced Breakdown Spectroscopy for Astrophysical applications

**Kodangil Supriya**[a], Masaomi Tanaka[b], Daiji Kato[c,d], Gediminas Gaigalas[e], Hajime Tanuma[f], Nobuyuki Nakamura[a]
[a]Institute of Laser Science, University of Electro-Communications, 1-5-1 Chofugaoka, Chofu, 182-0021, Tokyo, Japan
[b]Astronomical Institute, Tohoku University, 2-1-1 Katahira, Aoba-ku, Sendai, 980-8578, Miyagi, Tokyo
[c]National Institute for Fusion Science, 322-6 Oroshi-cho, Toki, 509-5292, Gifu, Tokyo
[d]Interdisciplinary Graduate School of Engineering Sciences, Kyushu University, 1-1 Minami-Osawa, Kasuga, 816-8580, Fukuoka, Japan
[e]Institute of Theoretical Physics and Astronomy, Vilnius University, Saul ˙atekio av. 3, LT-10257, Vilnius, Lithuania
[f]Department of Physics, Tokyo Metropolitan University, 1-1 Minami-Osawa, Hachioji-shi, 192-0397, Tokyo, Japan

Atomic data, such as transition probabilities, play an important role in astrophysical applications, especially in studying kilonovae emissions observed after the merging of two neutron stars. These events are responsible for the formation of heavy elements in the universe, and accurately quantifying their emissions requires precise atomic data [1]. However, for heavy elements like lanthanides, existing atomic spectral databases, such as the National Institute of Standards and Technology [2], remain incomplete. While several theoretical methods have been successfully applied to atomic data calculations [3,4], experimental measurements remain essential for validation and accuracy. In this study, we use Laser-Induced Breakdown Spectroscopy (LIBS), an atomic emission spectroscopy technique, which is usually used for qualitative and quantitative analysis. Recently, LIBS has also gained attention for atomic data measurements [5,6].
Here, we investigate three lanthanide elements—Lanthanum (La), Cerium (Ce), and Europium (Eu)—and measure transition probabilities (A-values) for several emission lines of singly ionized (La II, Ce II, Eu II) and neutral (Eu I) species. This work not only reports new A-values for these elements but also demonstrates the applicability and versatility of LIBS in atomic data measurements.

References

[1] Tanaka, M., Kato, D., Gaigalas, G., Rynkun, P., Radˇzi¯ut˙e, L., Wanajo, S., Sekiguchi, Y., Nakamura, N., Tanuma, H., Murakami, I., et al., 2018. Properties of kilonovae from dynamical and post-merger ejecta of neutron star mergers. The Astrophysical Journal 852, 109.
[2] Ralchenko, Y., 2005. Nist atomic spectra database. Memorie della Societ`a Astronomica Italiana Supplement, v. 8, p. 96 (2005) 8, 96.
[3] Bar-Shalom, A., Klapisch, M., Oreg, J., 2001. Hullac, an integrated computer package for atomic processes in plasmas. Journal of Quantitative Spectroscopy and Radiative Transfer 71, 169–188
[4] Fischer, C.F., Gaigalas, G., J¨onsson, P., Biero´n, J., 2019. Grasp2018—a fortran 95 version of the general relativistic atomic structure package. Computer Physics Communications 237, 184–187.
[5] Messaoud Aberkane, S., Safi, A., Botto, A., Campanella, B., Legnaioli, S., Poggialini, F., Raneri, S., Rezaei, F., Palleschi, V., 2020. Laser-induced breakdown spectroscopy for determination of spectral fundamental parameters. Applied Sciences 10, 4973
[6] Kodangil, S., Domoto, N., Tanaka, M., Kato, D., Gaigalas, G., Tanuma, H., Nakamura, N., 2024. Measurement of transition probabilities of la ii using laser induced breakdown spectroscopy (libs). Journal of Quantitative Spectroscopy and Radiative Transfer 322, 109011

A-15

# Gaunt factor, collision strength and electron-impact excitation cross-section for Sn ions

**S. Aggarwal**[1,2], J. Sheil[1,2]

[1]Advanced Research Center for Nanolithography, Science Park 106, 1098 XG Amsterdam, The Netherlands

[2]Department of Physics and Astronomy, and LaserLaB, Vrije Universiteit Amsterdam, De Boelelaan 1081, 1081 HV Amsterdam, The Netherlands

One of the challenging topics in plasma physics is the calculation of the populations of energy levels of the various ions produced in the plasma. It is important to know these populations to quantify the radiation produced by plasma in relevance to extreme ultraviolet nanolithography [1]. Very recently, Sheil *et al.* [2] found that the populations of these systems can be approximated using the so-called two-level model by calculating effective temperatures (see Eq. (1)). This two-level model is as follows: Let $n_2$ and $n_1$ denote the populations of the two levels, $E_{21}$ denotes the energy separation between these two levels, $n_e$ denotes the number of free electrons in the plasma (the so-called free-electron density) and $T_e$ denotes the plasma temperature (specifically the electron temperature). The populations can be shown to follow a simple analytic relation:

$$\frac{n_2}{n_1} = \frac{g_2}{g_1} \exp\left(\frac{-E_{21}}{T_e}\right) \left[1 + \frac{\mathcal{C} E_{21}^3 T_e^{1/2}}{n_e \bar{g}}\right]^{-1} = \frac{g_2}{g_1} \exp\left(\frac{-E_{21}}{T_{eff}}\right) \tag{1}$$

The symbol $\mathcal{C}$ is a constant, $g_{1(2)}$ represents the statistical weights of levels 1 and 2, $T_{eff}$ is the effective temperature, and $\bar{g}$ is the so-called Gaunt factor. This Gaunt factor introduces quantum mechanical corrections to classical cross-sections. Accurate determination of the Gaunt factor is crucial for estimating the population densities of atomic levels. Several formulations exist in the literature for calculating the Gaunt factor [3], with some providing analytical expressions while others offer tabulated or fitted values based on the specific transitions and energy ranges involved. In this work, the Jena Atomic Calculator (JAC) has been employed to compute the collision strengths ($\Omega$), which are fundamental quantities describing the probability of electron-impact excitation. These collision strengths are then used to derive the corresponding electron-impact excitation cross-sections. To assess the accuracy and applicability of various Gaunt factor formulations, the computed cross-sections from JAC are compared with those obtained via analytical cross-section formulas incorporating Gaunt factors. By performing this comparison, an effective Gaunt factor can be deduced—one that best reproduces the numerically predicted cross-sections.

References

[1] F. Torretti *et al.* 2020 *Nat. Commun.* **11 2334**.

[2] J. Sheil *et al.* 2025 *in preparation.*

[3] S. M. Younger and W. L. Wiese, 1979 *J. Quant. Spectrosc. Radiat. Transfer* **22 161-170**.

A-16

# Evaluation of the electron impact excitation cross-sections of atomic hydrogen for incident energy upto 1 MeV

**Gajendra Singh**[1], M. B. Chowdhuri[1] and Joydeep Ghosh[1,2]

[1]Institute for Plasma Research, Bhat 382 428, Gandhinagar, India
[2]Homi Bhaba National Institute, Anushaktinagar, Mumbai 400 094, India

Electron impact excitation (EIE) cross-sections of the states having n = 2 - 6 of atomic hydrogen and their respective rate coefficients have been calculated for a wide range of incident electron energies (1.0 eV to 1 MeV) using the fully relativistic distorted wave method. A huge range of incident energies i.e. 1 eV to 1 MeV are considered here for the calculation since the tokamak plasma consists of both thermal and non-thermal electrons with wide range of energies. The cross-sections and collisional rate coefficients at lower energies, i.e. ≤ 10 keV are readily available but for very high energies, these are sparsely available. Thus, the present work aims to provide these atomic data, which is very crucial to do accurate collision radiative modelling of the spectral lines in Blamer series, mainly $H_\alpha$, $H_\beta$, $H_\gamma$ and $H_\delta$, from tokamak plasmas [1]. Here, the computed transition energies and prominent transition probabilities have been compared with NIST experimental values and other calculations performed in the past for the evaluation purpose. It has been observed that the presently computed collision strengths associated with prominent lines in Balmer series are reduced more than 5 order in magnitude at 1 MeV from its highest value at low energy. The excitation rate coefficients have been also computed and have been compared to existing data.

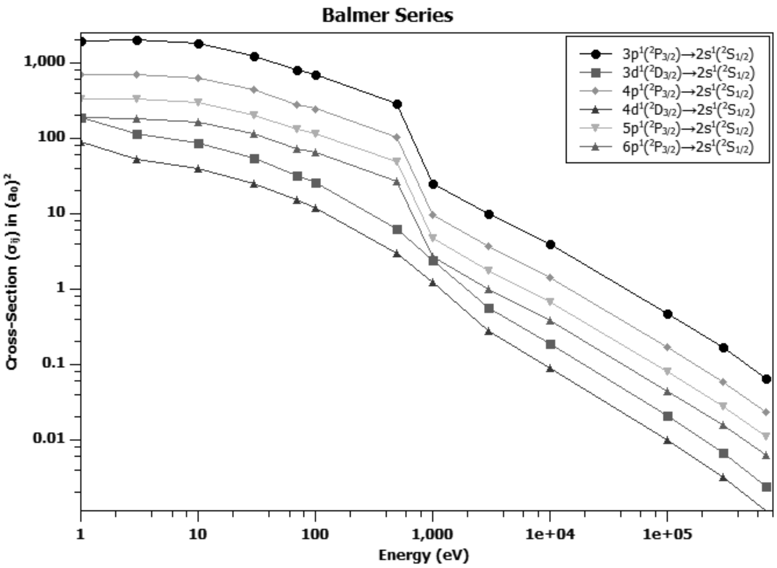


Figure 1: EIE cross-section of prominent Balmer series lines in H atom with electron incident energy from 1 eV to 1 MeV.

References

[1] R. L. Tanna, T. Macwan, J. Ghosh, *et al*. Nuclear Fusion **62**, 042017 (2022).

A-17

# Electronic collisions with molecular cations: species relevant in the edge of the fusion plasma and plasma facing material in the fusion devices.

R. Ghosh,[1,*] K. Chakrabarti,[2] and B. S. Choudhury[1]

[1] *Department of Mathematics, Indian Institute of Engineering Science and Technology, Shibpur, Howrah 711103, India*
[2] *Department of Mathematics, Scottish Church College, 1 & 3 Urquhart Sq., Kolkata 700006, India*

The impetus behind this abstract comes in relation with studies in experimental nuclear reactors with walls made up of materials containing simple atoms (e.g., Be, C, N), referred to as PFPs or plasma facing materials, that may react with the fuel atoms (H, D, T) producing BeH, CH, NH, and their cations, all this related to the long-time elusive quest for controlled nuclear fusion energy employing magnetic-field confinement, particularly related to ITER. Generally, for kinetic modeling of low temperature plasmas, it is not only essential to know all the constituent species present in the plasma, but also the reaction rate coefficients (which can be obtained from cross sections) for dominant collision processes that are pathways to final products.

Molecular ions are a constituent of many low temperature plasmas, where collision of these ions with electrons play an important role governing their chemistry. Hydrocarbon ions, and in particular $CH^+$, are found in the edge plasmas in those fusion reactors operating with graphite or carbon fiber composite as plasma facing material[1]. Sometimes these ions occur as an impurity in the plasma of fusion reactors operating with graphite as plasma facing material and plays a crucial role in understanding carbon erosion and redeposition. Collision cross sections for these processes are therefore important for modeling of the plasma environment and to understand the chemistry of formation and destruction of $CH^+$ as well as the carbon erosion and redeposition in the plasma facing components.
Many nitrogen plasmas contain $NH^+$ and therefore the kinetic modeling of these plasmas require cross sections for different electron induced processes in $NH^+$. $NH^+$ is also to be observed in a fusion plasma (or indeed any other sort of plasma for example ammonia plasmas) and it will be via emissions from its electronically excited states.
The competitive model of quantum mechanics can be used to describe Feshbach resonances, which are extremely excited bound states superposed with the continuum. Because they generate dissociation at low energy, these bound states are essential for explaining the dissociative recombination of the molecule that often occurs in this plasma environment. One effective theory that yields quantitative findings for identifying the interaction indicated by potential energy curves is the R-Matrix technique. The contribution of Feshbach resonances to the dissociation of molecules, as indicated by the dissociative rates, will be discussed in this presentation. The illustrations are based on $CH^+$ [2]and $NH^+$[3] cations and corresponding to CH and NH molecules.
We have obtained a detailed construction of the potential energy curves for the ions $CH^+$, $NH^+$, and resonant states and corresponding their widths as the inter-nuclear distance R varies. Other collisional calculations should benefit from these resonant states, particularly the dissociative recombination of the $CH^+$ and $NH^+$ ions. Several resonant states of different symmetries, which were unknown till now, have been systematically identified and their widths calculated, which proved much more challenging due to the presence of many avoided crossings. It is hoped that the bound and the new resonant states we obtained will open up other molecular dynamics studies so that the fusion devices can be improved in the future.

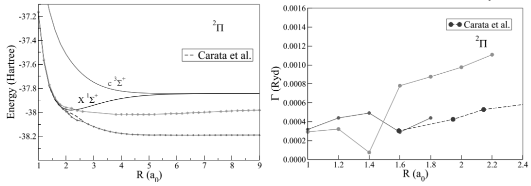


FIG. 1. Resonance and width curves (starred) of $^2\Pi$ symmetry. The dashed curve in the left panel is the $2^2\Pi$ diabatic state of Carata *et al* (2000) shifted up by 0.082 Hartree. Shown also are the ground state $X^1\Sigma^+$ and the c $^3\Sigma^+$ excited state of $CH^+$ ion.

[1] H. Tawara, Atomic and Molecular Processes in Fusion Plasmas ed R K Janev (New York: Plenum) 461–96(1995)
[2] K. Chakrabarti, A. Dora, R. Ghosh, B. S. Choudhury, and J. Tennyson J. Phys. B: At. Mol. Opt. Phys. 50 175202 (2017)
[3] R. Ghosh, K. Chakrabarti, and B. S. Choudhury, Plasma Sources Sci. Technol. 31 065005 (2022)
[4] Ghosh et al.(comminicated).

* rajughosh152@gmail.com

A-18

# Polarization spectroscopy of He I $2^3S$-$2^3P$ emission line in an ECR plasma with quantification of instrumental polarization

Yuki Watanabe, **Taiichi Shikama**, Hiroto Inagaki, and Masahiro Hasuo

Graduate School of Engineering, Kyoto University, Kyoto 615-8540, Japan

A diagnostic technique that utilizes the polarization of atomic and ionic emission lines to measure the anisotropy of the electron velocity distribution in plasmas is known as plasma polarization spectroscopy. In most experimental studies on discharge plasmas, the observed degree of polarization is typically a few percent or less. Consequently, instrumental polarization originating from reflections off the vacuum chamber walls and spectroscopy system poses a limitation to measurement accuracy. In this study, we performed polarization spectroscopy of the He I $2^3S$-$2^3P$ emission line, with quantification of the instrumental polarization.

The He I $2^3S$-$2^3P$ emission line has a fine structure with *J-J'* = 1-0, 1-1, and 1-2 transitions [1]. The wavelength separation between 1-0 and the other transitions is approximately 120 pm, which exceeds the Doppler width in a typical discharge plasma (13 pm at 0.1 eV). As a result, the spectral profile exhibits two distinct peaks. The smaller peak corresponds to the 1-0 transition, which does not exhibit collisional polarization due to the presence of only a single upper-state sublevel. Furthermore, its low opacity suppresses polarization arising from radiative transfer [2]. Based on these characteristics, we regarded the polarization of the smaller peak as the instrumental polarization.

The spectroscopy system consisted of two photoelastic modulators [3], a linear polarizer, and a spectrometer. Plasma emission was collected along a single line of sight (LOS) and the spectrometer output light intensity was detected using a photomultiplier tube. The wavelength resolution was approximately 65 pm, and the normalized Stokes parameters $q$, $u$, and $v$ were measured in two wavelength regions centered at 1082.91 nm and 1083.03 nm, corresponding to the smaller and larger peaks, respectively. The experiment was conducted using a helium ECR plasma produced in a cusp magnetic field under various pressures ranging from 6.8 to 550 mPa. The plasma was sustained for approximately 140 ms, and measurements were performed over an 80 ms period. The LOS was aligned to cross the ECR surface, and a viewing dump was installed on the opposite wall to minimize reflected light.

The measured degree of polarization at the smaller peak was below 1%, and this was regarded as the instrumental polarization. This value was subtracted from polarization observed at the larger peak. After subtraction, the degree of polarization at the larger peak was approximately 6%, and the polarization direction was nearly perpendicular to the local magnetic field at the LOS-ECR surface intersection. The obtained $q$, $u$, and $v$ all showed significant values, suggesting the possible presence of both collisional polarization and polarization induced by radiative transfer.

References

[1] T. Shikama, *et al., J. Phys. D: Appl. Phys.* **49**, 025206 (2016).
[2] T. Shikama, *et al., Jpn. J. Appl. Phys.* **53**, 086101 (2014).
[3] T. Teramoto, *et al., Appl. Phys. Lett.* **112**, 214101 (2018).

# Results on VIS and VUV Spectroscopy of hydrogen atoms and molecules in linear plasma device PSI-2

O. Marchuk, M. Sackers, S. Brezinsek, V. Kotov, M. Reinhart, G. Sergienko and A. Kreter

*Forschungszentrum Jülich GmbH, Institute of Fusion Energy & Nuclear Waste Management - Plasma Physics*

Emission of atomic and molecular lines of hydrogen plays an essential role in low-temperature laboratory, astrophysical and fusion plasma. The absolute and/or relative intensity of the lines as well as the line shape provide us with the valuable information on plasma parameters (density and temperature, magnetic or electric field strength, concentration of species, etc.) and in many cases serve as a reliable instrument to determine and characterize the physical and chemical processes at plasma-surface interaction. So, for example, the series of Balmer-lines represents a reliable tool to monitor the development of detachment at plasma-surface interaction in fusion plasma.

The linear plasma devices serve for many years as a testbed to perform the measurements in a controlled environment to benchmark the reactions collected in different plasma codes and thus, prove their reliability. One should admit, however, that the emission of molecular and atomic lines at linear plasma device PSI-2 [1] is still not completely understood. So, for instance, the two-component profile of Balmer lines as observed at linear plasma devices PSI-2 [2, 3] and MAGNUM [4] is still a subject of an ongoing discussion in the literature in the last decade. And if on one hand, the broad rotating component of Balmer lines was explained by the MAR process due to the presence of molecular ions $H_2^+$ in the plasma [4], another explanation is based on the symmetric charge-exchange reaction between $H^+$ ions and atoms [2]. Also, the transition to the recombined plasma demonstrated the clear role of molecular ions in the past, though full agreement with the modelling was not achieved [5].

In this work we performed the absolute calibrated measurements of the molecular lines, Balmer series of hydrogen lines (360-900 nm) but also the high-resolved line shapes (measurements of the first three Balmer ($\alpha$, $\beta$, $\gamma$) lines along the plasma radius) with the aim to collect the complete spectroscopic sets of experimental data for subsequent line intensity modelling using the Yacora code and AMJUEL database [6, 7]. Finally, the measurements are supported by the recently obtained VUV spectra in the range of 120-200 nm. The comparison of the data with the collisional radiative model using AMJUEL and Yacora code would be presented.

**References**

1. Kreter A et al 2015 Fusion Sci. Technol. 68 8.
2. O. Waldmann, Meyer H, and Fussmann G. Contrib. Plasma Phys. **47**, No. 10, 691 – 702 (2007).
3. O Marchuk et al 2018 J. Phys. B: At. Mol. Opt. Phys. **51** 025702.
4. H. J. van der Meiden, W. A. J. Vijvers, J. Westerhout, N. J. Lopes Cardozo and G. J. van Rooij, Phys. Rev. E **78**, 046405 (2008).
5. A. Pospieszczyk et al, Journal of Nuclear Materials,438 S1249-S1252 (2013).
6. Reiter D. 2020 AMJUEL database (available at: www.eirene. de/Documentation/amjuel.pdf)
7. D. Wünderlich, M. Giacomin, R. Ritz and U. Fantz, J. Quant. Spectrosc. Radiat. Transfer 240, **2020**, 106695, doi:10.1016/j.jqsrt.2019.106695

# BH molecular emission in the divertor region of LHD: Q-branch analysis and rotational temperature measurement

**A. Kuzmin**[1], T. Shikama[1], T. Kawate[2], S. Masuzaki[3,4], M. Shoji[3,4], F. Nespoli[5], R. Lunsford[5], E. Gilson[5], M. Hasuo[1]

[1]*Graduate School of Engineering, Kyoto University, Kyoto, Japan*
[2]*National Institutes for Quantum Science and Technology, Naka, Japan*
[3]*National Institute for Fusion Science, Toki, Japan*
[4]*Graduate University for Advanced Studies, SOKENDAI, Toki, Japan*
[5]*Princeton Plasma Physics Laboratory, Princeton, NJ, United States of America*

kuzmin.arseniy.6x@kyoto-u.ac.jp

In the context of real-time wall conditioning for fusion devices, boron plays a central role as a gettering material capable of reducing impurity content and hydrogen recycling. Recent experiments on the Large Helical Device (LHD), including those by Kawate *et al.* [1], have demonstrated the effectiveness of boron powder injection in modifying plasma-facing surfaces and enhancing plasma performance. Among the observed signatures, boron monohydride (BH) molecular emission has emerged as a potentially useful diagnostic for surface interactions and boron-related chemistry near the divertor.

In this work, we analyze spectrally resolved BH emission during LHD discharges with boron powder injection. We focus on the Q-branch of the $X^1\Sigma^+$–$A^1\Pi$ transition, which appears prominently in lines of sight viewing the divertor region. This localization supports the idea that BH is formed predominantly near material surfaces, likely through surface reactions or sputtering processes.

The observed spectra (Fig. 1) show a clear Boltzmann distribution in rotational states, suggesting that the BH molecules are in or near thermal equilibrium. Spectral fitting yields a rotational temperature of approximately 3600 K, with only minor variation depending on the line of sight. This value is notably higher than might be expected for a purely sputtering-driven origin, raising the possibility that additional energy input—such as from chemical reactions on the surface—may contribute to the formation and excitation of BH.

These findings underscore the relevance of BH as a sensitive tracer of surface conditions and boron-related chemistry in fusion devices. Further analysis, including modeling and comparison with theoretical cross sections, will help clarify the formation pathways and diagnostic utility of BH emission.

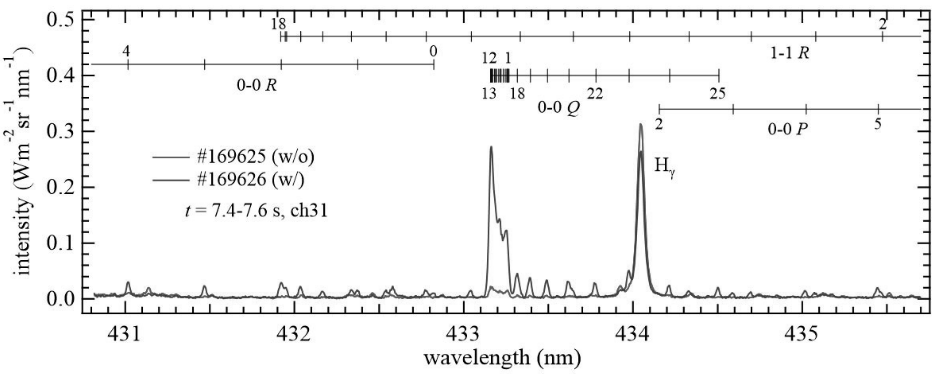


Fig. 1. Observed ro-vibrational structure in the BH molecular spectra during LHD discharges #169625 (without boron injection) and #169626 (with boron injection), for the time interval $t$ = 7.4–7.6 s, as measured on channel 31.

[1] T. Kawate *et al.*, *Nucl. Fusion* **62**, 126052 (2022).

# A-21

## Quantifying Prompt Tungsten Redeposition in the WEST Tokamak Using High-Resolution UV Spectroscopy

**C.A. Johnson**[1], E.A. Unterberg[1], Y. Corre[2], A. Grosjean[3], C. Guillemaut[2], N. Fedorczak[2], N. Rivals[2], C.P. Ballance[4], and the WEST team[5]

[1]Oak Ridge National Laboratory, Oak Ridge, TN 37831-6169, USA
[2]CEA, Institute for Research on Fusion by Magnetic confinement, 13108 St-Paul-Lez-Durance, France
[3]Department of Nuclear Engineering, University of Tennessee, Knoxville, Tennessee 37996, USA
[4]School of Mathematics and Physics, Queen's University Belfast, Belfast BT7 1NN, Northern Ireland, United Kingdom
[5]See http://west.cea.fr/WESTteam.

Prompt redeposition of tungsten is a critical process influencing impurity transport and surface evolution in fusion devices, particularly in long-pulse, full-metal tokamaks like WEST. In this work, we use high-resolution ultraviolet spectroscopy and collisional-radiative modeling to quantify prompt redeposition fractions in the lower divertor of WEST. Measurements focus on emission from both neutral and singly ionized tungsten using the W I 400.9 nm and W II 364.1 nm lines, respectively.

Tungsten particle fluxes were inferred from line-integrated brightness measurements using the S/XB method, with electron temperature and density profiles obtained from Langmuir probes. The atomic data used for the collisional-radiative modeling were taken from Smyth *et al.* [1] for neutral tungsten and Dunleavy *et al.* [2] for singly ionized tungsten. Under X-Point Radiator (XPR) plasma conditions, the comparison of neutral and ionized tungsten fluxes indicates that 90–97% of the grossly eroded tungsten is promptly redeposited within the divertor region, consistent with expectations for high-density, high-recycling regimes.

Preliminary spatial analysis suggests asymmetry in redeposition behavior, with higher prompt redeposition observed on the high-field side (HFS) compared to the low-field side (LFS). These results demonstrate the capability of combining W I and W II emission spectroscopy with simplified yet robust modeling to resolve key parameters for impurity transport. The W II 364.1 nm line, in particular, is shown to be spectrally isolated and well-suited for use in prompt redeposition studies, provided sufficient resolution and calibration are achieved. This work lays the foundation for future experimental campaigns aimed at correlating spectroscopically inferred redeposition with post-mortem surface analysis of tungsten deposits in WEST and ITER-relevant conditions.

This work was funded under DE-AC05-000R22725

References
[1] R.T. Smyth, , C.P. Ballance, C.A. Ramsbottom, C.A. Johnson, D.A. Ennis, and S.D. Loch. Physical Review A 97, no. 5 (2018)
[2] N.L. Dunleavy, C.P. Ballance, C.A. Ramsbottom, C.A. Johnson, S.D. Loch, and D.A. Ennis. Physics B: Atomic, Molecular and Optical Physics 55, no. 17 (2022)

A-22

# Hydrogen Recycling Model using Machine Learning

**S. Saito**[1*], H. Nakamura[2,3], K. Sawada[4], K. Hoshino[5], Y. Homma[6], S. Yamoto[7]

[1] Graduate School of Science and Engineering, Yamagata University, Yonezawa, Japan
[2] Department Research, National Institute for Fusion Science, Toki, Japan
[3] Graduate School of Engineering, Nagoya University, Nagoya, Japan
[4] Graduate School of Science and Technology, Shinshu University, Nagano, Japan
[5] Department of Applied Physics and Physico-Informatics, Keio University, Yokohama, Japan
[6] National Institutes for Quantum Science and Technology, Rokkasho, Japan
[7] National Institutes for Quantum Science and Technology, Naka, Japan

Understanding the mechanisms of hydrogen recycling is a key factor in accurately predicting and managing plasma behavior in nuclear fusion reactors. In the present study, we develop a machine learning (ML) model capable of predicting the translational energy distributions and rovibrational states of hydrogen atoms and molecules emitted from tungsten plasma-facing components. These predictions play a critical role in evaluating the influence of recycled hydrogen on edge plasmas through neutral transport simulations.

The training dataset for the ML model[1] is generated using molecular dynamics (MD) simulations[2-4], which replicate hydrogen atom injection into hydrogen-saturated tungsten under various conditions, including different incident energies, material temperatures, and hydrogen-to-tungsten (H/W) ratios. These simulations provide detailed information on the resulting energy and rovibrational distributions.

To strike a balance between computational efficiency and predictive accuracy across a broad parameter space, we employ a fully connected neural network trained on 120 datasets derived from 24 distinct simulation scenarios, enhanced via random sampling for data augmentation. This ML model demonstrates high fidelity in reproducing the emission behavior of hydrogen species under monochromatic injection conditions.

The model is further generalized to more realistic plasma conditions by incorporating a shifted-Maxwellian distribution for the incident energy, accounting for the energy gain of ions in the sheath region. Two methodologies are proposed: (1) numerical integration of the monochromatic ML model over the shifted-Maxwellian distribution, and (2) development of a new ML model trained directly on pre-integrated data with four input parameters—H/W ratio, material temperature, and ion and electron temperatures. The analysis reveals that elevated electron temperatures enhance atomic hydrogen emission, while lower electron temperatures favor the release of molecular hydrogen.

References

[1] S. Saito, et al., "Machine Learning-Based Hydrogen Recycling Model for Predicting Rovibrational Distributions of Released Molecular Hydrogen on Tungsten Materials via Molecular Dynamics Simulations", accepted to Nucl. Mater. Energy, (2025).
[2] S. Saito, et al., Contrib. Plasma Phys. e201900152 (2020).
[3] S. Saito, et al., Jpn. J. Appl. Phys. **60**, SAAB08 (2021).
[4] S. Saito, et al., Nucl. Fusion **64** 126067 (2024).

## A-23

# Atomic processes in laser-produced tin plasmas for the efficient emission of extreme-ultraviolet (EUV) radiation

**Akira Sasaki[1,2], Atsushi Sunahara[2], Katsunobu Nisihara[2], Nozomi Tanaka[2], Shinsuke Fujioka[2], Tomoyuki Johzaki[3], Kentaro Tomita[4], and Masashi Yoshimura[2]**

[1]*QST, Kizugawa, Kyoto, Japan*
[2]*ILE, The University of Osaka, Suita, Osaka, Japan*
[3]*Hiroshima University, Higashi Hiroshima, Hiroshima, Japan*
[4]*Hokkaido University, Sapporo, Hokkaido, Japan*

From tin, xenon, rare-earth elements, and tungsten to bismuth ions have signature EUV emission. The emission arises from 4d-4f and 4p-4d atomic transitions showing a broad, strong peak called an unresolved transition array (UTA) [1]. The wavelength scales as the atomic number from 13.5 nm using tin to ≈3 nm using bismuth. Due to the effect of configuration interaction, emission from a range of charged states in the plasma overlaps so that more than 5 % of conversion efficiency into 2% bandwidth at the wavelength of 13.5 nm using tin.

We developed a collisional radiative model of tin based on the computational atomic data calculated using the HULLAC code [2]. We investigated the energy level structure of 4 to 17 times the ion of tin and the excited states of each ion, which contribute to the emission. We calculated ion abundance and level population using configuration averaged atomic energy levels and then calculated EUV emission, taking the detailed spectral structure of each UTA into account [3].

Atomic transitions, which contribute to the main peak at 13.5 nm, broad tail structure in 14-20 nm, and peaks in 5-12 nm, are investigated. We also investigate the emission from multiply excited states, which may contribute to the broadening of the main peak at high densities [4].

The calculated wavelength of UTA is compared and corrected with respect to the experimental spectrum [5]. The calculated spectrum is also compared with the spectrum obtained from laser-produced plasmas, and the effect of radiative transfer is investigated [6].

Using the present model, the opacity table will be produced, which will be used in the radiation-hydrodynamics simulation to investigate the temporal and spatial evolution of the laser-proudced plasmas to determine the conditions to obtain high power with high efficiency.

References

[1] W. Svendsen, et al., Phys. Rev. A 50, 3710 (1994).
[2] A. Bar-Shalom, et al., J. Quant. Spectrosc. Radiat. Transfer, 71, 169 (2001).
[3] A. Sasaki, J. Appl. Phys. 107, 113303 (2010).
[4] A. Sasaki, Appl. Phys. Lett. 124, 064104 (2024).
[5] H. Ohashi, et al., J. Phys. B: At. Mol. Opt. Phys. 43 065204 (2010).
[6] R. Schupp, et al., Phys. Rev. Appl.12, 014010 (2019).

## A-24

# Charge Exchange X-ray Spectra of H-like and He-like Iron at Tokyo EBIT

Shinkichi Yamanaka, **Hajime Tanuma**, Nobuyuki Nakamura*

Department of Physics, Tokyo Metropolitan University, Tokyo 192-0397, Japan
(*) Institute for Laser Science, The University of Electro-Communications, Tokyo 182-8585, Japan

Emission from hydrogen-like and helium-like iron ions has been observed in X-ray spectra from high-temperature plasmas in the Universe. Observations of the Perseus cluster of galaxies by the Japanese Hitomi satellite attracted attention because of the clean separation of four emission lines from helium-like iron ions [1]. These emission lines are due to the electron impact excitation in high-temperature plasmas, but emission after the charge exchange reactions can also be observed from comets, supernova remnants, etc. To reproduce this phenomenon in ground-based experiments, an experiment was carried out at Lawrence Livermore National Laboratory, in which neutral gas was introduced to the electron beam ion trap, where the multiply charged ions are produced, to induce a charge exchange reaction, and the subsequent emission was observed [2]. This experimental result was investigated with the theoretical multi-channel Landau-Zener model calculation and understood precisely [3].

In this work, we performed similar experiments with a windowless silicon drift detector, which has better energy resolution than the Ge detector used in the previous work, and $CH_4$ gas, which has the same ionization potential energy as atomic hydrogen of 13.6 eV. We have observed not only 1s–$n$p and $1s^2$–1s$n$p transitions of H-like and He-like iron ions, but also transitions between excited states and emission from Li-like iron ions. Furthermore, we observed that the forbidden transition from 1s2s $^3S_1$ was enhanced in charge exchange spectra.

References

[1] Hitomi Collaboration, Nature **535**, 117 (2016).

[2] B. J. Wargelin *et al.* Astrophys. J. **634**, 1 (2005).

[3] P. D. Mullen *et al.*, Astrophys, J. Supple. Ser. **224**, 31 (2016).

A-25

# Polarization of VUV emission from highly charged ions studied with an electron beam ion trap

**Nobuyuki Nakamura**, Ryohko Ishikawa*, Motoshi Goto†

Institute for Laser Science, The University of Electro-Communications, Tokyo 182-8585, Japan
(*) National Astronomical Observatory of Japan, Tokyo 181-8588, Japan
(†) National Institute for Fusion Science, Gifu 509-5202, Japan

Plasma polarization spectroscopy is important for applications such as plasma anisotropy diagnostics [1]. The atomic processes in plasma such as collisions of ions with non-thermal electrons are responsible for the polarization; thus, it is important for the applications to study the polarization mechanism of emission arising from elementary processes in plasma. In this study, we present the polarization of the 2s–2p$_{3/2}$ transition at 124 nm in Li-like $N^{4+}$ measured with an electron beam ion trap (EBIT). Inside an EBIT, trapped highly charged ions are excited with a quasi-monoenergetic electron beam. It is thus an ideal device for studying the polarization of emission from highly charged ions excited by electron collisions. To measure the polarization for the vacuum ultraviolet (VUV) range, we have introduced the techniques used in the solar Lyman-$\alpha$ polarimeter in the CLASP rocket experiment [2] to the compact EBIT (CoBIT) [3] at the University of Electro-Communications in Tokyo.

In the experiment, the VUV emission from Li-like $N^{4+}$ trapped in CoBIT was diffracted with an aberration-corrected concave grating. A waveplate and a polarization analyzer specifically designed for the Lyman-$\alpha$ polarimeter in CLASP were introduced upstream and downstream of the grating, respectively. The waveplate was mounted on an ultra-high vacuum rotation stage to change the polarization state. The polarization analyzer selectively reflects $\sigma$-polarized radiation and the reflected radiation was observed with a position-sensitive detector with five microchannel plates and a resistive anode. The polarization can thus be obtained from the amplitude of the $\cos^2(2\theta)$ modulation when the intensity variation was observed as a function of the waveplate rotation angle $\theta$. The present result demonstrates a new experimental method for measuring the polarization in the VUV emission of highly charged ions.

This work was supported by the UEC-NAOJ matching fund project and JSPS KAKENHI Grant Number 24H00200.

References

[1] Fujimoto T and Kazantsev S A, Plasma Phys. Control. Fusion **39**, 1267 (1997)

[2] Kano R *et al.*, ApJ **839**, L10 (2017)

[3] Nakamura N *et al.*, Rev. Sci. Instrum. **79**, 063104 (2008)

A-26

# High Harmonic genertaion plasma wedge and laser interaction.

**Amar Pal[1], Bhuvanesh Ramakrishna[1,2]:**
[1]Department of Physics, Indian Institute of Technology Hyderabad, India:
[2]Department of Physics, Indian Institute of Technology Hyderabad, India:
email address: ph20resch11004@iith.ac.in

**Abstract:** In this study, we investigate the generation of high-order harmonics through laser-plasma interaction using both planar and wedge-shaped targets by EPOCH PIC 2D simulation. The focus of the research is to compare the efficiency and spectral characteristics of High Harmonic Generation (HHG) from these two target geometries. A high-intensity femtosecond laser is used to ionize the surface of the targets, creating plasma where the harmonic generation occurs. In the case of the wedge-shaped target, the plasma density varies along the interaction surface, providing a unique environment for enhancing phase matching and boosting the harmonic yield, especially at higher orders.

We systematically vary the laser-wedge interaction angle to explore its influence on the harmonic generation process. By adjusting the angle of incidence, we control the laser's interaction with the plasma density gradient, which directly impacts the efficiency of HHG and the emission direction of the harmonics. Our results show that the wedge target significantly enhances the generation of high-order harmonics compared to the planar target, particularly in the extreme ultraviolet (XUV) region, due to better phase matching and optimized electron dynamics.

Additionally, the variation in laser-wedge interaction angle enables fine-tuning of the harmonic spectrum, with sharper and more intense harmonic peaks observed at optimized angles. This study highlights the potential of structured targets like wedges in achieving more efficient HHG for applications requiring coherent XUV or soft X-ray sources and offers insights into the role of interaction geometry in optimizing plasma-based harmonic generation.

# Amplified Spontaneous Emission of 112-nm $Al^{3+}$ ion in neon-like aluminum laser plasmas

**Y. Takehiro**[1], Y. Nishii[1], M. Kishimoto[1], K. Yamasaki[1], T. Higashiguchi[2], and S. Namba[1]
[1] Graduate School of Advanced Science and Engineering, Hiroshima University, [2] Department of Electrical and Electronic Engineering, Utsunomiya University

Since the invention of lasers, research on laser oscillation with various wavelengths and pulse widths has been conducted. In particular, researches for short-wavelength lasers has been carried out extensively. The transient electron collision excitation (TCE) scheme [1] is one of the mechanisms for generating an inverted population in plasma x-ray laser oscillations. Using nickel-like and neon-like TCE methods, laser oscillations have been observed with wavelengths ranging from the shortest of 7.3 nm using Sm to the longest of 87.6 nm using Si, respectively. If an amplified spontaneous emission (ASE) for aluminum is realized between $Al^{3+}$ 3s-3p transition, it would be the longest wavelength of 111.9 nm by this scheme. It is expected to have various applications as it falls in the intermediate region between currently existing ultraviolet lasers ($F_2$ laser: 157 nm) and soft x-ray lasers. This study aims to demonstrate the ASE of 111.9 nm vacuum ultraviolet (VUV) wavelength in neon-like Al laser plasma for the first time.

In the TCE scheme, an aluminum target in the vacuum chamber was irradiated with two lasers (1064 nm wavelength), that is, pre-pulse and main pulse, with a time delay between them. The pre-pulse was line-focused onto the Al target normal to the target surface to generate a low-density and low-temperature plasma (pre-plasma). After an appropriate time delay, the main pulse was injected and further heated the pre-plasma (axial pumping). However, optimal plasma density heated by the main pulse (~$10^{18}$ $cm^{-3}$) efficiently is much higher than the critical density ($10^{21}$ $cm^{-3}$) of 1064 nm pump laser, so that the gain coefficient is even low due to both density mismatch. Therefore, the main pulse was irradiated onto the target at a grazing angle of ~4 degrees, by which the effective critical density in the gain region was similar to the density of $10^{18}$ $cm^{-3}$. By varying several parameters, such as time intervals between both pulses and each laser intensity, VUV spectra were measured with a normal incident VUV spectrometer. Besides, the incident angle and the position of the main pulse to heat the plasma was also varied in the experiments. Figure 1 shows a schematic diagram of the experimental setup. Two apertures were placed to reduce intense stray light (note that the axial pumping was used).

Under conditions of the incidence angles of 3.5~4°, very sharp spectrum of 111.9 nm was at pre-pulse energy of $2.5 \times 10^8$ W/cm$^2$ and main pulse of $4.2 \times 10^{13}$ W/cm$^2$. The result at 4° is shown at FIG.2. According to the NIST database [3], the spectral wavelength of the transition of neon-like ion 3p ($^1S_0$)-3s ($^1P_1$) is 111.9 nm, and thus we can demonstrate ASE of the longest wavelength by the TCE scheme. In this study, intense ASE was not observed due to the instability caused by the pump laser energies and pulse interval (timing jitter), thus making it impossible to optimize plasma parameters and laser irradiation conditions precisely.

In the future, we plan to improve the jitter of the pre-main pulses by stabilizing the pump lasers, and by optimizing the laser energies, pulse time intervals, as well as the incident angle and position, we will aim to achieve prominent ASE signal of the 111.9 nm spectrum with high signal to noise ratio.

**References**
[1] H. Daido, Rep. Prog. Phys. **65**, pp. 1513 (2002).
[2] Y. Li *et al.*, Physica Scripta. **57**, pp.237-241 (1998).
[3] NIST Atomic Spectra Database, https://physics.nist.gov/PhysRefData/ASD/lines_form.html

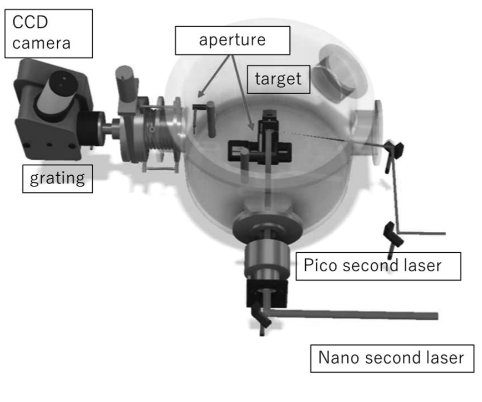


**FIG.1**.A schematic diagram of the experimental setup for VUV wavelength ASE measurement.

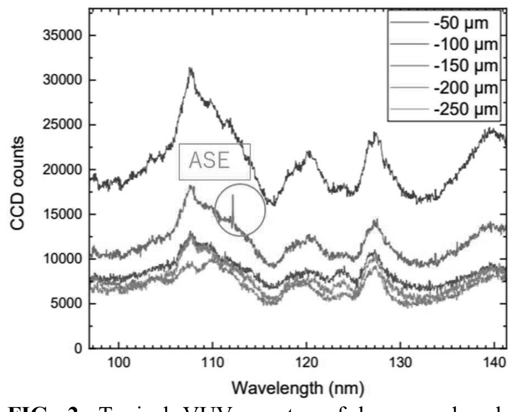


**FIG. 2**. Typical VUV spectra of laser produced Al plasma. Around 112 nm, sharp line spectrum is observed.

# POSTERS B

**B-01**

# Spectroscopic Characteristics of Ce- to Gd-like Highly Charged Ions in the Water Window range

**Dingbao Song**[1], Hayato Ohashi[2], Hiroyuki A. Sakaue[3], Nobuyuki Nakamura[4], Daiji Kato[3,1]

1. IGSES, Kyushu University, Kasuga, 816-8580, Fukuoka, Japan
2. ILAS, University of Toyama, Toyama, 930-8555, Toyama, Japan
3. National Institute for Fusion Science, Toki, 509-5292, Gifu, Japan
4. ILS, The University of Electro-Communications, Chofu, 182-8585, Tokyo, Japan

Studying highly charged heavy elements ions like bismuth, lead, and gold in laser plasmas shows promise for molecular microscopy, especially their emission spectra in the water window (23-44 Å)[1] range are useful for in vivo imaging. However, modeling these spectra is challenging due to dynamic variations in temperature and density. So that, Ohashi et al.[2] measured soft X-ray spectra from highly charged Bi ions in the water window range with a compact electron beam ion trap (CoBIT) [3]. CoBIT provides well-defined electron density conditions, but at lower densities ($10^{10}$ cm$^{-3}$), non-equilibrium plasma models are required. To analyze these emissions, we constructed a collisional-radiative models (CRMs) for $Bi^{19+}$ to $Bi^{25+}$ ions in CoBIT, utilizing atomic data from the HULLAC code[4].
As shown in Figure 1, in the soft-X ray spectra from $Bi^{19+}$ to $Bi^{25+}$ ions in CoBIT, a series of emission lines due to $4f-7g$, $6g$, $5g$ (A, B, C) transitions are identified, except for $Bi^{22+}$ (Pm-like) and $Bi^{23+}$ (Nd-like) ions. More complicated featues for these ions is due to the prominent lines (green arrows) from the metastable states: $4f^{13}5s^2$ ($Bi^{22+}$), $4f^{13}5s$ and $4f^{12}5s^2$ ($Bi^{23+}$) respectively. Additionally, emission lines of higher charge states, which are not produced by direct ionization from the ground states of lower charge states under the experiment energy condition, also take part in the spectra (yellow arrows). These line emissions can occur by ionization from long-lived metastable excited states of the lower charge states.

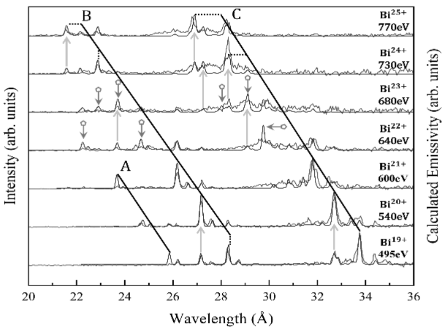


Figure 1: Emission line spectra of $Bi^{19+}$ to $Bi^{25+}$ ions in CoBIT (red) and calculated spectra (blue) by using HULLAC in the water window range. The wavelength scales of the calculated spectra from 495 eV to 770 eV are shifted +0.18, +0.14, +0.15, +0.31, +0.2 and +0.08 Å. The intensities contribution of each ion in the spectrum are calculated by using nonlinear least squares method.

References

[1] C. Spielmann, N. H. Burnett, S. Sartania, *Science* **278**, 661 (1997).
[2] H. Ohashi et al., *Proc. 20th Int. Conf. on the Physics of Highly Charged Ions* **B25** (2022).
[3] H. A. Sakaue, N. Nakamura, E. Watanabe, *J. Instrum.* **5**, C08010 (2010).
[4] A. Bar-Shalom, M. Klapisch, J. Oreg, *J. Quant. Spectrosc. Radiat. Transf.* **71**, 169 (2001).

## B-02

# Influence of Multiply Excited States of Tin ions on Laser-Produced EUV Light Emission

**Chun-Tse Wu**, Shih-Hung Chen
Department of Physics, National Central University, Taoyuan, Taiwan
and
Shivam Gupta, and Yao-Li Liu
Institute of Space and Plasma Sciences, National Cheng Kung University, Tainan, Taiwan

Nowadays, extreme ultraviolet (EUV) light sources at a wavelength of 13.5 nm with 2% bandwidth facilitates the state-of-the-art nanolithography. Tin liquid droplets are considered as target materials because they exhibit numerous strong resonance transitions in moderately ionized states ($Sn^{8+}$ to $Sn^{14+}$) within this wavelength range. The EUV light is generated in laser-produced plasmas (LPP) through complicated physical processes such as laser-plasma interactions, heat conduction, electron-ion collisions, and atomic processes of tin plasmas. Experimental optimization of EUV generation within the desired wavelength band is challenging, highlighting the essential role of accurate simulations.

Among the involved physical processes, accurately modeling atomic processes is critical for calculating in-band EUV emission and radiated power loss from tin plasmas. Previously, the numerical simulation of LPP-EUV light emission on the assumption of dominant contributions from one-electron-excited states of tin ions was proved to give inaccurate estimation of EUV light emission. Torretti et al. [1] demonstrated significant contributions from multiply excited states of tin ions on EUV light emission . Although multiply excited states typically exhibit lower excitation probabilities, their large number of levels results in strong aggregate transitions. Based on this finding and employing Flexible Atomic Code (FAC) [2] for simulation, our recent research indicates that $Sn^{15+}$ ions also exhibit notable in-band EUV emission when multiply excited states are considered. These higher charge states of tin ions arise under high energy laser pulse [3], influencing the optimal conversion efficiency of EUV light sources predicted by simulations and providing important insights for further advancements in EUV lithography technology.

References

[1] F. Torretti et al. Nature communications, 11(1), 2334 (2020).
[2] M. F. Gu, Canadian Journal of Physics. 86, 675 (2008).
[3] F. Torretti et al. Journal of physics D: applied physics, 53(5), 055204 (2019).

**B-03**

# Electric octupole transitions of Ta and Hf observed in an EBIT plasma

**H. A. Sakaue**[1)], E. Takacs[2,3)] and Dipti[2,3)], M. Kimura[1)], D. Kato[1,4)], N. Nakamura[5)], H. Staiger[3)], C.A. Faiyaz [3)], C. Suzuki[1),6)], I. Murakami[1,6)], H. Ohashi[7)], Yu. Ralchenko[2)]

1)National Institute for Fusion Science, Toki, Gifu 509-5292, Japan
2)National Institute of Standards and Technology, Gaithersburg, Maryland 20899, USA
3)Department of Physics and Astronomy, Clemson University, Clemson, South Carolina 29634, USA
4)Interdisciplinary Graduate School of Engineering Sciences, Kyushu University, Kasuga, Fukuoka 816-8580, Japan
5)Institute for Laser Science, The University of Electro-Communications, Tokyo 182-8585, Japan
6) Graduate Institute for Advanced Studies, SOKENDAI, Toki, Gifu 509-5292, Japan
7)Institute of Liberal Arts and Sciences, University of Toyama, Toyama 930-8555, Japan

The atomic spectrum is generally dominated by electric dipole (*E1*) transitions; however, forbidden transitions, which are restricted by the dipole selection rule, can also occur. This decay process is explained by higher-order terms in the multipole expansion of the radiation field. As the intensity of forbidden transitions is sensitive to the electron density, these long-lived and low-probability decay processes are often useful as diagnostic tools in the study of fusion, astrophysics, and laser-generated plasmas. We have conducted spectroscopic studies of emission line spectra from tungsten highly charged ions (HCI) using an electron beam ion trap (EBIT). In the emission spectra, we observed two strong forbidden electric octupole (*E3*) transitions, specifically the 5s-4f transitions of the $W^{27+}$ Ag-like ion. We predicted that these transitions appear in a narrow Z atomic number region of elements due to the crossing of excited levels feeding the 5s upper level [1]. To date, we have systematically observed the emission lines of Ag-like ions and successfully detected the *E3* transitions of the Ag-like ions of Ir (77), Os (76), Re (75), W (74), and Lu (71) [2].
In the present study, an electron impact heating evaporation source, which can introduce new high-melting-point metal atoms into the EBIT, was installed to measure Ta (73) and Hf (72), for which E3 transitions have not yet been confirmed. The *E3* transitions were successfully observed in the Ag-like charge state of both elements. These observations help to clarify the atomic number dependence of the emission mechanism of these highly forbidden transitions in highly charged ions.

Details of the measurements and the modeling work will be presented at the meeting.

References

[1] H.A. Sakaue et al., Phys. Rev. A **100**, 052515 (2019)
[2] H.A. Sakaue et al., Phys. Rev. A, Accepted for Publication (2025)

B-04

# NIFS Atomic and Molecular Numerical Database for Collision Processes

**Izumi Murakami**[1,2], Masatoshi Kato[1)], Masahiko Emoto[1)], Hiroyuki A. Sakaue[1,2)], Naoki Kimura[1)], Daiji Kato[1,3)]

1) National Institute for Fusion Science, National Institutes of Natural Sciences, Toki, Gifu 509-5292, Japan
2) Graduate Institute for Advanced Studies, SOKENDAI, Toki, Gifu 509-5292, Japan
3) Department of Advanced Energy Engineering Science, Kyushu Univ., Kasuga, Fukuoka 816-8580, Japan

We have compiled numerical atomic and molecular data for collision processes in plasmas and constructed the retrievable database, NIFS Atomic and Molecular Numerical Database, which is open to the public at http://dbshino.nifs.ac.jp. Data compilation has been done for 50 years with the help of collaborators inside/outside Japan. The first compiled data sets were published in IPPJ-DT-48 report in 1975 from Nagoya University [1], for fusion science research. Nowadays, various atomic and molecular (AM) data for collision processes in various plasmas, such as astrophysical, low-temperature, and high-temperature plasmas, are compiled in the database.

The NIFS AM Numerical Database consists of 5 sub-databases, namely, AMDIS (electron collision cross sections/rate coefficients for atoms and ions), CHART (ion-atom collision cross sections), MOL (cross sections of collision processes for molecules), SPUTY (sputtering yields by atomic ions for solid surface), and BACKS (back-scattering coefficients of light ions from solid surface). Each data set consists of numerical data and bibliographic information on the data source. So, users can trace the original paper of the data. Almost all data are compiled from the literature. The database has 1,881,982 datasets in total as of Apr. 1, 2025, which is the largest database on AM collision processes available in the world [2]. Users can search for their targeted data through a query from the database system, and the found data are listed in the form of a collision process, such as, $C + e^- \rightarrow C^+ + 2e^-$ for electron-impact ionization. The numerical data are shown in a table or a graph plotted with different symbols for different data sets (Fig.1). Such a graph is useful for comparing datasets from different sources to find a good dataset or evaluate data. Some of the sub-databases provide curves drawn with empirical formulae, such as the Lotz's empirical formula [3] for electron-impact ionization cross sections for atomic ions.

We also provide small databases without a retrievable system, constructed under collaborations. All are available from the web page.

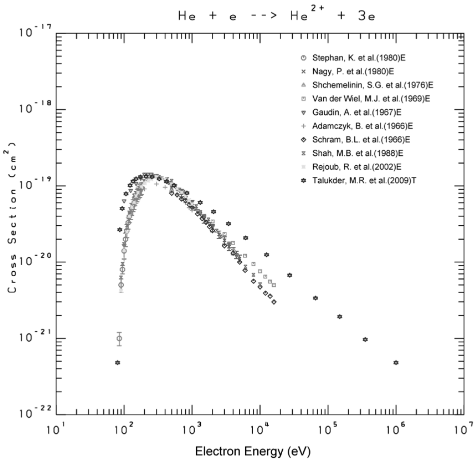


Fig.1 An example of a graph from AMDIS. Double ionization cross section for He by electron impact as a function of collision energy. E in legends means experimental data, and T means theoretical data.

References

[1] K. Takayanagi and H. Suzuki, IPPJ-DT-48 report, Institute of Plasma Physics, Nagoya University: Nagoya, Japan (1975).
[2] I. Murakami et al., Atoms **8**, 71 (2020).
[3] W. Lotz, Astrophys. J. Suppl. **14**, 207 (1967).

B-05

# Electronic state density modeling in hydrogen-like plasmas by Nearest Neighbor Approximation

**Takeshi NISHIKAWA**

Faculty of Environmental, Life, Natural Science and Technology, Okayama University
3-1-1 Tsushima-naka, Kita-ku, Okayama 700-8530, Japan

The continuous spectrum region outside the broadening of the bound-bound spectrum from plasma composed of hydrogen-like ions is considered. The position, broadening width and shape of bound-bound spectrum, and position of the bound-free edge have been studied for a long time, but in the case of simple atoms and ions such as hydrogen-like, the positional spacing of the bound-bound spectra are relatively wide, and from the viewpoint of energy transport by radiation, the transport coefficient is determined by the strength of this bottom region. In particular, it should have a significant contribution when solving radiation transport in plasma by computaer simulations, but its intensity has not been carefully examined so far. The absorption and emission of radiation in this region have been evaluated in two ways: as an extension of the broadening of the bound-bound spectrum or as a form of incorporating a continuous bound-free edge as a form of compensating for the disappearance of the bound state due to the plasma effect[1]. The most successful model of this disappearance is the classical model, in which atoms and ions in the plasma exist in an electric field statistically calculated from the positional distribution of the ions, and when the potential falls below the energy level of the atoms and ions of the isolated system, the level disappears. To compensate the disappearance of the bound state density, pseudo-continuum is introduced below bound-free edge. Consider the potential profile of the simplest system consisting of two hydrogen atoms (Fig. 1). In this case, when the two nuclei approach a distance of 8 $a_0$, the potential saddle point created by the potential profiles of nuclei corresponds to the energy of the 1s level of the hydrogen atom of the solitary system, so in such a state the level of 1s is calculated as disappearing. ($a_0$ is the Bohr radius) However, if we consider that the two hydrogen atoms are close to each other up to 8 $a_0$, the wave functions of the electrons are almost non-overlapping, and the potential for the contribution from the nucleus and electrons at the middle 4 $a_0$ is almost zero, and the two atoms can exist without interference. In this paper, the physical meaning of this pseudo-continuum is considered by solving the electronic state with as a hydrogen molecule ion by quantum mechanically and evaluating the electronic state density by considering the kinetic energy distribution of the ions in plasmas. As a result, we were able to obtain a pseudo-continuum state without introducing any ad hoc consideration.

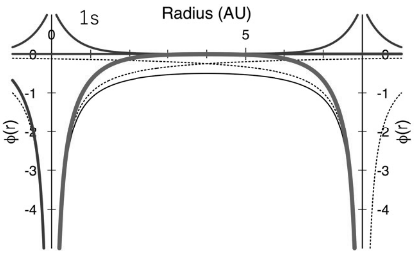


Figure 1: Potential profile between two hydrogen atoms 8 $a_0$ apart

[1] W. Däppen, L. Anderson, and D. Mihalas, Astrophys. J. **319**, 195 (1987).

**B-06**

# Contribution of multiply excited states to the EUV emission of $Sn^{12+}$

F J Zhang, X B Ding, D H Zhang and **C Z Dong**

Key laboratory of Atomic and Molecular Physics & Functional Materials of Gansu Province, College of Physics and Electronic Engineering, Northwest Normal University, Lanzhou 730070, China

Sn is the material of extreme ultraviolet (EUV) light sources. In industry applications, Sn is heated into a plasma with the temperatures of several tens of eV and the electron densities of $10^{18}-10^{19}$ $cm^{-3}$ , which has strong emissions in EUV region near the 13.5 nm band. At this temperature and density, the main types of ions in the Sn plasma are $Sn^{8+}$- $Sn^{14+}$ ions. To optimize the efficiency of the EUV light source, the calculations of the spectral intensity, opacity and the spectrum emission of Sn ions are necessary[1-2].

In 2020, Torretti *et al*. proposed that transitions between multiply-excited states make a significant contribution to EUV light, and not just from the decay of a singly-excited state to the ground state[1] . In 2024,the spectral emission rate of $Sn^{11+}$ ions is investigated as the typical ion by Sasaki *et al*., their results show that the excited states below the ionization threshold have a contributes significantly to the EUV emission[2].

In this work, we further investigate the EUV emission between multiply-excited states of $Sn^{12+}$ ions. Considering that most of the multiply-excited states are above the ionization threshold, the radiative branching ratios of these multiple-excited states are calculated in detail. Figure 1 shows the profile of emission rate of $Sn^{12+}$ ions. The results indicate that EUV light not only originates from the single-excited state decay to ground state, but also from the transition between multiple-excited states. As can be seen from the figure 1, the contribution emission rate from the transition between multiple-excited states after considering the radiative branching ratio is stronger than that of the single excited-state, but weaker than that of the multiple-excited state without considering the radiative branching ratio.

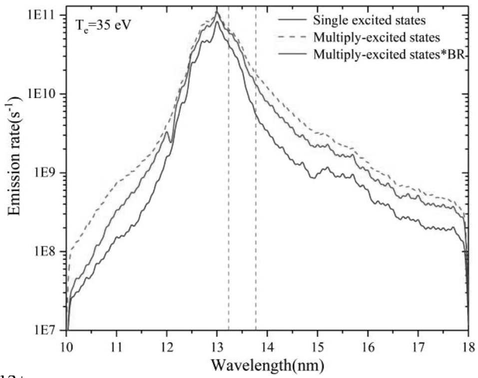


Figure 1: Emission rate of $Sn^{12+}$ ions, calculated assuming local thermal equilibrium state of the plasma with the electron temperature of 35 eV. (The black solid line and the red dashed line represent the emission rate of the single-excited state and the multiply-excited states, respectively. The blue solid line represent the emission rate of the multiply-excited state multiplied by the radiation branch.)

References
[1] F. Torretti, J. Sheil, R. Schupp, M. M. Basko, *et al.* Nat. Commun. 11, 1 (2020)
[2] Sasaki A, Appl. Phys. Lett. 124, 6 (2024)
E-mail:dongcz@nwnu.edu.cn

**B-07**

# A detailed collisional radiative model for Ti plasma

**Nitish Ghosh**, Lalita Sharma

Indian Institute of Technology Roorkee, Roorkee 247667, India

Titanium plasmas are widely studied due to their applications in thin-film deposition, biomedical coatings, and advanced material processing. Accurate plasma diagnostics are essential for optimizing these applications, with laser-induced breakdown spectroscopy serving as a powerful non-intrusive technique. A reliable collisional radiative (CR) model is crucial for extracting plasma parameters such as electron temperature and density from spectral emissions. However, existing Ti plasma studies are limited by the lack of comprehensive atomic and collisional data. This study presents a detailed CR model for Ti plasma by validating it using laser-induced breakdown spectroscopy (LIBS) measurements of Mejia et al. [1]. Radiative rates for 194 fine-structure levels considered in the model of Ti I are computed using the multiconfiguration Dirac-Hartree-Fock (MCDHF) method. Electron impact excitation cross-sections are calculated from the ground and metastable sates $3d^2 4s^2$ ($a\ ^3F$, $a\ ^1D$, $a\ ^3P$) and $3d^3 4s$ ($a\ ^5F$) up to upper fine structure levels using relativistic distorted wave (RDW) [2] theory for a wide range of incident electron energy from excitation threshold to 250 eV. The CR model incorporates key plasma processes, including radiative decay, electron impact excitation, and de-excitation, ionization, and three-body recombination. Incorporating all of the key plasma processes into a collisional radiative solver, a system of rate equations is solved to get the upper-level population of the fine structure energy levels. Theoretical spectra are generated and compared with experimental LIBS measurements from Mejia et al. [1] for validation. Eight Ti I spectral lines are analyzed and electron temperature ($T_e$) and density ($n_e$) at different delay times of 0.5 and 3.5 $\mu$s are extracted. A strong agreement between computed and experimental results confirms the accuracy of our model as shown in Figure 1 for the time delay of 3.5 $\mu$s. The validated atomic data and CR model pave the way for future applications in Ti plasma studies.

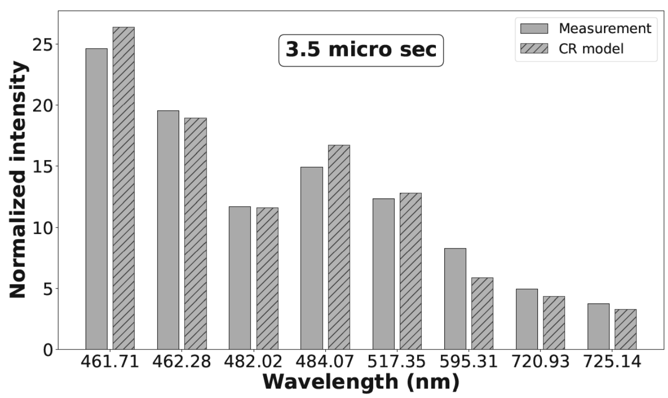


Figure 1: Comparison of theoretical and experimental intensities at optimized $T_e$ and $n_e$.

References

[1] R. E. Mejia, M. Raineri, R. Sarmiento, J. C. Álvarez & P. Pacheco, IEEE Transactions on Plasma Science, **51**(10), 3035–3052 (2023).

[2] L. Sharma, A. Surzhykov, R. Srivastava, & S. Fritzsche, Phys. Rev. A **83**, 062701 (2011).

## B-08

# Electron-Impact Ionization Cross Sections of Beryllium and Its Ions for Plasma Modeling

**A. Pandey[1],** K. C. Dhakar[1], D. Kato[2,3], G. Purohit[1]
[1]Department of Physics, University College of Science, Mohanlal Sukhadia University, Udaipur-313001, India
[2]National Institute for Fusion Science, 322-6 Oroshi-cho, Toki, Gifu 509-5292, Japan
[3]Interdisciplinary Graduate School of Engineering and Sciences, Kyushu University, 816-8580, Kasuga, Fukuoka, Japan

We report a detailed investigation of the electron-impact ionization cross sections of neutral beryllium (Be) and its ions ($Be^+$, $Be^{2+}$, $Be^{3+}$) using three theoretical methods: Binary Encounter Dipole (BED), Coulomb-Born Exchange (CBE), and Distorted Wave (DW). The calculations were performed with the fully relativistic Flexible Atomic Code (FAC) [1], considering both ground and first excited states over an incident electron energy range from threshold up to 10 keV. Our results are benchmarked against several state-of-the-art theoretical models including RMPS, TDCC, CCC, and BSR, and for $Be^+$, compared with available experimental data. The BED and CBE methods show excellent agreement with measurements in the 52–116 eV range, while DW aligns closely with non-perturbative models across charge states. In addition, Maxwell rate coefficients were calculated to provide thermally averaged ionization data for plasma modelling. This study provides essential atomic data for understanding beryllium behaviour in fusion environments, where it is widely used as a plasma-facing component.

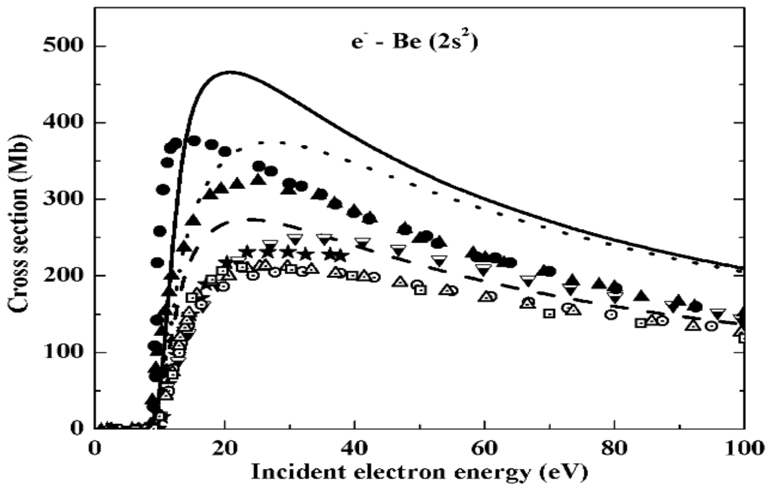


Fig. 1. Ground state electron impact ionization of Be as a function of incident electron energy. Dotted black line: present Binary Encounter Dipole (BED) results, dashed line: Present Distorted Wave (DW) results, solid black line: present Coulomb Born Exchange (CBE) results, solid black up triangle: results of distorted-wave with incident and scattered electrons calculated in $V^N$ potentials (DWIS(N-1)), solid circle: results of distorted wave with incident, scattered, and ejected electrons were calculated in a $V^{N-1}$ potentials (DWIS(N)) , black half filled down triangle: results from Time Dependent Close Coupling (TDCC), black star: results from R-Matrix with Pseudo States (RMPS) , open dot circle: results from B-Spline R-matrix (BSR-660) , open dot triangle: results from Convergent Close-Coupling (CCC-409) , open dot rectangle: results from Convergent Close-Coupling (CCC) .

References
[1] Gu, M. F. The flexible atomic code. Canadian Journal of Physics, 86(5), 675-689. (2008).

**B-09**

# Adiabatic Expansion Methods for Hydrogen Atoms in Ultra-High Magnetic Fields

**Kazuyoshi Yamada**, Daiji Kato*

IGSES, Kyushu University 6-1, Kasugakoen, Kasuga City, Fukuoka, Japan 816-8580
* National Institute for Fusion Science, 322-6 Oroshi-cho, Toki City, Gifu, Japan 509-5292

In recent years, high magnetic fields of 1000 T have become possible in the laboratory environment [1, 2]. In addition, thanks to the successful launch of the XRISM satellite, it is now possible to observe magnetic plasmas in space with an advanced X-ray microcalorimeter [3]. For these reasons, the study of elementary processes in ultra-high magnetic fields has attracted much attention. In order to understand the unique spectral structure of atoms/ions in strong magnetic fields quantum mechanically, an accurate theoretical description of the non-perturbative external magnetic field effects (diamagnetic Kepler motions of bound electrons) is required.

In the present study, the Schrödinger equation of hydrogen atoms in a uniform magnetic field is solved accurately by using the adiabatic expansion method adopting the radial coordinate $r$ as the adiabatic parameter. The adiabatic Hamiltonian and the Schrödinger equation in the spherical coordinates is expressed as,

$$\hat{H}_{ad} = \frac{1}{2}\frac{\hat{l}^2}{r^2} - \frac{1}{r} + \frac{m}{2}\gamma + \frac{1}{8}\gamma^2 (r\sin\theta)^2,$$

$$\hat{H}_{ad}\varphi_\mu = U_\mu \varphi_\mu,$$

where $\gamma = B_z/B_0$ and $B_0 \approx 2.35 \times 10^5$ T . Adiabatic potential energies and associated channel functions are obtained by diagonalizing the adiabatic Hamiltonian matrix with the spherical harmonics. Fig.1 shows the adiabatic potential energies as a function of the radial coordinate obtained for $B_z = 470$ T$(m = 0)$.

The adiabatic potential near the origin represents the centrifugal potentials of each orbital angular momentum (Kepler motion). On the other hand, at large distances, the adiabatic potentials of the pair of adjacent even and odd parity states become degenerated which converge to each Landau level of the cyclotron motion. The azimuthal distribution of the channel function also corresponds to the Kepler motion near the origin and the cyclotron motion at large distances.

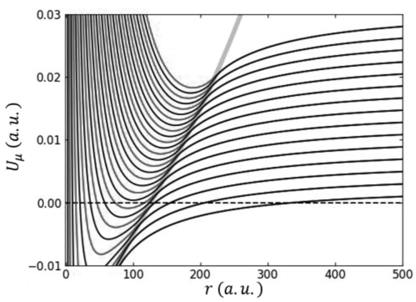


Fig. 1: Adiabatic potential energy $U_\mu(\mu = 1\sim15, B_z = 470$ T$, \mathrm{m} = 0)$ and the effective potential curve $V$ (gray) on $z = 0$ plane. Even parity (black), odd parity (red). $1\ a.u. \simeq 27.21$ eV (energy), $1\ a.u. \simeq 5.292 \times 10^{-11}$ m (length).

The two regions are separated by a sequence of avoided-crossings between the adjacent adiabatic potential curves of each parity along the effective potential on the plane of $z = 0$ perpendicular to $B_z$. The local wave functions astride on that plane are, therefore, affected by the non-adiabatic couplings. The finding has important implications for obtaining accurate wave functions of the adiabatic expansion.

References
[1] D. Nakamura et al., *Rev. Sci. Instrum.* 89, 095106(2018).
[2] S. Fujioka et al., *Sci Rep* **3**, 1170(2013).
[3] XRISM Science Team, arXiv:2003.04962 [astro-ph.HE].

**B-10**

# Explicit Numerical Scheme for Milne's Phase-Amplitude Equations and Applications

**Robin Piron**, Mikael Tacu

CEA, DAM, DIF
F-91297 Arpajon, France.
Université Paris-Saclay, CEA, Laboratoire Matière en Conditions Extrêmes
F-91680 Bruyères-le-Châtel, France.

Accurate modeling of many atomic processes in plasmas requires precise computation of continuum electron orbitals. The traditional approach consisting in directly sampling the oscillatory radial wavefunctions faces a significant computational burden due to the Nyquist-Shannon sampling limit [1]. Milne's phase-amplitude representation [2] offers a computationally efficient alternative, circumventing this sampling limit. However, existing numerical methods for solving the associated nonlinear amplitude equation on a fixed grid are either iterative [3,4] or prone to the growth of a spurious, rapidly varying component in the solution [5,6], hindering their systematic use in practice.

We propose a fully explicit numerical method based on a linear third-order equation equivalent to the nonlinear amplitude equation. This equation was originally derived by Kiyokawa for analysis of the Coulomb wavefunctions [7]. Our approach effectively decouples the solution from spurious components, resulting in a robust and stable scheme that allows for systematic improvement of accuracy when grid resolution is increased.

In this presentation, we comment on the limitations of existing methods [5,6] for solving Milne's equation, highlighting their susceptibility to numerical errors. We then expose our fully explicit method [8], showing its advantages in terms of stability. Finally, we present examples of applications which show its potential for advancing self-consistent, quantum-mechanical modeling of plasmas and more efficient calculations of atomic cross-sections.

References

[1] C. Shannon, Proceedings of the IRE 37:10–21 (1949)

[2] W. E. Milne, Phys. Rev. 35:863–867 (1930)

[3] M. J. Seaton, G. Peach Proceedings of the Physical Society 79:1296 (1962)

[4] L. Trafton, Journal of Computational Physics, 8:64–72 (1971)

[5] A. Bar-Shalom, M. Klapisch, J. Oreg, Comput. Phys. Commun. 93:21–32 (1996)

[6] B. Wilson, V. Sonnad, P. Sterne, W. Isaacs, J. Quant. Spectrosc. Radiat. Transf. 81:499–512 (2003)

[7] S. Kiyokawa, AIP Advances 5:087150 (2015)

[8] R. Piron, M. Tacu, submitted (2025)

**B-11**

# Spectroscopic Analysis of Impurity Ions (B, W, Xe) in ITER Plasmas Using Collisional-Radiative Modeling

**Runjia Bao**[1,2], Darío Mitnik[3], Ling Zhang[1*], Zhifeng Cheng, Fengling Zhang[1,2]

1 Institute of Plasma Physics, Chinese Academy of Sciences, Hefei 230031, China
2 University of Science and Technology of China, Hefei 230026, China
3 Instituto de Astronomía y Física del Espacio (CONICET-Universidad de Buenos Aires), Buenos Aires 1428, Argentina

Intrinsic impurities in a magnetically confined fusion (MCF) plasma dilute the reaction fuel in the hot plasma core and, through their radiation, are detrimental to global energy confinement [1, 2]. Thus, the radiative patterns of impurity elements in a fusion plasma must be understood across the full range of temperatures achieved in present day MCF experiments.

For this purpose, we present a comprehensive atomic processes investigation of impurity ions ($B^{4+}$, W, and $Xe^{44+}$, $Xe^{47+}$, $Xe^{51+}$) in ITER plasmas. Using the FAC code [3], we calculated excitation rate coefficients and radiative transition rates, then solved the collisional-radiative model (CR) to derive emission spectra across 100 eV–100 keV. Prominent spectral lines were identified, and their photon emissivity coefficients (PEC) were evaluated. Then by employing ITER's half-field, 7.5 MA scenario with impurity concentrations (B: $10^{-2}$, W: $10^{-4}$, Xe: $10^{-5}$) and $T_e$ and $n_e$ profiles, we computed emissivity profiles for key spectral lines. This work provides critical atomic data for diagnosing impurity transport and radiation losses in ITER, benchmarking CR model and FAC calculation with ADAS database. The results highlight the role of charge-state distribution and line emission in fusion-grade plasmas, supporting spectroscopic diagnostics for ITER.

As shown in our synthetic spectrum (Fig. 1 top panel), $B^{4+}$ dominates the emission near 255 eV, Xe ions dominate the emission around 4590 eV, while W lines contribute broadly across 100 eV–100 keV.

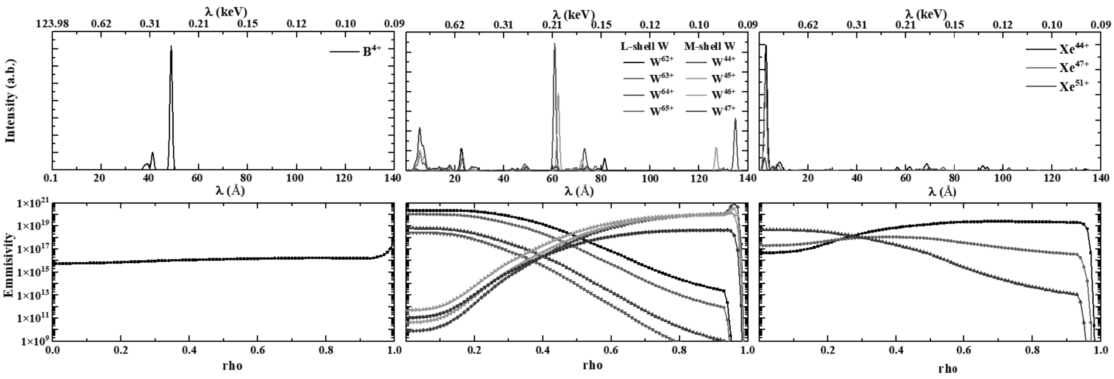


Figure 1: Top panel shows the simulated spectrum with wavelength from our large-scale FAC calculations and intensity from our CRM simulation; The bottom panel plots calculated emissivity of impurities ions (key transition) with PEC-FAC of ITER plasma.

References
[1] C. De Michelis, M. Mattioli, Rep. Prog. Phys. **47**, 1233 (1984)
[2] D.E. Post, J. Abdallah, R. Clark, N. Putvinskaya, Phys. Plasmas **2**, 2328 (1995)
[3] M. F. Gu, Can. J. Phys. **86**, 675 (2008).

## B-12

# R-matrix Atomic Data for Kilonova Applications in Astrophysics

**C. P. Ballance**, C. A. Ramsbottom, L. P. Mulholland, M. McCann, N. E. McElroy, D. J. Dougan

Astrophysics Research Centre, Queen's University Belfast, Belfast BT71NN, United Kingdom

The spectra currently emerging from ground- and space-based facilities are of exceptional quality and resolution, and cover a broad range of wavelengths. To meaningfully analyse these spectra, astronomers utilise complex modelling codes to simulate the astrophysical observations. The main inputs to these codes are radiative and collisional atomic data to include energy levels, transition probabilities, collision cross sections for the processes of electron-impact excitation, electron-impact ionisation and photoionisation, as well as the reverse processes of radiative and dielectronic recombination. The quality and quantity of the atomic data available to the modellers is thus crucial, and complete atomic datasets are necessary for understanding and calculating stellar structure.

In 2017 the first gravitational wave from a binary neutron star merger (NSM) was detected and the ejected matter created a bright glow called a kilonova via r-process nucleosynthesis. This r-process is one channel through which elements heavier than Fe can be created, elements such as the lanthanides, actinides and platinum group elements. Disentangling r-process abundances from the broad spectra of NSM is a challenging task that demands a high degree of rigour in calculations of the ejecta opacity and the atomic calculations that underpin them. Recent publications by McCann et al (2022, 2025a, 2025b) [1], [2], [3] and Mulholland et al (2024a, 2024b) [4], [5], report on extensive relativistic atomic structure and electron-impact excitation collision calculations for the species Au I-III, Pt I-III, W III, Zr I-III, Sr II, Y II and Te I-III, which were subsequently used in collisional-radiative models to investigate line ratio diagnostics in NSM environments. The W III dataset was also used in [3] to provide luminosity predictions and probe for potential sources of emission in kilonova.

The R-Matrix approach is credited as one of the most powerful and reliable tools in calculating these atomic data. Recent and ongoing developments of the relativistic parallel DARC codes have enabled an order of magnitude advance in the accuracy of the atomic structure and subsequent collision calculations that are now feasible for lowly ionised high Z ions. The research group at QUB has a longstanding track record not only in the evaluation of these vital data, but also in the development, maintenance and testing of current and new variants of the R-matrix codes, on numerous platforms from local clusters to HPC facilities worldwide [6].

References

[1] M. McCann, S. Bromley, S.D. Loch and C.P. Ballance, MNRAS, Vol 509, 4, 4723-4735, 2022

[2] M. McCann, L.P. Mulholland, Z. Xiong, C.A. Ramsbottom, C.P. Ballance, O. Just, A. Bauswein, G. Martinez-Pinedo, F. McNeill and S.A. Sim, MNRAS, Vol 538, 1, 537-552, 2025.

[3] M. McCann, C.P. Ballance, F. McNeill, S.A. Sim and C.A. Ramsbottom, MNRAS (submitted for publication March 2025)

[4] L. P. Mulholland, N. E. McElroy, F.L. McNeill, S.A. Sim, C.P. Ballance and C. A. Ramsbottom, MNRAS, Vol 532, 2, 2289-2308, 2024.

[5] L. P. Mulholland, F. McNeill, S.A. Sim, C.P. Ballance and C. A. Ramsbottom, MNRAS, Vol 534, 4, 3423-3438, 2024.

[6] C.P. Ballance, http://connorb.freeshell.org

# Development of a compact electron beam ion trap for application to astronomy and spectroscopic experiments of highly charged ions at the synchrotron radiation facility SPring-8

**Leo Hirata**[A B], Yuki Amano[A], Moto Togawa[C], Hiroyuki A. Sakaue[D], Nobuyuki Nakamura[E], Makoto Sawada[F], Hiromasa Suzuki[G] and Hiroya Yamaguchi[A B]

[A]*Institute of Space and Astronautical Science (ISAS), JAXA, Kanagawa, Japan*
[B]*Department of Physics, The University of Tokyo, Tokyo, Japan*
[C]*Max-Planck-Institut für Kernphysik (MPIK), Heidelberg, Germany*
[D]*National Institute for Fusion Science (NIFS), NINS, Gifu, Japan*
[E]*Institute for Laser Science (ILS), The University of Electro-Communications, Tokyo, Japan*
[F]*Department of Physics, Rikkyo University, Tokyo, Japan*
[G]*Faculty of Engineering, University of Miyazaki, Miyazaki, Japan*

The X-ray microcalorimeter *Resolve* onboard the latest X-ray astronomy satellite, *XRISM*, has shown an outstanding spectral resolution of $< 5$ eV(FWHM@6 keV)[1], resolving fine structures in the X-ray spectra of hot plasma composing astrophysical objects. This enables unprecedentedly precise measurements of their key physical properties. The accuracy of atomic data is crucial when analyzing such fine spectra. However, current spectral models, heavily relying on theoretical calculations, entail non-negligible uncertainties[2], thus precise experimental values are required as substitutes. To address this issue, we explored the use of an "Electron Beam Ion Trap (EBIT)[3]," a device that produces and traps highly charged ions using a monochromatic electron beam and detects their X-ray emission.

The JAXA-EBIT was developed based on the Heidelberg Compact EBIT[4], with a design that allows combined operation with a synchrotron radiation facility, for instance SPring-8, to reproduce various atomic processes occurring in astrophysical environments. We assessed its performance, including the monochromaticity of the electron beam, as well as the ion production and trapping ability, based on dielectronic recombination measurements. Our EBIT demonstrated performance comparable to the same type EBIT at MPIK[4]. Aiming for comprehensive atomic data measurement using our EBIT, this study focused on the L-shell transition lines of iron, which are frequently highlighted in observational studies of galaxy clusters and supernova remnants. In particular, we examined the resonance lines from 3d–2p and 3s–2p transitions in Ne-like Fe ions, where discrepancies between observation and theory have been known[5]. To obtain precise values for the wavelengths and the oscillator strength ratio of these lines, we brought the JAXA-EBIT to the soft X-ray beamline BL17SU at SPring-8 and conducted a six-day beamtime experiment in June 2024 (Fig. 1). In this experiment, monochromatized synchrotron radiation was irradiated onto ions produced in the EBIT, and X-ray photons that were resonantly absorbed and re-emitted by the ions were detected. By measuring the dependence of detected count rates on the incident photon energy, we successfully obtained high-resolution spectra (Fig. 1. Inset), utilizing the excellent monochromaticity afforded by the beamline. Details of the results and the methods employed will be presented at the conference.

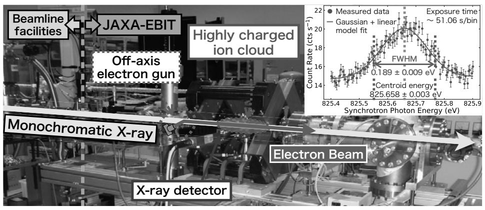


Fig. 1. Photograph of JAXA-EBIT connected to BL17SU, SPring-8, with key components in our experimental setup. Inset: the obtained X-ray spectrum of 3d–2p transition in Ne-like Fe ions.

References

[1] XRISM Collaboration et al., PASJ **76**, 6 (2024)
[2] Hitomi Collaboration et al., PASJ **70**, 2 (2018)
[3] R. E. Marrs et al., Phys. Rev. Lett. **60**, 1715 (1988)
[4] P. Micke et al., Rev. Sci. Instrum. **89**, 063109 (2018)
[5] L. Gu et al., Astron. Astrophys. **627**, A51 (2019)

B-14

# Anomalous Fe XXV triplet structures in a *textbook* plasma revealed by XRISM

**Fukushima, Kotaro**, on behalf of the A1795 team

JAXA/ISAS, Sagamihara, Kanagawa, Japan

Clusters of galaxies are one of the largest structures in the universe as a relaxed self-gravitating system. Dark matter constitutes a significant fraction of the cluster mass, whereas the rest of the mass is primarily comprised of hot ($10^7$–$10^8$ K) and tenuous ($10^{-3}\,\mathrm{cm}^{-3}$) plasma, called the intracluster medium (ICM). X-ray spectra of clusters are dominated by emissions from this ICM, a plasma in collisional ionization equilibrium (CIE), and X-ray line emission from highly charged ions therein plays a key diagnostic role. For example, we have evaluated essential characteristics of the ICM, such as temperature and chemical composition, by comparing their simple X-ray spectra to well-established prototypical plasma emission models (e.g., Astrophysical Plasma Emission Code; APEC [2]). Nevertheless, the situation is being challenged with the new X-ray observatory, X-ray Imaging and Spectroscopy Mission (XRISM; [3]). With the advent of an X-ray microcalorimeter (Resolve) with an energy resolution of about 4.5 eV at 6 keV, XRISM achieved an unprecedented resolving power of the X-ray emission from hot cosmic plasmas, especially at the Fe K emission band ([4, 5]).

Here, we provide a preliminary result of the 225 ks observation of the A1795 cluster with XRISM in January 2025. A1795 is a nearby cluster at 0.8 Gly with a relatively high temperature of about $7 \times 10^7$ K, where the prominent Fe XXV line from He-like ions is expected. Figure 1(a) gives the X-ray image in the 2–8 keV band obtained by Chandra, superimposed on the $3' \times 3'$ field of view of Resolve. Spectra are extracted from six equal segments of this 0.7 Mly covering the central region. Figure 1(b) shows a zoomed-up view of the Resolve spectrum in the southeast part, which is spectrally dominated by the triplet structure of Fe XXV as prospected. The standard CIE plasma model with APEC reproduces the fine structures well, including the resonance $w$, forbidden $z$, and intercombination $x$ and $y$ lines. On the other hand, the spectrum in the northeast region displays an anomalously stronger $y$ line than the CIE prediction by about 60% (Figure 1(c)). We tested redshifted line contamination ($+1400\,\mathrm{km\,s^{-1}}$ from A1795, if any) but found no supporting evidence, suggesting that the anomaly originates from within the ICM itself. This deviation implies atomic processes beyond CIE, such as recombination or possible density-dependent effects, in this dilute environment. These findings highlight the importance of continued cross-disciplinary efforts between the atomic and astrophysical communities, especially in the era of high-resolution X-ray spectroscopy dawned with XRISM.

References

[1] R. K. Smith et al., 2001, ApJ, **556**, 91

[2] M. S. Tashiro et al., 2025, PASJ, in press

[3] XRISM Collaboration et al., 2024, ApJ, **977**, 34

[4] XRISM Collaboration et al., 2025, Nature, **638**, 365

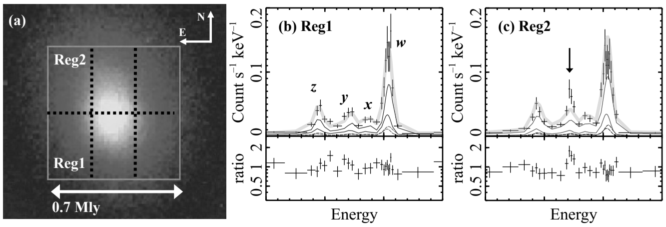


Figure 1: X-ray image and spectra of a galaxy cluster A1795. (a) 2–8 keV image by *Chandra*. (b, c) Zoom-up spectra of the Fe XXV line in Reg1 and Reg2, labelled in (a). Thick lines indicate the best-fit model with several CIE components from each part.

B-15

# Low-Ionized Iron in Cen X-3 Determined by Fe K$\alpha$ and K$\beta$ Fluorescent Lines

**Yutaro Nagai**, on behalf of XRISM Cen X-3 Target Team

Kitashirakawa-Oiwakecho, Sakyo, Kyoto 606-8502, Japan

The high-mass binary Centaurus X-3 (Cen X-3) was observed with the XRISM X-ray observatory on 2024 February 12–15, covering the entire 2.09-day binary orbit. The sinusoidal radial velocity (RV) modulation was found by the orbital phase-resolved spectroscopy of the fluorescence Fe K$\alpha$ line [1]. However, the offset of this RV curve was shifted at $-3.0$ eV, corresponding to $-140$ km s$^{-1}$ (redshift) much larger than the line-of-sight system velocity of $-39$ km s$^{-1}$ reported from optical observations [2]. In order to solve this discrepancy, we further include the energy shift due to Fe ionization, which is coupled with the kinetic Doppler effect of the orbital motion. Since the energy of the weak Fe K$\beta$ line is much more sensitive to the ionization degree than Fe K$\alpha$ [3], we calculated the energy difference between the Fe K$\beta$ and Fe K$\alpha$ lines to cancel out the contribution from the kinematic Doppler shift. Comparing the two atomic calculations at the sub-eV level, we identified for the first time that the fluorescent emission originates from Fe VI (ionization degree of $q = 5$), where five electrons are stripped from the neutral Fe. After disentangling the two effects, the revised Fe K$\alpha$ RV curve was found to be a sinusoidal form with $263 \pm 20$ km s$^{-1}$ ($5.60 \pm 0.43$ eV) and the offset velocity of $-50 \pm 15$ km s$^{-1}$ ($-1.1 \pm 0.3$ eV). The former amplitude stays consistent with the previous results [1], whereas the latter offset becomes consistent within $1\sigma$ with the optically measured systemic velocity. The low-ionized Fe ions are expected to be photoionized at the surface of the O6-8 III supergiant V779 Cen or between the O-star surface and the Lagrangian point $L_1$, as suggested by the RV amplitude. The primary ionizing source is assumed to be either the neutron star or V779 Cen, of which estimated ionization degrees (electron density) are $\log\xi \sim -1$ ($10^{15}$ cm$^{-3}$) and $\log\xi \sim 2$ ($10^{13}$ cm$^{-3}$), respectively.

References

[1] Mochizuki, Y. et al. 2024, ApJL, 977, L21.

[2] Hutchings, J. B. et al. 1979, ApJ, 229, 1079.

[3] Palmeri, P. et al. 2003, A&A, 410, 359.

**B-16**

# Resonant Auger-Meitner Destruction of He-like K$\alpha$ Lines in Photoionized Plasmas

**Gabriel Grell**[1], Roi Rahin[1], Maurice Leutenegger[1], Ehud Behar[2]

[1]NASA Goddard Space Flight Center 8800 Greenbelt Road, Greenbelt, Maryland 20771, USA
[2]Physics Department, Technion, Haifa 32000, Israel

The helium-like K$\alpha$ line complexes are valuable diagnostics of electron density, temperature, and ionization conditions of astrophysical plasmas. The ratios of these lines, however, can be altered by the presence of lithium-like ions, both through inner-shell ionization as well as the process of resonant Auger-Meitner destruction (RAD) [1], in which the He-like intercombination lines are diminished by line absorption from near-coincident Li-like lines [2]. We used the Flexible Atomic Code [3] and line energy values published on the NIST Atomic Spectra Database to model the effect of increased Li-like presence on the He-like line ratios $\mathcal{R} = z/(x + y)$ and $\mathcal{G} = (x + y + z)/w$ for astrophysically important ions in a photoionized plasma, by solving the steady-state rate equations as a function of Li-like column density $N_{Li}$, He-like column density $N_{He}$, velocity dispersion $\sigma_v$, electron density $n_e$, and UV photoexcitation rate $\phi$. We also define and analytically solve for a ratio $\mathcal{Q} = (q+r)/w$; we found that $\mathcal{Q}$ is a diagnostic of the Li-like column density in observed astrophysical spectra. We find that a high Li-like column density can significantly modify $\mathcal{R}$ and $\mathcal{G}$, primarily through enhancement of $z$ and suppression of $x$ and $y$, and that the effects of RAD are highly dependent on the energy difference between the emitting and absorption transitions. Due to this dependence, we stress the importance of a carefully curated database as a reference for transition energies. We will apply our diagnostic framework to spectra of active galactic nuclei (AGN) observed by space-based X-ray spectrometers such as $XRISM$ Resolve.

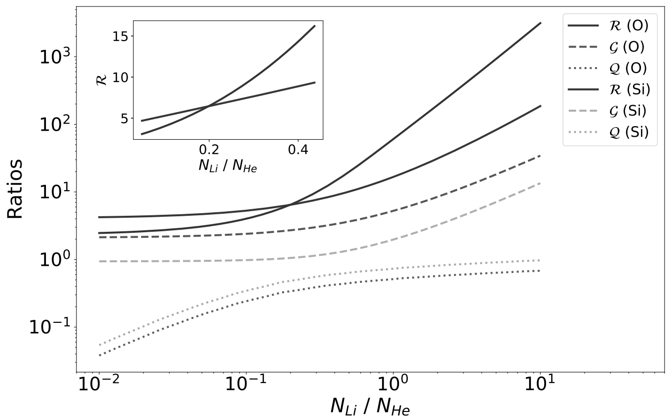


Figure 1: Analytic model calculations of $\mathcal{R}$, $\mathcal{G}$, and $\mathcal{Q}$ ratios for oxygen and silicon as a function of the lithium-like to helium-like column density ratio $N_{Li}/N_{He}$.

References

[1] Liedahl, D. A., American Institute of Physics Conference Series, **774**, 99–108 (2005)

[2] Mehdipour, M., Kaastra, J. S., & Raassen, A. J. J., A&A, **579**, A87 (2015)

[3] Gu, M. F., Canadian Journal of Physics, **86**, 675-689 (2008)

# Dependence of Hydrogen Molecular Dissociation Degree on Discharge Conditions in an ECR-Based Atomic Hydrogen Source

**Yuya Inokuchi**, Kazutaka Mitsui*, Toshiro Kasuya, Hidenori Takahashi*, Yoshihiro Yamada*, Takahiro Kenmotsu, Shinichi Iwamoto*, Koichi Tanaka*, Motoi Wada

Doshisha University, Kyotanabe Kyoto 610-0321, Japan
(*) Shimadzu Corporation, Nakagyoku, Kyoto 604-8511, Japan

Post-translational modification (PTM) binding patterns are considered correlated with lesion such as cancer and Alzheimer's disease [1, 2]. Accurate identification of PTM sites of large molecules may lead to accurate diagnostics of diseases in early stages. In 2016, Shimadzu Corporation reported that Hydrogen Attachment/Abstraction Dissociation (HAD) method enables a fragmentation mass analysis to selectively cleave peptide backbones while preserving PTM binding by using neutral hydrogen radicals [3]. HAD is a promising process for PTM site analysis, but the initial HAD validation used thermally dissociated hydrogen radicals produced by a hot tungsten capillary tube, which exhibited a short life. To prolong the operational lifetime of the system, an ECR-based hydrogen radical source shown in Fig. 1 is being developed for HAD reactions.

One important factor of the atomic hydrogen source for HAD is the velocity distribution function of the produced hydrogen atoms. To estimate the velocity distribution, the hydrogen Balmer-α spectrum is measured with a high-resolution spectrometer. Significant self-absorption by hydrogen atoms is observed in the wavelength spectrum of Balmer-α. To quantitatively evaluate the absorption rate due to produced hydrogen atoms, a LED at 650 nm wavelength serves as the source of light passing through the plasma to measure the absorption spectra shown in Fig. 2. The dependence of the degree of hydrogen dissociation upon ECR discharge source conditions is investigated.

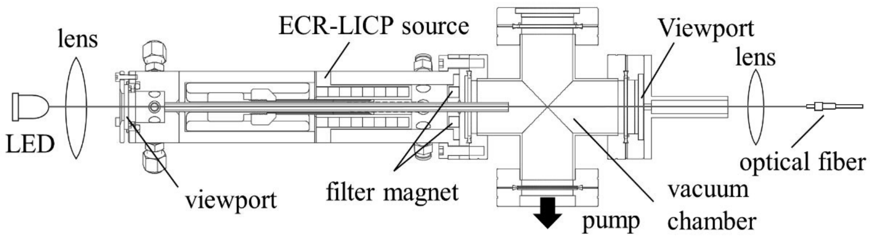


Figure 1: A schematic of experimental system.

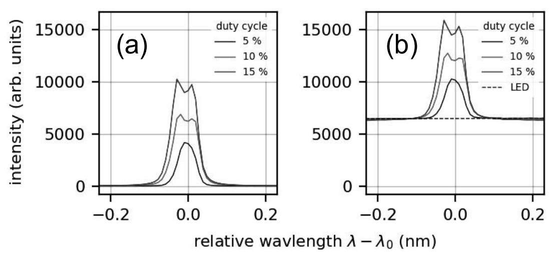


Figure 2: Measure spectrum data for 5, 10 and 15% duty cycle operations at 1 kHz PWM and 250 W peak microwave input power: (a) only plasma, (b) plasma with LED.

References
[1] H. Wang, L. Yang, M. Liu, and J. Luo, Cancer Gene Ther. **30**, 4 (2023)
[2] H. Wesseling et al., Cell., **183**, 6 (2020)
[3] H. Takahashi et al., Anal. Chem. **88**, 7 (2016)

B-18

# Effects upon sheath formation due to plasma surface interaction at the plasma grid surface of a negative hydrogen ion source

**Motoi Wada**, Yuya Inokuchi*, Takahiro Kenmotsu*

Organization for Research Initiatives and Development, Doshisha University, Kyotanabe, Kyoto 610-0321, Japan
(*) Graduate School of Life and Medical Sciences, Doshisha University, Kyotanabe, Kyoto 610-0321, Japan

Successful operation of a cesium (Cs) shower system has realized quasi-steady state beam extraction for 1000 s from a radio frequency (RF) power driven negative hydrogen ($H^-$) ion source [1]. The most significant improvement by the direct introduction of Cs from the shower tube was the suppression of electron current co-extracted with $H^-$ ions. Density of Cs measured by Tunable Diode Laser Absorption Spectroscopy (TDLAS) indicated the time constants smaller than several tens of seconds, while the coextracted electron current varied with longer time constants against the open and close of the Cs shower valve. Surface work function of the plasma grid (PG) that is determined by the plasma-surface interaction affects the $H^-$ ion emission rate and thus the electron density in the vicinity of extraction holes.

The measured Cs density by TDLAS was as high as $4\text{X}10^{10}$ $\text{cm}^{-3}$ during operation of the shower. The density was three orders of magnitude smaller against 0.3 Pa hydrogen in the ion source. However, Cs transport in plasma requires longer time due to its large mass compared with hydrogen ions and neutrals. Reaction cross sections of Cs atoms are larger in low energy regions. For example, the electron impact ionization cross section exceeding $10^{-15}$ $\text{cm}^{-2}$ at the peak as shown in Fig. 1. Low temperature low density extraction region electrons can ionize Cs due to the low ionization threshold. Besides, once Cs are ionized near the PG of the ion source, they can be trapped in a region of negative space potential created by surface produced $H^-$ ions. The sheath structure around the PG is currently investigated by modifying the one-dimensional model developed by McAdams *et al* [3].

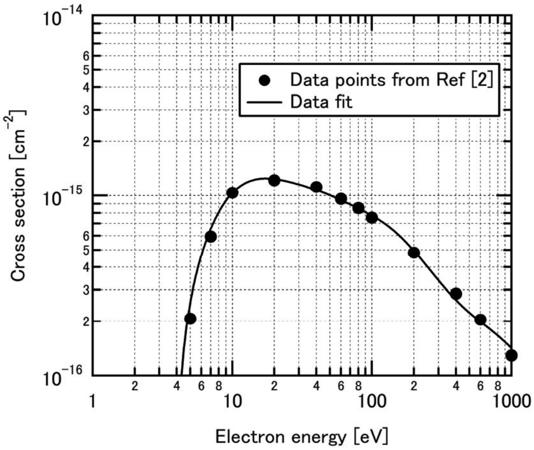


Figure1: Electron impact ionization cross section for Cs and the numerical data fit.

This work was supported by JSPS KAKENHI Grant Number 23K25855.

References

[1] C. Wimmer, A. Döring, Tl Fellinger, M. Fröschle, A. Heiler, D. Mussini, U. Fantz, Fusion Eng. Design, **215**, 114949(2025).
[2] E.J. McGuire, Phys. Rev. **A20**, 445(1979).
[3] R. MacAdams, D.B. King, A.J.T. Holmes, E. Surrey, Rev. Sci. Instrum. **83**, 02B109(2012).

**B-19**

# Photoionized Plasma Production Experiments Using the Synchrotron Light Source UVSOR

**Masahiro Kobayashi[1], Shinji Yoshimura[1], Hiroshi Ota[2,3], Hiroki Chimura[1], Kohei Shimizu[3], Tatsuo Kaneyasu[3], Masahiro Katoh[3,4]**

[1] National Institute for Fusion Science, Toki city, 509-5292, Japan
[2] Japan Synchrotron Radiation Research Institute, Sayo-gun, Hyogo, 679-5198, Japan,
[3] UVSOR Synchrotron Facility, Institute for Molecular Science, Okazaki city, 444-8585, Japan
[4] Reserach Institute for Synchrotron Radiation Science, Hiroshima University, Higashi-Hiroshima 739-0046, Japan

Photoexcitation and photoionization are pivotal processes in astrophysical environments for plasma production. These processes are expected to play a crucial role in the divertor region of nuclear fusion reactors, driven by increased gas pressure and plasma emission. Unlike plasma production via conventional electric fields, photoionized plasmas bypass threshold conditions like Paschen's law. The photoionization rate coefficients peak in the photon energy range of several tens of eV for most atoms and molecules, and diminishes rapidly as photon energy increase. For photon energies exceeding the ionization potential, the additional energy is converted to electron kinetic energy. These features set photoionized plasmas apart from their electrically induced ones.

Despite their potential, the collective behavior of photoionized plasmas has not been systematically explored across varying photon energy ranges, especially in the VUV/EUV range. To address this, experimental apparatus capable of generating photoionized plasmas using synchrotron radiation has been developed [1]. The UVSOR synchrotron light source [2] provides a continuously tunable energy beam spanning X-ray, EUV, VUV, visible, and infrared ranges, enabling a comprehensive study of photoionized plasma properties.

In this study, VUV/EUV beams were generated using the undulator beamline BL1U at UVSOR. An upstream aluminum mirror effectively eliminated higher-order light components, ensuring spectral purity. The experimental gas cell was integrated with a multi-stage differential pumping system, avoiding window-induced photon flux attenuation. Photon flux of $10^{15}$ photons/s/mm$^2$ and beam radius of approximately 1 mm were achieved at the gas cell center. Sample gases introduced at pressures between 1 and 10 Pa maintained ultra-high vacuum conditions $10^{-6}$ to $10^{-7}$ Pa in the upstream storage ring chamber.

Beam energy scanning between 16 and 36 eV facilitated plasma production characterization through emission spectroscopy and Langmuir probe diagnostics. Figure 1 illustrates visible light camera images of the plasma, revealing localized emission along the beam trajectory. The plasma parameters were estimated as $n_e = 10^{14} \sim 10^{15}$ m$^{-3}$ and $T_e \sim 1$ eV at 1 mm from the beam axis. The $n_e$ rapidly decreased within 2 mm from the beam axis, while $T_e$ remained spatially almost constant. The plasma parameter change is found not monotonic against the beam energy. Further details of the experiments will be presented at the conference.

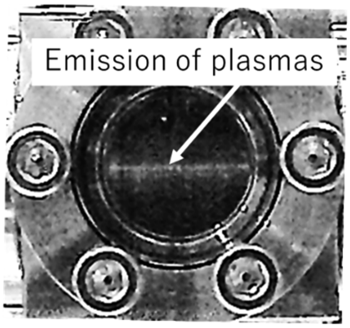


Figure 1 : Visible camera image of photoionized plasma produced along the beam.

References

[1] M. Kobayashi et al., Plasma and Fusion Research **19**, 1301028 (2024).
[2] H. Ota et al., J. Phys.: Conf. Ser. **2380**, 012003 (2013).

# Ion fractional abundance measurement in linear plasma device NUMBER

**A. Okamoto**, K. Sato, K. Takeda, K. Torii, Y. Kawachi, T. Fujita

Graduate School of Engineering, Nagoya University

Ion fractional abundance is an important parameter. While it is easily estimated from ionization equilibrium in magnetically confined plasmas, what determines the fractional abundance is not so clear in low temperature plasmas. Spectroscopic measurement of fractional abundances for helium and argon discharges in a linear plasma device NUMBER is presented.

Experiments were performed in a linear plasma device NUMBER [1]. Helium and argon plasmas were produced by the electron cyclotron resonance (ECR) in the magnetic beach configuration with a 2.45 GHz microwave. Intensities of visible line emissions were measured between the ECR region and a uniform high field region. Electron temperature and density were measured by a Langmuir probe.

For helium plasmas, typical electron temperature and density were $T_{\mathrm{e}} = 8 - 12\,\mathrm{eV}$ and $n_{\mathrm{e}} = 0.6 - 1 \times 10^{17}\,\mathrm{m}^{-3}$. Transitions in He I with upper state of $n^1\mathrm{S}$ were observed to minimize the effects of radiation trapping and the quasi-steady-state approximation for metastable states. Collisional-radiative models (CRM) for helium atoms [2,3] and singly charged ions were used to calculate the population coefficients. Density ratio between the atoms and singly charged ions was then easily obtained. In order to determine the density ratio between singly and doubly charged ions, particle loss timescales were introduced [4], which can be estimated from observables. The fractional abundance for helium plasmas indicate that the density of singly charged ions is one order of magnitude smaller than that of atoms, and that the doubly charged ions have a density 4 orders of magnitude smaller than the singly charged ions. We also note that the atom density is one order of magnitude smaller than that estimated from gas pressure before discharge.

For argon plasmas, typical electron temperature and density were $T_{\mathrm{e}} = 4 - 6\,\mathrm{eV}$ and $n_{\mathrm{e}} = 0.6 - 1.3 \times 10^{18}\,\mathrm{m}^{-3}$. Line emissions of Ar I – Ar III were observed. Because the dataset for argon ions available from OPEN-ADAS degenerates in levels, the total intensity of the degenerate level was complemented based on intensities of observed transitions. The fractional abundance for argon plasmas indicate that the density of singly charged ions is 1/3 - 1/100 of that of atoms depending on the electron temperature, and that the doubly charged ions have a density 4 orders of magnitude smaller than the singly charged ions.

References

[1] D. Hamada, A. Okamoto, T. Fujita, *et al.*, Plasma Fusion Res. **13** (2018) 3401044.

[2] T. Fujimoto, J. Quant. Spectrosc. Radiat. Transf. **21** (1979) 439.

[3] M. Goto, J. Quant. Spectrosc. Radiat. Transf. **76** (2003) 331.

[4] K. Sato, A. Okamoto, T. Fujita, *et al.*, Plasma Fusion Res. **20** (2025) in press.

B-21

# Machine learning approach to measuring electron density and temperature from high-density helium plasmas

[1]**Shin Kajita**, [2]Daisuke Nishijima, [3]Keisuke Fujii, [4]Hirohiko Tanaka, [5]Jordy Vernimmen, [5]Ivo Classen, and [6]Noriyasu Ohno

[1] Graduate School of Frontier Sciences, The University of Tokyo, Japan
[2] Center for Energy Research, University of California, San Diego, United States of America
[3] Fusion Energy Division, Oak Ridge National Laboratory, United States of America
[4] Institute of Materials and Systems for Sustainability, Nagoya University, Nagoya 464-8603, Japan
[5] DIFFER—Dutch Institute for Fundamental Energy Research, Eindhoven, The Netherlands
[6] Graduate School of Engineering, Nagoya University, Nagoya 464-8603, Japan

In the divertor region of a nuclear fusion device, low-temperature plasmas dominated by mixed helium (He) and hydrogen (H) isotope plasmas, including recombining plasmas, predominate. Optical emission spectroscopy using H and He lines has been widely used. The He line intensity ratio (LIR) method using collisional radiative models (CRMs) has been used for a long time to measure electron density and temperature [1], and its potential and limitations in fusion plasmas have been discussed. This approach has been reported to be extremely useful, while also potentially causing errors in helium-hydrogen mixed plasmas and recombining plasmas [2,3]. One method to overcome these issues has been the consideration of machine learning techniques in recent years [4,5]. This presentation reports results of measuring electron density and temperature using a neural network-based LIR method with spectroscopic data from helium-hydrogen mixed recombining plasmas at the Magnum-PSI divertor simulator.

Mixed plasmas have more complex spectral shapes, hence the spectroscopic data uses the intensity of each line directly in machine-learning, with temperature and density measured by Thomson scattering. The prediction uncertainty is found to be extremely low, approximately 10% for density (see Fig. 1) and 7% for temperature. Sensitivity analysis conducted using SHAP (SHapley Additive exPlanations) reveals that, while helium line intensity is important in pure helium plasma, hydrogen Balmer lines contribute significantly in helium-hydrogen mixed plasma. The machine learning approach has the potential to provide a robust and simple analytical method for evaluating electron temperature and density from visible spectroscopic measurements of helium-hydrogen mixed plasmas

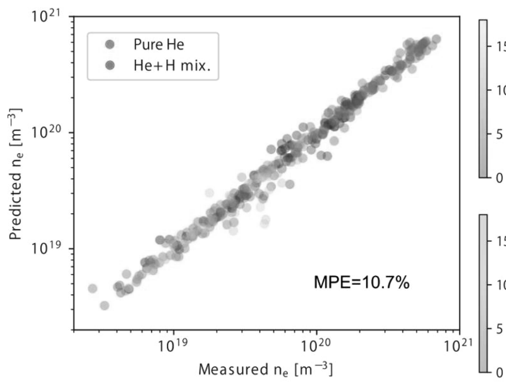


Figure 1: The predicted values of the electron density as functions of the TS-measured value.

References
[1] S Kajita, D Nishijima, Journal of Physics D: Applied Physics 57 (2024), 423003.
[2] S Kajita, K Suzuki, H Tanaka, N Ohno, Physics of Plasmas 25, 063303 (2018).
[3] S. Kajita, G. Akkermans, K. Fujii, H. van der Meiden, and M. C. M. van de Sanden, AIP Advances 10, 025225 (2020).
[4] D. Nishijima, S. Kajita, and G. R. Tynan, Review of Scientific Instruments 92, 023505 (2021).
[5] S. Kajita, S. Iwai, H. Tanaka, D. Nishijima, K. Fujii, H. van der Meiden, and N. Ohno, Nuclear Materials and Energy 33, 101281 (2022).

**B-22**

# Residual Stress and Related Properties of Copper Oxide Thin Films Deposited by Ion Energy Modulated ALIS and Magnetron Sputtering Hybrid Process

**Yuan-Ming Chang**[1]*, Chuen-Lin Tien[1,2], Yi-Lin Wang[1,2]

[1]Ph.D. Program of Electrical and Communications Engineering, Feng Chia University, Taichung 40724, Taiwan;
[2]Department of Electrical Engineering, Feng Chia University, Taichung 40724, Taiwan;
*p1200407@o365.fcu.edu.tw;

This study investigates a hybrid co-deposition method that integrates an anode layer ion source (ALIS) with a magnetron sputtering system to enable the controlled fabrication of copper oxide (CuO) thin films [1]. To optimize ion beam bombardment characteristics, magnetic field simulations were conducted for both high-energy and low-energy ALIS configurations [2, 3]. These simulations were experimentally validated using a three-dimensional magnetic field mapping system, allowing direct comparison between simulated and measured field distributions under various ion channel widths [4]. In this dual-source configuration, ALIS functions as an auxiliary ion source, providing adjustable ion energy that both suppresses substrate damage during sputtering and enhances film densification and adhesion [5]. In the experimental phase, the CuO thin films were deposited on B270 and H-K9L optical glass substrates under varying oxygen/argon gas flow rates and ALIS power conditions, employing both high-energy and low-energy ion modes. Surface morphology and residual stress were characterized using a Twyman–Green interferometer and a Linnik microscopic interferometer. The results indicate that variations in ion energy and sputtering configuration significantly affect the film microstructure, optical reflectance, and internal stress distribution. By appropriately tuning the ion-assisted deposition parameters, grain density can be increased and pore formation suppressed, enabling precise control over stress states and surface roughness. This hybrid co-deposition strategy provides a versatile and controllable platform for tailoring the microstructural and mechanical properties of thin films, making it particularly suitable for high-performance optical coatings, protective surface layers, and advanced functional material applications.

References

[1] W. Zheng, Y. Chen, X. Peng, K. Zhong, Y. Lin, Z. Huang, The Phase Evolution and Physical Properties of Binary Copper Oxide Thin Films Prepared by Reactive Magnetron Sputtering. Materials, **11**, 1253 (2018).

[2] Y. Xi, J. Zhao , J. Zhang , C. Zhang, Q. Wu, The Influence of Ion Beam Bombardment on the Properties of High Laser-Induced Damage Threshold HfO2 Thin Films, Crystals, **12**, 117, 2022.

[3] A. G. Guglya and I. G. Marchenko, "Ion beam-assisted deposition," in Comprehensive Guide for Nanocoatings Technology, M. Aliofkhazraei, Ed. New York: Nova Science Publishers, 2015, ch. 3, pp. 45–69(2015)

[4] K.G. Ressler, N. Sonnenberg, M.J. Cima. Mechanism of biaxial alignment of oxide thin films during ion-beam-assisted deposition. *Journal of the American Ceramic Society*, 80, 2637–2648 (2005)

[5] Z.Z. Wu, Fabrication of Nitrogen Ion Sources and Their Applications on Nitriding of Titanium Metal. Master's Thesis, National Yang Ming Chiao Tung University, Hsinchu, Taiwan (2024)

[6] M.M.M. Bilek, D.X. Fu, Y. Yin, D.R. McKenzie, Use of low energy and high frequency PBII during thin film deposition to achieve relief of intrinsic stress. Surface and Coatings Technology, **186**, 21-28 (2004)

**B-23**

# Characterization of laser induced plasma: Analysis of rocks using calibration-free LIBS

**S.U. Haq*,** Qamar Abbas, and Ali Nadeem

National Institute of Lasers and Optronics College, Pakistan Institute of Engineering and Applied Sciences, Nilore, Islamabad, 45650, Pakistan.

## Abstract:

The laser-induced plasma of rock samples has been characterized by determining plasma parameters such as the plasma temperature and electron number density. The plasma was produced by irradiating focused laser pulses of the fundamental wavelength of 1064 nm with a Nd:YAG laser. The plasma emissions were collected and analyzed via a LIBS2500+ spectrometer. The emission spectra were used to determine the plasma temperature using iron emission lines in the Saha Boltzmann plot, whereas the electron number density was estimated using Stark broadened emission line of hydrogen ($H\alpha$) at 656.27 nm. To characterize the laser-induced plasma, the plasma was produced as a function of laser energy from 80–150 mJ per pulse and in the presence of a magnetic field of 1–3.5 kG strength. The plasma electron temperature and the number density of electrons being determined were used to verify the condition of local thermodynamic equilibrium (LTE). The normalized emission spectra and calibration-free laser-induced breakdown spectroscopy technique were employed to measure the concentrations of the rock constituents. Compositional analysis was performed via the calibration-free technique, which revealed that Li, B, Na, Mg, Si, K, Ca, Fe, Cu, and Zn are present in almost all the rock samples, but their concentrations vary from sample to sample.

* Corresponding author
E-mail: sami_ulhaq2002@yahoo.com

B-24

# Measurement of visible emission from Laser-Produced Sn Plasma in a Hydrogen Atmosphere

**G. Shusen** [1], K. Watanabe [1], Y. Nishii [1], M. Kishimoto [1], T. Jozaki [1,2], A. Sunahara [2,3], K. Yamasaki [1], T. Higashiguchi [4] and S. Namba [1]

[1] Graduate School of Advanced Science and Engineering, Hiroshima University, [2] Institute of Laser Engineering, Osaka University, [3] Center for Material under Extreme Environment, Purdue University, [4] Department of Electrical and Electronic Engineering, Utsunomiya University

Extreme Ultraviolet (EUV) lithography at a 13.5 nm wavelength is essential for high-volume manufacturing of next-generation semiconductors with a 22 nm node. A critical issue in EUV light source is debris mitigation emitted from laser-produced tin (Sn) plasma, which can severely damage EUV mirrors. Introducing hydrogen gas into the Sn plasma has been proven to reduce the debris, extending the lifetime of the large, expensive mirror. [1-3] In this study, we have investigated the emission behavior in laser produced Sn plasma under a hydrogen atmosphere. Particular attention is paid to understand the formation mechanism of gaseous $SnH_4$ due to complicated reactions with Sn atom/ion and hydrogen radicals. To elucidate this, spatiotemporal visible emission spectra were measured and analyzed for identification of dominant atomic/molecular processes in plasmas.

Figure 1 illustrates a schematic of the experimental setup. A Sn target was irradiated by a Nd:YAG laser (1064 nm, 7 ns, < 650 mJ) to produce Sn plasma. A pinhole camera was used to capture two-dimensional EUV emission images. EUV spectra were measured using a grazing incidence spectrometer. Visible emission spectra were observed with a 250-mm visible spectrometer equipped with an ICCD. The gas was introduced into the chamber to maintain a constant pressure of 100 Pa.

Figure 2 presents a photograph of laser-produced Sn plasmas in vacuum and hydrogen atmosphere. For vacuum, the plasma exhibits a predominantly green light, attributed to strong emissions of Sn I–Sn III line emissions around 550 nm. In contrast, for $H_2$ atmosphere, a prominent color transition—from white near the target, to blue in the target periphery , and then pink at the outermost region. The white emission originates from continuum radiation of the target surface. The blue region is dominated by H atom Balmer series, particularly $H_\beta$ and $H_\gamma$, indicating hydrogen excitation and plasma formation. At greater distances, the mixture of $H_\alpha$, $H_\beta$, $H_\gamma$, and $H_\delta$ lines results in a pink emission, indicating that H is majority plasma particles. The color change is caused by interaction of electron/ion/atom and $H_2$, resulting in the plasma cooling and strong recombination (three-body recombination). On the other hand, $H_2$ gas suffers from dissociation, excitation and ionization, which emits Balmer lines ($H_\beta$, $H_\gamma$) at a specific plasma density and temperature position. Spatiotemporal line emissions of Sn I, II and H atom show that this interpretation is reasonable.

## References

[1] H. Komori, SPIE **5374**, pp. 710-719 (2000).
[2] P. Mirkarimi, Applied Optics **39** (10), pp.1617-1625 (2000).
[3] V. Bakshi, "EUV Sources for Lithography," SPIE Press, Bellingham, WA (2006).

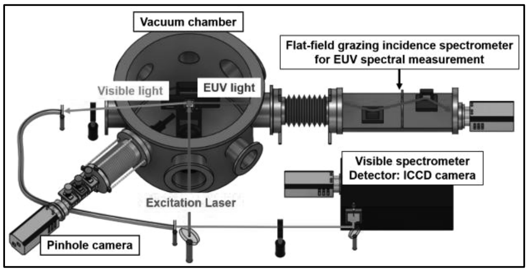


**FIG. 1:** Schematic of the experimental setup for visible and EUV emission measurements.

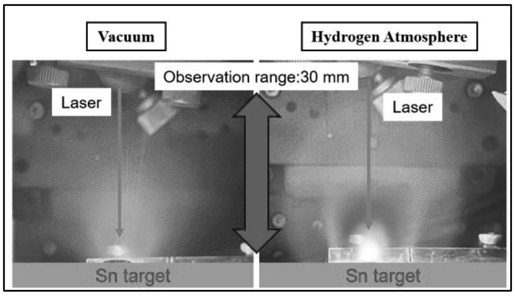


**FIG. 2:** Photographs of laser Sn plasma under vacuum and hydrogen atmosphere.

**B-25**

# Development of CoBIT-III for studying atomic processes in plasmas

Ryohei Ishigami[1], Ayumu Iso[1], Omi Miyauchi[1], Yugo Nagata[1], Nobuyuki Nakamura[2], Hiroyuki Sakaue[3], Naoki Kimura[3]

[1]Department of Physics, Tokyo University of Science, 162-8601, Japan
[2]Institute for Laser Science, The University of Electro-Communications, Tokyo 182-8585, Japan
[3]National Institute for Fusion Science, Gifu 509-5292, Japan

Highly charged ions (HCIs) play important roles for atomic processes in various plasmas. To understand their details, laboratory simulations with experimental devices which can well-defined plasma conditions are useful. An electron beam ion trap (EBIT) is a representative experimental apparatus with a well-defined laboratory plasma as well as a powerful tool for emission spectroscopy of HCIs.

Here, we report recent progress on our development for a compact EBIT (CoBIT-III). A compact electron beam ion trap in Japan, called CoBIT, is a useful device for studying moderate charge state ions. The first CoBIT (CoBIT-I) was developed at the University of Electro-Communication (UEC) in Tokyo [1]. The second CoBIT (CoBIT-II) was installed at the National Institute for Fusion Science (NIFS) in Gifu [2]. They are available for low-cost operation without liquid helium. To date, many emission spectra for various HCIs have been measured in a wide wavelength range. The spectroscopic activity using CoBIT has contributed to a variety of research applications, such as astrophysics, fusion reactors, and HCI clocks.

Recently, we started development of the third CoBIT (CoBIT-III) at Tokyo University of Science (TUS). CoBIT-III will employ a flat- or hollow- cathode, which is different from the prior CoBIT design. By taking the advantage of the hollow-cathode setup, we plan to challenge advanced experiments such as HCI laser spectroscopy for probing plasma conditions. In the poster, we report the progress of the design and development.

Figure 1: Photo of CoBIT-III.

References
[1] N. Nakamura, et al., Rev. Sci. Instrum. 79, 063104 (2008).
[2] H. A. Sakaue, et al., JINST 5 C08010 (2010).

**B-26**

# Origin of Polarized Emission from Laser Produced Plasma

**Geethika B R**, Jinto Thomas, Renjith Kumar R, Judhistir Shamal, H C Joshi

Institute For Plasma Research, Bhat, Gandhinagar, Gujarat, India &
Homi Bhabha National Institute, Training School Complex, Anushaktinagar, Mumbai, India

Laser Produced Plasma (LPP) is a highly suitable medium for studying atomic emissions, as the high temperature provides access to transitions involving excited states that are rarely populated under normal conditions. Furthermore, LPP exhibits sharp spatial and temporal gradients in both electron density and temperature. These gradients make LPP an excellent platform for studying non-equilibrium plasma dynamics and spectroscopic line broadening mechanisms. The steep gradients also allow time-resolved and space-resolved spectroscopy to probe the evolution of plasma parameters across different regions and stages of the plasma plume.

Polarized emission from laser-produced plasmas has been observed for several decades and continues to fascinate researchers due to the insights it offers into the fundamental physics of plasma formation and evolution. In earlier studies, polarized light has been found to carry information about anisotropic electron velocity distributions [1], self -generated magnetic fields [2] etc. Despite these observations, the actual mechanisms responsible for polarization in LPP still remains challenging and are often debated. In the present study, we undertake a comprehensive spatio-temporal investigation of polarized emission from LPP, employing localized measurements of key plasma parameters (ref Figure 1). Our results reveal a remarkable feature in the degree of polarization (DOP): a spatial sign reversal along the axis of the expanding plume. This behavior not only highlights the complexity of polarization processes in transient plasmas but also prompts deeper inquiry into possible causes.

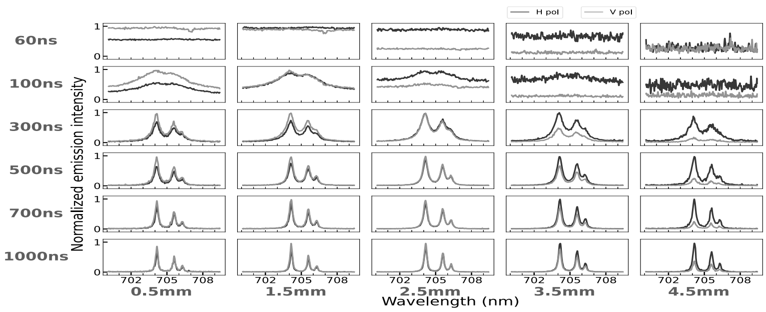


Figure 1: Polarization resolved spatio-temporal evolution of the emission spectra of Al II [3].

References

[1] P . Hammond, W. Karras, A. G. McConkey, & J. W. McConkey, Phys. Rev. A **40**, 1804-1810 (1989)

[2] A.K. Sharma & R.K. Thareja, Applied Surface Science **253**, 3113-3121 (2007)

[3] B. R. Geethika, J. Thomas, M. Patel, R. Kumar & H. C. Joshi, J. Anal. At. Spectrom. **38**, 2477-2485 (2023)

# Spatially resolved spectroscopy and plume splitting of soft x-ray emitting laser-produced iron plasmas in a high pressure helium environment

**E Sokell[1] *, K Mongey[1], R Brady[1], E Gallagher[1], B Delaney[1] and F O'Reilly[1]**

[1]School of Physics, University College Dublin, Belfield, Dublin 4, Ireland

**Synopsis** Emission spectra from iron laser-produced plasmas recorded in vacuum and at helium pressures of up to 900 mb reveal features at ~820 eV. This emission is predomintately attributed to $Fe^{16+}$ and $Fe^{17+}$. Spatially resolved spectra indicate a second source of this x-ray emission far from the plasma, the intensity and location of this emission show a strong dependence on helium pressure.

X-ray emitting laser-produced plasmas are relevant for a number of applications including the creation of soft x-ray light sources [1]. Buffer gases can be used to confine laser-produced plasmas and helium is often used as it transmits soft x-ray photons.

This work reports spectra obtained with a set up that has been described in detail elsewhere [2] and is shown schematically in figure 1. In these experiments 1064 nm laser radiation at an energy of 40 mJ per pulse was focused through a 20 mm focal length lens onto an iron slab target. The resulting x-ray emission was imaged using a 5 μm slit orientated perpendicularly to the laser axis, producing an image of the plasma along the laser axis. X-ray photons were detected using a raspberry pi camera with a Sony IMX477R silicon chip with a pixel size of 1.55 μm covered with a 600 nm aluminium filter. Photon counts were converted to photon energies to perform spectroscopic measurements. The technique facilitates the production of spectra corresponding to specific points in the image. In this work bins of 20 μm were used.

The one-dimensional spatial profiles of the laser plasmas resulted in skewed distributions along the laser axis, which has been observed for tin [2] and other elements under similar irradiation schemes before. The length of the plasma (away from the target) was observed to decrease by approximately 8% as the helium pressure changed from 0 mb to 500 mb. At higher pressures the length remained constant within the experimental uncertainties.

As the helium pressure was increased from 0 mb secondary source of soft x-ray emission was observed far, 100s μm, from the primary plasma emission. Increasing the helium pressure reduced the intensity of this secondary source emission. The spatial separation of the emission from the primary emission decreasing as the helium pressure increased. Software to model the Stopping Range of Ions in Matter (SRIM) using Monte Carlo simulations has been used to determine a feasible range of kinetic energies for the ions responsible for the emission.

Spatially resolved spectroscopy of the regions corresponding to the secondary source emission indicate that $Fe^{16+}$ and $Fe^{17+}$ ions [3] are predominantly responsible for the emission, although the mechanism by which these ions survice for so long in the high pressure helium environments is still under consideration.

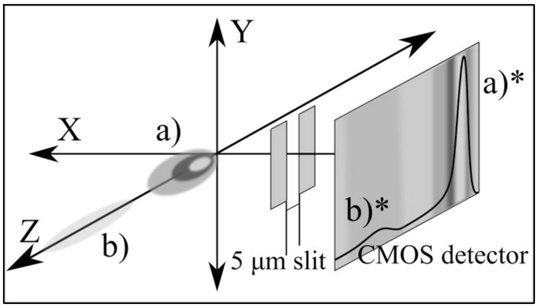


**Figure 1.** Schematic of the experimental set up used. The laser axis is along the z-axis.Soft x-ray emission is imaged through a 5μm slit and recorded with a CMOS detector.

This work was funded by Science Foundation Ireland (SFI), "Frontiers for the Future" programme; 19/FFP/6795.

## References

[1] O'Sullivan G *et al* 2015 *J. Phys. B: At. Mol. Opt. Phys.* **48** 144025
[2] Mongey K *et al* 2024 Applied Physics **124** 102104
[3] Fuhr J *et al* 1981 *J. Phys. Chem. Ref. Data.* 10 1.555644

* E-mail: emma.sokell@ucd.ie

# AUTHOR INDEX

(Presenter Only)


| | |
|---|---|
| Aggarwal, Surabhi | A-15 |
| Agrawal, Ayushi | O-23 |
| Amano, Yuki | O-16 |
| Aybar, Nicholas A | A-01 |
| Balance, Connor | B-12 |
| Bao, Runjia | B-11 |
| Belmonte, Maria Teresa | I-16 |
| Benredjem, Djamel | A-08 |
| Chang, Yuan-Ming | B-22 |
| Cho, Patricial | I-19 |
| Deprince, Jerome | I-20, A-11, A-12 |
| Dey, Ritu | O-01 |
| Dong, Chen Zhong | A-02, B-06 |
| Dowd, Kirsten | O-21 |
| Fernadez, Lucas Ansia | O-15 |
| Fujii, Keisuke | O-05 |
| Fujioka, Shinsuke | I-08 |
| Fukushima, Kotaro | B-14 |
| Gao, Shusen | B-24 |
| Gawne, Thomas | I-15 |
| Geethika, B R | B-26 |
| Ghosh, Nitish | B-07 |
| Ghosh, Raju | A-17 |
| Goto, Motoshi | I-01 |
| Grell, Gabriel Jonathan | B-16 |
| Gupta, Shivam | O-07 |
| Hannachi, Ibtissem | O-02 |
| Hayashi, Yuki | O-03 |
| Hirata, Leo | B-13 |
| Humphries, Oliver | I-12 |
| Inokuchi, Yuya | B-17 |
| Ishigami, Ryohei | B-25 |
| Ishikawa, Ryohko | I-18 |
| Johnson, Curtis | A-21 |
| Kajita, Shin | B-21 |
| Kato, Daiji | A-05, A-06 |
| Kawate, Tomoko | I-03 |
| Kobayashi, Masahiro | I-05, B-19 |
| Kodangil, Supriya | A-14 |
| Kuzmin, Arseniy | A-20 |
| Langenberg, Andreas | I-02 |
| Le, Hai P | O-10 |
| Lee, Hae Ja | O-12 |
| Losada, Ulises | I-06 |

| | | | |
|---|---|---|---|
| Marchuk, Oleksandr | A-19 | Sasaki, Akira | A-23 |
| Miron, Canelia | I-13 | Schaeuble, Marc-Andre | I-10 |
| Morita, Tsunehiro | O-04 | Sheil, John | M-02 |
| Murakami, Izumi | B-04 | Shikama, Taiichi | A-18 |
| Nagai, Yutaro | B-15 | Singh, Gajendra | A-16 |
| Nagler, Bob | I-11 | Sokell, Emma Jane | B-27 |
| Nakamura, Hiroaki | O-20 | Song, Dingbao | B-01 |
| Nakamura, Nobuyuki | A-25 | Song, Mi-Yong | O-13 |
| Nasr, Sirine Ben | A-13 | Stambulchik, Evgeny | I-09 |
| Nishikawa, Takeshi | B-05 | Suzuki, Chihiro | A-04 |
| Okamoto, Atsushi | B-20 | Takehiro, Yu | A-27 |
| O'Mullane, Martin | M-01 | Tanuma, Hajime | A-24 |
| Pain, Jean-Christophe | A-07 | Telmini, Mourad | O-22 |
| Pal, Amar | A-26 | Togawa, Moto | O-11 |
| Pandey, Alpana | B-08 | Tsujimoto, Masahiro | O-17 |
| Patel, Mehul V | A-03 | Ulhaq, Sami | B-23 |
| Perks, Conor | I-04 | Velarde, Pedro | O-14 |
| Piron, Robin | B-10 | Wada, Motoi | B-18 |
| Quinet, Pascal | A-09, A-10 | Wang, Xing | O-09 |
| Rahin, Roi Avraham | O-18 | Wu, Chun-Tse | B-02 |
| Ralchenko, Yuri | I-07 | Yamada, Kazuyoshi | B-09 |
| Renaudin, Patrick | O-08 | Yamaguchi, Hiroya | I-17 |
| Sackers, Marc | I-14 | Yuan, Jianmin | O-06 |
| Saito, Seiki | A-22 | Zhang, Chunyu | O-19 |
| Sakaue, Hiroyuki A. | B-03 | | |

| July 21 (Mon) | July 22 (Tue) | July 23 (Wed) | July 24 (Thu) | July 25 (Fri) |
|---|---|---|---|---|
| | 08:30 Registration | *chair: G. D. O'Sullivan* | *chair: H. J. Lee* | *chair: P. Quinet* |
| | 09:30 Opening | 09:30 [I-07] Yu. Ralchenko | 09:30 [I-15] T. Gawne | 09:30 [I-19] P. Cho |
| | *chair: Yu. Ralchenko* | 10:00 [O-06] J. Yuan | 10:00 [O-14] P. Velarde | 10:00 [I-20] J. Deprince |
| | 09:50 [I-01] M. Goto | 10:20 [O-07] S. Gupta | 10:20 [O-15] L. Ansia Fernadez | 10:30 [O-19] C. Zhang |
| | 10:20 [I-02] A. Langenberg | | | 10:50 [O-20] H. Nakamura |
| | 10:50 Coffee | 10:40 Coffee | 10:40 Coffee | 11:10 Coffee |
| | *chair: C. Ballance* | *chair: E. Stambulchik* | *chair: D. Kato* | *chair: C. A. Ramsbottom* |
| | 11:10 [M-01] M. O'Mullane | 11:00 [M-02] J. Sheil | 11:10 [I-16] M. T. Belmonte | 11:40 [O-21] K. Dowd |
| | 11:40 [I-03] T. Kawate | 11:30 [I-08] S. Fujioka | 11:40 [I-17] H. Yamaguchi | 12:00 [O-22] M. Telmini |
| | 12:10 [O-01] R. Dey | 12:00 [O-08] P. Renaudin | 12:10 [O-16] Y. Amano | 12:20 [O-23] A. Agrawal |
| | 12:30 [O-02] I. Hannachi | 12:20 [O-09] X. Wang | 12:30 [O-17] M. Tsujimoto | 12:40 Closing |
| | 12:50 Lunch | 12:40 Lunch | 12:50 Lunch (IPC meeting) | |
| | *chair: O. Marchuk* | *chair: S. Fujioka* | *chair: I. Murakami* | |
| | 14:10 [I-04] C. Perks | 14:00 [I-09] E. Stambulchik | 14:10 [I-18] R. Ishikawa | |
| | 14:40 [I-05] M. Kobayashi | 14:30 [I-10] M. Schaeuble | 14:40 [O-18] R. Avraham Rahin | |
| | 15:10 [O-03] Y. Hayashi | 15:00 [O-10] H. P. Le | | |
| | 15:30 Coffee | 15:20 Coffee | 15:00-17:00 | |
| | *chair: C. Johnson* | *chair: J. Sheil* | Poster A | |
| | 15:50 [I-06] U. Losada | 15:40 [I-11] B. Nagler | | |
| | 16:20 [O-04] T. Morita | 16:10 [I-12] O. Humphries | | |
| | 16:40 [O-05] K. Fujii | 16:40 [O-11] M. Togawa | | |
| 16:00-18:00 Registration Reception | | 17:00 [O-12] H. J. Lee | | |
| | 17:00-19:00 | 17:20 Break | | |
| | Poster B | *chair: H. Tanuma* | | |
| | | 17:35 [I-13] C. Miron | | |
| | | 18:05 [I-14] M. Sackers | | |
| | | 18:35 [O-13] M. Y. Song | 18:30-20:30 Banquet | |
| | | 18:55 End | *Hachioji Nihonkaku* | |

Presentation time:

Invited: 25+5 min

Memorial: 25+5 min

Oral: 15+5 min